uOttawa

L'Université canadienne
Canada's university

FACULTÉ DES ÉTUDES SUPÉRIEURES ET POSTOCTORALES

uOttawa

L'Université canadienne
Canada's university

FACULTY OF GRADUATE AND POSDOCTORAL STUDIES

Chantal Medina

AUTEUR DE LA THÈSE / AUTHOR OF THESIS

M.Sc. (Biochemistry)

GRADE / DEGREE

Department of Biochemistry, Microbiology and Immunology

FACULTÉ, ÉCOLE, DÉPARTEMENT / FACULTY, SCHOOL, DEPARTMENT

The Chromatin Remodeling Protein ATRX is Required for Interneuron Survival in the Mammalian Retina

TITRE DE LA THÈSE / TITLE OF THESIS

Dr. David Picketts

DIRECTEUR (DIRECTRICE) DE LA THÈSE / THESIS SUPERVISOR

CO-DIRECTEUR (CO-DIRECTRICE) DE LA THÈSE / THESIS CO-SUPERVISOR

EXAMINATEURS (EXAMINATRICES) DE LA THÈSE / THESIS EXAMINERS

Marie-Andrée Akimenko

Catherine Tsilfidis

Gary W. Slater

Le Doyen de la Faculté des études supérieures et postdoctorales / Dean of the Faculty of Graduate and Postdoctoral Studies

The Chromatin Remodeling Protein ATRX is Required for Interneuron Survival in the Mammalian Retina

Chantal Medina

THESIS

Submitted to the School of Graduate Studies in partial fulfilment
of the requirements for the degree of
Master of Science

University of Ottawa
Ottawa, Ontario, Canada
May 2008

Your file Votre référence
ISBN: 978-0-494-48616-0
Our file Notre référence
ISBN: 978-0-494-48616-0

Abstract

ATRX is a SWI/SNF-like chromatin remodeling protein mutated in several X-linked mental retardation syndromes. In addition to severe mental retardation, α-thalassemia and urogenital abnormalities, several vision defects are present in patients, although these have been greatly under reported. Upon closer examination, visual defects were noted in 23% of patients, with optic atrophy, pale disc and refractive errors being the most commonly reported abnormalities. We report here that Atrx is abundantly expressed in the neuroprogenitor pool during retinal differentiation as well as in all cell types of the mature retina with the exception of rod photoreceptors. To further investigate the impact of *ATRX* ablation on vision, we used a conditional gene-targeting approach to generate transgenic mice in which inactivation of *Atrx* occurs under the control of the retina specific element of murine *Pax6*. Our results show that inactivation of *Atrx* results in a ~25-30% reduction in amacrine and horizontal interneurons. The loss of amacrine and horizontal cells resulted from increased cell death in a period which corresponds with a change in Atrx nuclear localization and retinal synaptogenesis in these cell types. Furthermore, our work illustrates that *Atrx* inactivation is associated with attenuated b-wave amplitude as measured by ERG analysis. Based on these findings it seems that ATRXmay play a critical role in the mediation of retinal synaptogenesis and that increased cell loss may contribute to the visual defect observed in ATR-Xpatients.

Acknowledgements

First and foremost I would like to express my sincere gratitude to my supervisor Dr. David Picketts as well as my co-supervisor Dr. Valerie Wallace for giving me this wonderful opportunity. Over the last couple of years, they have given great support, guidance, and encouragement. I must also thank my thesis advisory committee members, Drs. Alan Mears and Stefanny Bennett whose support has been much appreciated.

I would also like to acknowledge all past and present members of the Picketts and Wallace lab: Andrew Ha, Brian McNeil, Chantal Mazerolle, Darren Yip, Dana Wall, Emma Goodall, Marilyne Delorme, Matt Todd, Matt Cwinn, Mike Huh, Maureen Curtin, Steve Rennick, Tina Price-O'Dea and YaPing Wang for making graduate school a pleasant experience. More specifically, I would like to express my gratitude to Darren for helping me getting oriented at the OHRI and for all the countless little things he helped me out with throughout the last two years. In addition I would like to thank Brian for sharing his knowledge and expertise as well as Dana, Andrew and Matt who were always happy to answer my questions at any time of the day. I would also like to thank YaPing and Chantal who were both enormous help to me over the last two years. Without their help and technical expertise I would not have been able to complete this project. Many thanks also go to Adam Baker who was an enormous help in dissecting my ERG data, as well as Dr. Stuart Coupland whose expertise was much appreciated.

Finally I would like to thank my husband Victor for always supporting me no matter what and spending countless evenings and weekend with me at the lab.

Table of Contents

List of Figures

List of Tables

Nonstandard abbreviations

ADD: Atypical PHD domain common to ATRX, DNMT3a and DNMT3b

ADP: Adenosine diphosphate

ATMDS: Alpha-Thalassemia myelodysplasia syndrome

ATP: Adenosine triphosphate

ATRX: Alpha-thalassemia X-linked mental retardation gene

ATR-X: Alpha-thalassemia X-linked mental retardation syndrome

ATRX KO: α-cre;ATRX $^{f/y}$ mouse

BDNF: Brain-derived neurotrophic factor

BFLS: Börjeson–Forssman–Lehman syndrome

bHLH: Basic-helix-loop-helix transcription factor

BPTF: Bromodomain PHD finger transcription factor

BrdU: Bromodeoxyuridine

BRG1: Brahma-related gene 1

ChAT: Choline Acetyltransferase

CHD family: Chromodomain/helicase/DNA binding domain family

CNS: Central nervous system

COFS syndrome: cerebro-oculo-facio-skeletal syndrome

DAB: 3,3'-diaminobenzidine

DAPI: 4',6-diamidino-2-phenylindole

DIG: Digoxigenin

ERG: Electroretinograms

GABA: Gamma-aminobutyric acid

GFP: Green fluorescent protein

Gly: Glycine

GlyT1: Glycine transporter 1

GCL: Ganglion cell layer

H1: Histone 1

H2A: Histone 2a

H2B: Histone 2B

H3: Histone 3

H4: Histone 4

HD: Homeodomain

HDAC: Histone deacetylase

HOX: Homeobox

IHC: Immunohistochemistry

INL: Inner nuclear layer

INBL: Inner nuclear blast layer

IPL: Inner plexiform layer

ISWI: Imitation Switch

MeCP2: MethylCpG-binding protein 2

NURF: Nucleosome remodeling factor

ONBL: Outer nuclear blast layer

ONL: Outer nuclear layer

OPL: Outer plexiform layer

PBS: Phosphate buffered saline

PFA: Paraformaldehyde

PHD: Plant homeo domain

PML: Promyelocytic leukemia protein

PML-NB: Promyelocytic leukemia nuclear bodies

Q-RT PCR: quantitative reverse transcriptase-polymerase chain reaction

RGC: retinal ganglion cells

RNA: Ribonucleic acid

RPE: retinal pigmented epithelium

SNF2: sucrose non-fermenting 2

TH: Tyrosine hydroxylase

XLMR: X-linked mental retardation

1.0 Introduction

1.1 An overview of chromatin

The genetic code of each single eukaryotic cell is contained within DNA molecules that, collectively, span over two meters in length and are compacted within a nucleus to one hundred thousandth times smaller dimensions than the DNA itself. Such a great feat is accomplished by mechanisms which involve a hierarchical scheme of folding with an equal mass of proteins, thereby forming the nucleoprotein complex known as chromatin (1, 2). Since its identification in 1882 by Walther Flemming, chromatin has emerged to be much more than a simple building block for chromosomes and over the last century, much has been learnt about its structure and function.

1.12 Basic Chromatin structure

The expression "beads on a string", was long ago coined to describe the primary repeating subunit of chromatin, the nucleosome. This basic unit consists of the wrapping of 146-147bp of DNA onto histone octamers in ~1.7 helical turns. Long arrays of nucleosomes are then connected by linker DNA of variable length which is bound by histone H1 to facilitate higher order compaction (Figure 1) (3). As the fundamental component of the nucleosome, the four proteins which make up the histone core, histone H2A, H2B, H3 and H4 have been well studied. The histone proteins are relatively small varying from 102-135 amino acids in length and, not surprisingly, represent some of the

most conserved proteins amongst eukaryotes. The histone core itself is comprised of an histone octamer which consists of histone tetramer of H3-H4 flanked by two dimers of the H2A and H2B histones (3-5). The globular structure of the histone core arises from the protein-protein interactions between the different histones. The two H3–H4 pairs interact through a 4-helix bundle formed by H3 dimers to define the H3–H4 tetramer. Each H2A–H2B pair can then interact with the tetramer through a second set of homologous 4-helix bundles between H2B and H4 histone folds (6). The histone fold domains created by these interactions is directly responsible for the wrapping of the DNA around the histone octamer as each histone fold pair can associate with ~30 bp of DNA by binding to the phosphodiester backbone (6).

This linear string of nucleosomes is further condensed to form the structure often referred to as the 30-nm fiber. Formation of this more condensed structure is believed to involve histone H1, which serves to pull the nucleosomes together, as well the histone tails which may help attach one nucleosome to another thereby allowing for their condensation (7). As the 30-nm fiber, the typical human chromosome would still be 0.1 cm in length and span the nucleus more than 100 times. Therefore, a higher order of folding is required. Although the process by which the 30-nm fiber condenses to form the chromosomes is poorly understood, it is known to involve the formation of loops as depicted in Figure 1 (7) .

Albeit a complex structure, the nature of chromatin does not allow it to remain static for very long. During such processes as cell cycle progression and cellular differentiation, the chromatin state must undergo a number of architectural changes,

Figure 1: Schematic diagram illustrating the compaction of DNA into a chromosome structure

146-147bp of double strand DNA wraps around histone octamers in ~1.7 helical turns to form the beads on a string structure. Long arrays of nucleosomes are connected by linker DNA of variable length which is bound by histone H1 to facilitate higher order compaction. The linear string of nucleosomes is further condensed to form the 30-nm chromatin fiber.The chromatin fiber then forms a series of loops in order to condense into the well known chromatin structure. Figure modified from Alberts and al 2002 (7).

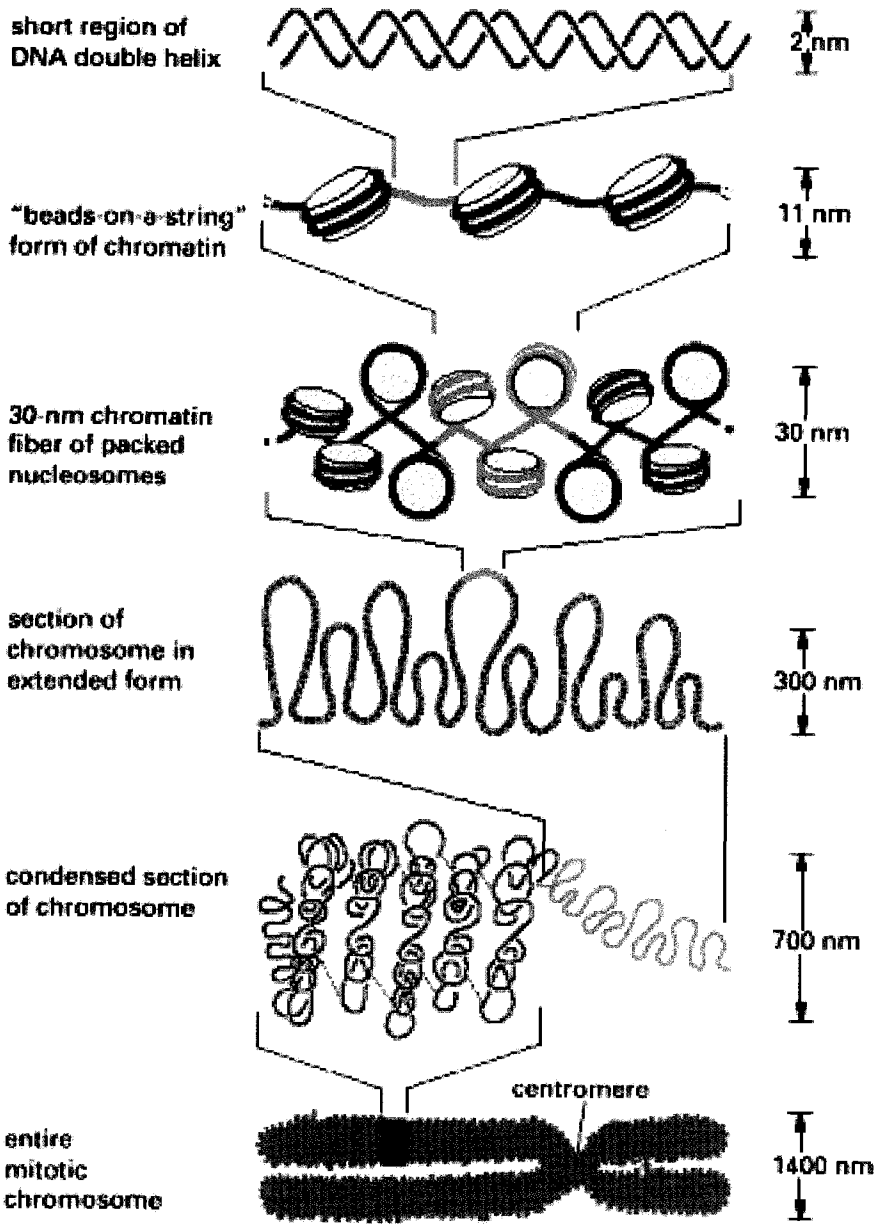

NET RESULT: EACH DNA MOLECULE HAS BEEN PACKAGED INTO A MITOTIC CHROMOSOME THAT IS 10,000-FOLD SHORTER THAN ITS EXTENDED LENGTH

which are often referred to as epigenetic changes, as they can alter the gene expression profile without changing the DNA sequence. These conformational changes in the chromatin structure are modulated by two distinct mechanisms. The first is by covalent modification of histones, while the second involves the direct introduction of conformational changes in chromatin by ATP-dependent chromatin remodeling complexes.

1.2 Covalent histone modifications

While the histone core itself forms a globular structure, the N-terminal tail of histones that flank the core domain are relatively flexible and unstructured. These N-terminal tails which extend out from the face of the nucleosome and through the DNA grooves into the area surrounding the nucleosome, contain a striking number of sites which are susceptible to post-translational modifications (6, 8). To date, eight different types of modifications at 60 distinct residues on the histone tails have been described (9, 10). These post-translational modifications include acetylation, methylation, phosphorylation, ubiquitination, sumoylation, ADP-ribosylation, deimination and proline isomerization and play an important role in regulating basic cellular functions such as transcription, repair, DNA condensation and replication. As summarized in Table 1, the nature, as well as the position of the modified residues is crucial in order to regulate the specificity of these processes.

Histone modifications function by two discrete mechanisms. The first is to disrupt the contacts between histone and DNA or between distinct nucleosomes in order to

Table 1: Overview of the different histone tail modifications
Identified histone modifications and their respective associated function are listed above. Figure modified from Kouzarides, T. 2007. Chromatin modification and their function. *Cell* 128:693-705. (9)

Chromatin Modifications	Residues Modified	Functions Regulated
Acetylation	K-ac	Transcription, Repair, Replication, Condensation
Methylation (lysines)	K-me1 K-me2 K-me3	Transcription, Repair
Methylation (arginines)	R-me1 R-me2a R-me2s	Transcription
Phosphorylation	S-ph T-ph	Transcription, Repair, Condensation
Ubiquitylation	K-ub	Transcription, Repair
Sumoylation	K-su	Transcription
ADP ribosylation	E-ar	Transcription
Deimination	R > Cit	Transcription
Proline isomerization	P-cis > P-trans	Transcription

loosen the chromatin. An example of such a process is the acetylation of lysine residues of histone tails. This modification has long been believed to be one of the key modifications in the unraveling of chromatin, as it can neutralize the basic charge of lysine residues. Most recently this proof of principle was illustrated in an *in vitro* system. In 2006, Shogren-Knaak, M., et al. demonstrated that acetylation of Histone 4 on lysine 16 (H4K16) had a negative effect on the formation of the 30-nanometer fiber and the generation of higher chromatin structure (11).

The second mechanism by which histone modifications operate is by promoting or occluding the recruitment of non-histone proteins. Based on their functional domains, proteins can be recruited to the modified histone sites. For example histone methylation is recognized by the chromo-like domains of the Royal family and some PHD domains (12). Moreover, acetylated histone residues are recognized by bromo domains while phosphorylation is recognized by 14-3-3 family members (9). Proteins that are recruited by their structural domains can subsequently recruit enzymes which can further modify the histone tails. A good example of such a phenomenon is the methylation of H3K27 which is bound by the chromodomain of the polycomb protein PC2, thereby promoting the recruitment of additional interacting proteins including one associated with ubiquitin ligase activity specific for histone H2A (13, 14). Proteins recruited to modified histone residues can also serve as an anchor to recruit larger protein complexes. Case in point is the recruitment of BPTF, a component of the NURF remodeling complex, via its PHD domain that interacts with H3K4 trimethylation sites (15). Large complexes such as the

NURF complex can serve to further modify the chromatin structure through ATP-dependent chromatin remodeling mechanisms.

1.3 ATP-dependent chromatin remodeling proteins

While the affinity of the DNA for the histones is primarily modulated by the post-translational modification of histones tails, it is the role of ATP-dependent chromatin remodeling complexes to non-covalently reposition histones along the chromatin to generate nucleosome free or dense regions consequently modulating the access to DNA (16). In addition, recent studies have shown that ATP-dependent remodellers can also remove or exchange histone dimers between nucleosomes in order to further regulate chromatin structure and subsequently gene expression (17, 18).

All chromatin remodeling complexes identified to date contain a core sucrose non-fermenting 2 (SNF2) related ATP hydrolyzing region, which shares considerable sequence homology with the large helicase superfamily 2 (SF2) and includes known DNA and RNA helicases such as DNA translocase and the bacterial helicase RecG (19, 20). The diverse nature of the core ATP hydrolyzing regions of these chromatin remodeling complexes has led to their classification based on similarities extending beyond their helicase domain. Such classification resulted in the identification of seven subfamilies, the three most prominent being the SNF2, CHD and ISWI (21). A summary of the most characterized human ATPase-dependent chromatin-remodeling complexes and their respective cellular functions are listed in Table 2

Table 2: Identified human ATP-dependent chromatin-remodeling complexes and their respective cellular functions

Human ATP dependent chromatin complexes are listed above based on the subfamily of their core ATP hydrolyzing region. If known, the respective function of each complex is also listed. Only the most common subfamilies are listed above. Reviewers are refered to Havas, K. and al for information on the other subfamilies which include ATRX (12). Figure modified from Wang,G et al 2007 (22).

Family and complexes	Remodeling-complex subunits	Complex functions
SWI/SNF family		
BAF	BRM or BRG1, SNF5/INI1, BAF155, BAF170, BAF250, BAF53, β-actin, BAF60a, BAF57	Tumor suppressor, cell-cycle progression, DNA replication, development, differentiation, elongation, signaling, splicing, DNA-damage repair
PBAF	BRG1, SNF5/INI1, BAF155, BAF170, BAF180, BAF53, β-actin, BAF60a	
BRM	BRM, SNF5/INI1, BAF155, BAF170, BAF250, BAF53, BAF60a	
BRG1-complex I	BRG1, SNF5/INI1, BAF155, BAF170, BAF250, BAF53, BAF60a	
BRG1-complex II	BRG1, SNF5/INI1, BAF155, BAF170, BAF250, BAF53	
EBAFa	BRG1, SNF5/INI1, BAF155, BAF170, BAF250a, BAF53, β-actin, BAF60a, ENL, EBAF70, EBAF100, EBAF140	
EBAFb	BRG1, SNF5/INI1, BAF155, BAF170, BAF250b, BAF53, β-actin, BAF60b, ENL, EBAF70, EBAF100, EBAF140	
ISWI family		
ACF/WCRF	SNF2H, WCRF180/ACF1	X-chromosome regulation, cohesion, embryonic development and differentiation, transcriptional activation and repression, DNA replication, DNA repair response
CHRAC	SNF2H, ACF1, CHRAC17, CHRAC15	
RSF	SNF2H, p325	
WICH	SNF2H, WSTF	
SNF2H/Cohesin	SNF2H, Mi-2, Rad21, HDAC1, HDAC2, MTA1, MTA2, SA1/SA2, RbAp46, RbAp48, MBD2, MBD3, SMC1, SMC3	
NURF	SNF2L, BPTF, RbAp46, RbAp48	
NURD/Mi-2/CHD family		
NuRD/Mi-2/CHD	Mi2-α/CHD3 or Mi2-β/CHD4 or CHD1–2 or CHD5, HDAC1, HDAC2, RbAp46, RbAp48, MTA1 or MTA2 or MTA3, MBD2 or MBD3	Tumor suppressor, transcriptional repression and silencing, transcriptional activation, pluripotency of embryonic stem cell
INO80 family		
INO80	hINO80, Tip49a, Tip49b, BAF53a, Arp5, Arp8, hles2, hles6, Amida, NFRKB, MCRS1, FLJ90652, FLJ20309	
TRRAP/Tip60	P400, Tip49a, Tip49b, BAF53a, actin, GAS41, DMAP1, YL-1, Brd8, TRRAP, Tip60, MRG15, MRGX, FLJ11730, MRGBP, EPC1, ING3	
SRCAP	SRCAP, Tip49a, Tip49b, BAF53a, Arp6, GAS41, DAMP1, YL-1, ZnF-HIT1	

Abbreviations: ACF, ATP-utilizing chromatin-assembly and remodeling factor; BAF, BRG1-associated factor; CHRAC, chromatin-accessibility factor; EBAF, partner of MLL in mixed-lineage leukemia)-associated BAF-containing complex; ENL, eleven-nineteen leukemia gene; MBD, methyl-CpG-binding domain p polybromo and BRG1-associated factor; RSF, remodeling and spacing factor; SA1, stromal antigen 1; SMC1, structural maintenance of chromosomes 1A; WICI chromatin remodeling; WSTF, Williams syndrome transcription factor.

1.3.1 The SWI2/SNF 2 family

The distinctive element of the SWI2/SNF2 family is the presence of a C-terminal bromodomain (12, 21). SWI/SNF chromatin remodeling complexes are capable of sliding histone octamers as well as distorting the path of DNA within the nucleosome without nucleosome relocation (23, 24). These complexes have been implicated in a variety of cellular processes. To this effect, the SWI/SNF complex in yeast has been shown to be involved in the cell cycle dependent transcriptional activation and repression of gene expression (25). Furthermore, in *Drosophila,* the Swi2/Snf2 protein Brm has been shown to be required for RNA polymerase II association with chromatin, implicating that Brm is required for transcription (26, 27). In humans, the SNF2 family member BRG1 has been shown to collaborate with Rb in the regulation of E2F1, as well as in the regulation of cell cycle progression (28, 29). Recent studies have further highlighted the importance of BRG/BRM SNF2 ATPases in the mediation of cell cycle exit and p53 mediated apoptosis (30). In addition to their important role in the mediation of cell cycle control, SWI/SNF complexes have also been shown to associate with C/EBP beta and the heat shock protein *hsp* 70, as well as being important regulators of steroid hormone receptors in humans (31-33).

1.3.2 The chromodomain/helicase/DNA binding domain family

The chromodomain/helicase/DNA binding domain (CHD) family of chromatin remodelers was first described in the early 1990's and now encompasses nine family members (CHD 1-9) which can be found in a broad range of eukaryotic organisms

including mice and humans (34, 35). The CHD family is characterized by the presence of three fundamental structural domains: an N-terminal chromodomain, an ATPase/helicase domain, which bears resemblance with the SWI2/SNF2 ATPase, and a C-terminal DNA binding region which shows preferential binding to A-T rich regions. In addition to the three main functional domains, CHD family members also contain a PHD zinc finger domain and/or a SANT domain (35).

Like other chromatin remodeling proteins, the CHD family plays both an active and repressive role in the regulation of gene expression. For example, CHD1 and CHD2 are thought to be involved in the activation of transcription and elongation. In support of this, work in yeast have shown that CHD1 can associate with both Paf1 and Rdf1 which are known regulators of polymerase II and transcription elongation respectively (36). Moreover, using the yeast two-hybrid system it was shown that CHD1 can interact with both the transcriptional repressor NCor and the histone modifying enzyme HDAC1 (37). In addition to HDAC, the CHD family of proteins was also shown to associate with large protein complexes such as NURD. Within such complexes, the CHD proteins regulate the expression of the developmentally important HOX genes in *Drosophila* and the DNA repair protein ATR in humans, thus highlighting the biological relevance of these proteins (12, 38, 39).

1.3.3 Imitation Switch (ISWI) family

First identified in *Drosophila*, the Imitation Switch (ISWI) family is comprised of two homologs ISW1 and ISW2 in yeast and SNF2L and SNF2H in mammals. These

proteins are characterized by the presence of an ATPase domain homologous to the one found in *Drosophila* as well as a SANT domain (12, 40). The redundancy of ISWI in yeast and mammals has made it a difficult task to study the function of these proteins. Nevertheless, the ISWI family seems to play a crucial role in development, as disturbance of the ISWI gene in *Drosophila* resulted in late larval or early pupal lethality possibly due to aberrant chromosome structure (41, 42). In the case of mammalian ISWI homologs, loss of SNF2H in mice results in early embryonic lethality at the peri-implantation stage (43). While recent work in our laboratory has shown that loss of the other mammalian ISWI homolog, SNF2L, does not affect viability, these mouse mutants exhibit abnormal cell number suggesting that the protein is important in the regulation of cell cycle exit and differentiation (DJP, unpublished data). In support of the hypothesis that SNF2L regulates CNS development, SNF2L has been found within the human nucleosome-remodeling factor (NURF) complex which regulates the homeodomain protein Engrailed a critical mediator of neuronal development of the mid-hindbrain (44). In addition to playing a critical role in CNS development and maturation, ISWI proteins have also been implicated in the maintenance of chromatin structure during DNA replication via their interaction with the William's syndrome transcription factor (45, 46).

Chromatin remodeling proteins play important and diverse biological functions. It therefore comes as no surprise that mutation which leads to altered function of histone modifiers or ATP dependent chromatin remodeling complexes, has a severe impact on development and are the cause of numerous human diseases.

1.4 Chromatin remodeling and disease

In recent years, the identification of many disease causing genes have revealed the importance of chromatin structure both in the development and the pathogenesis of human diseases. Indeed, both histone modifying enzymes and ATP-dependent nucleosome remodeling complexes have been implicated in human diseases such as cancer, immune disorders, autism and a broad spectrum of mental retardation disorders.

1.4.1 Relationship between chromatin structure and cancer

Covalent histone modifications are a central process in the regulation of gene expression. Therefore, it seems inevitable that alterations in this process are associated with human diseases such as cancer. Proof in principle, the global loss of H4K16 acetylation and H4K20 trimethylation have been linked to breast and liver cancer respectively (47-49). Moreover, a chromosome translocation which implicates the histone acetylases MOZ and MORF is a common feature of acute myeloid leukemia, myelodysplastic syndromes and uterine leiomyomata (50). Translocations of MOZ and MORF that result in the production of fusion proteins such as the CREB binding protein (CBP)-MOZ and CBP-MORF result in aberrant histone acetylation and abnormal gene expression (50). Data obtained from transgenic animals also supports the role of covalent histone modifications in cancer development. Transgenic mice which lack Suv39h, a methyltransferase important for H3K9 methylation, are prone to B-cell lymphoma and the development of other cancers (51). Further emphasizing the biological importance of

the preservation of chromatin structure, genetic screens have identified mutations in proteins involved in ATP-dependent remodeling complexes in human cancers and diseases (52). Case in point, mutations in three different SWI/SNF ATPases: BRM, BRG1 and SMARCB1 have been identified in tumor cell lines (53). In addition, inactivating mutations in the SWI/SNF ATPase SNF5 has been associated with the production of rhabdoid tumors (54-56). These tumors, which arise primarily in the kidney and the brain, are an extremely aggressive and lethal example of inherited childhood cancer (57, 58).

1.4.2 Role of chromatin modifying complexes in inherited human diseases

In addition to cancer development, aberrant modification of histones has also been linked to inherited human diseases such as Rubinstein-Taybi syndrome, a congenital malformation syndrome characterized by mental retardation, short stature and facial abnormalities (59). The disease is the result of mutations in the CREB binding protein, a histone acetyltransferase (52, 60). Rett syndrome is another example of human disease caused by abnormal modification of chromatin. Mutations in the *MECP2* gene, which encodes a methyl-CpG-binding protein, have been found as the underlying cause of Rett syndrome and have also been linked to autism (61). It is believed that MeCP2 serves as an anchor for histone deacetylase activity thereby inducing transcriptional silencing (62). Consistent with this hypothesis, histone H4 was found to be hyperacetylated in Rett syndrome patients (63).

Histone modifications such as acetylation are reversible. Therefore, pharmacological intervention for the treatments of disorders such as Rubinstein-Taybi

syndrome is an intense area of investigation. To this effect, histone deacetylase inhibitors such as sodium butyrate and Trichostatin A, have already been tested using an *in* vitro system and a mouse model of Rubinstein-Taybi syndrome both with positive outcomes (60, 64). As histone deacetylase inhibitors have already been used in clinical trials against acute promyelocytic leukemia with an optimistic clinical outlook, in the future, these drugs might provide some therapeutic benefit for Rubinstein-Taybi syndrome patients (65).

ATP dependent chromatin remodeling complexes have also been linked to inherited diseases. Examples of this include COFS (cerebro-oculo-facio-skeletal) and Cockayne syndrome, which are both caused by mutations in the excision repair cross-complementing rodent repair deficiency, complementation group 6 (ERCC6) protein, a SWI/SNF related ATPase. COFS and Cockayne syndrome are characterized by neurological degeneration and dysmorphic features, as well as UV sensitivity in the case of Cockayne syndrome. This phenotype is believed to arise from the impaired function of ERCC6 in transcription-coupled DNA repair (52, 66). Mutations in another SWI/SNF related ATPase, SMARCAL1, have also been linked to Schimke immuno-osseous dysplasia. However, the link between the T-cell immunodeficiency and bone marrow failure observed in these patients and SMARCAL1 function remains to be elucidated (67).

Aberrant chromatin remodeling activity has also been linked to a broad spectrum of mental retardation syndromes which embraces a wide range of developmental defects. Of these, the previously mentioned Rubinstein-Taybi and Rett syndrome are good examples.

1.4.3 X-linked mental retardation

Mental retardation is one of the most common human disorders affecting 2–3% of the population. Mental retardation is defined by the American Association on Mental Retardation as a disability characterized by an IQ <70 and significant limitations both in intellectual functioning and in adaptive behavior as expressed in conceptual and social skills (68).

The X chromosome is an area particularly rich in mutations causing mental retardation, which can partly explain the increased prevalence of this disease in males and is often referred to as X-linked mental retardation (XLMR) (69). To date, more MR causing mutations have been identified on the X-chromosome than on any other chromosome, although this is postulated to be due in part to the hemizygous state of these genes in males which allows for disease manifestation, and easier target gene identification (68). Of the numerous mental retardation genes identified on the X chromosome, a number of them have been postulated to be epigenetic regulators. Probably the most characterized of these XLMR related genes is the *FMR1* gene. When mutated, the *FMR1* gene gives rise to Fragile X syndrome, a disorder that accounts for approximately 20 % of all diagnosed cases of XLMR (70). Altered histone methylation and acetylation pattern at the FMR1 locus in patients have been reported and suggest a role for epigenetics in the pathogenesis of this disease (69).

BFLS syndrome, which is caused by mutations in the plant homeodomain (PHD)-like finger *(PHF6)* gene located at Xq26.2, and JARID1C-related XLMR which arises due to mutations in the histone H3K4 demethylase *SMCX/JARID1C*, are both additional examples of epigenetic regulators involved in mental retardation disorders (71-73). Other

less characterized genes which also give rise to XLMR include the *PHF8* gene, which is associated with the presence of cleft lip/cleft palate in addition to mental retardation (74).

One of the most studied forms of XLMR caused by mutations within an ATP dependent chromatin remodeling protein, is the alpha-thalassemia X-linked mental retardation syndrome (ATR-X). This disease and a number of other inherited mental retardation disorders such as Juberg–Marsidi syndrome, Carpenter–Waziri syndrome, Sutherland–Haan syndrome and Smith–Fineman–Myers syndrome have been linked to mutations within the *ATRX* gene, which lies at Xq13.3 (75, 76).

1.5 X-linked alpha thalassemia mental retardation (ATR-X) syndrome

ATR-X syndrome (ATR-X, MIM# 300032) is a rare disease with a prevalence believed to be less than 1-9/1,000,000 in the general population. To date, approximately 200 cases have been positively identified (77). As *ATRX* is encoded within the X-chromosome, the disease affects almost exclusively males, as female carriers show preferential inactivation of the mutated X chromosome and are generally unaffected. One incidence of ATR-X syndrome in a female patient has recently been reported althought in this case, skewed X-inactivation which lead to ATR-X syndrome was attributed to *in* vitro fertilization (78). ATR-X syndrome is characterized by severe mental retardation and global developmental delay. Alpha-thalassemia and skeletal abnormalities are present in 90% of patients, while microencephaly and some degree of genital abnormalities have been described in over 75% of the cases (77). Short stature, seizures, cardiac defects, as well as renal and urological abnormalities, have also been described in a small percentage

of ATR-X patients. However, it is the distinctive facial traits of these patients that are the most readily recognized. As shown in Figure 2, ATR-X patients display facial dysmorphia characterized by epicanthic folds, mid-face hypoplasia, a flat nasal bridge and a small triangular upturned nose, as well as a tented upper lip, a full everted lower lip and a protruding tongue. In addition to the classical presentation which includes severe mental retardation and facial dysmorphia, it is postulated that ATR-X patients also suffer from subtle sensory defects, such as visual system abnormalities. To date, a few clinical reviews have briefly stated the presence of visual problems in ATRX patients albeit little follow up of these original diagnosis has been reported (77, 79). As vision deficiency would only mildly impact overall quality of life of these patients, it is therefore very likely that such defects are often overlooked and therefore underreported.

1.6 Aetiology of the ATR-X syndrome

As previously stated, mutations within the *ATRX* gene, which lies at Xq13.3, have been identified as the underlying cause of several inherited mental retardation disorders including the ATR-X syndrome. The *ATRX* gene spans 36 exons and 300kb of genomic DNA. It encodes for two alternatively spliced transcripts which generate a full length 280 kD protein and a shorter 180 kD isoform that contains the first 11 exons (Figure 3) (80). Although the exact function of ATRX remains unclear, some information may be gained by comparing its homology to proteins whose function is already known. To this effect, the full length ATRX protein contains an ADD domain (an atypical PHD domain common to ATRX, DNMT3a and DNMT3b) and a C-terminal SNF2 ATPase/helicase

Figure 2: Child presenting with facial features characteristic of ATR-X syndrome patients

Eight years old ATR-X patient presenting with the characteristic facial features of ATR-X syndrome. Note the upswept frontal hair line, hypertelorism, epicanthic folds, flat nasal bridge, small triangular upturned nose, tented upper lip, everted lower lip and hypotonic facies. Figure modified from Gibbons, RJ, 2006 (77).

domain that shares considerable homology with the yeast protein RAD54 (81). Mutations linked with ATR-X syndrome are mostly single base pair missense mutations, 25% of which are located within the ATPase/helicase domain while another 60% can be found in the PHD zinc finger motif, thus highlighting the importance of these two highly conserved functional domains. Moreover, mutations within either domain give rise to similar clinical manifestations, thereby suggesting that these mutations result in a loss of function. Although a genotype/phenotype correlation has yet to be identified, it appears that some level of full length protein is required for survival, as low levels of the full length protein can be detected by Western blots in patients (82, 83).

1.7 ATRX function and localization

The homology of ATRX with other chromatin remodeling proteins, as well as the relationship between mutations in the *ATRX* gene and inherited and acquired alpha-thalassemia suggests that it may play a role in gene regulation via chromatin-based epigenetic mechanisms, although this premise remains to be confirmed (75, 84). Protein studies have revealed that the protein is abundantly expressed in the nucleus in a punctate speckled pattern. In human cells, the full length protein was found to interact with Daxx, a transcriptional co-activator and regulator of apoptosis, as well as a component of the promyelocytic leukemia protein (PML) nuclear bodies (85, 86). This ATRX-Daxx complex was found to mediate ATPase and chromatin remodeling activities *in* vitro on reconstituted nucleosomes supporting the idea that this is a chromatin remodeling

Figure 3: Schematic of the *ATRX* gene and the resulting protein products
A) Diagram of the *ATRX* gene. The whit boxes represent the 35 exons (excluding the spliced exon 7), while the thin vertical lines represent introns (not to scale). The 3'and 5' untranslated region (UTR) are shown flanking the open reading frame. In the upper part of the diagram, previously identified ATR-X causing mutations are identified while acquired somatic mutations in *ATRX* that causes alpha thalassemia myelodysplastic syndrome (ATMDS) are identified below. *ATRX* encodes two protein products ATRX (280 kDa) and ATRXt (180 kDa) which are illustrated in (B). The full length protein contains an ADD domain, a C-terminal SNF2 helicase domain as well as a P box (P) and a glutamine-rich region (Q). The truncated 180 kDa isoform only contains the ADD domain. Figure modified from Gibbons, RJ, 2008 (87).

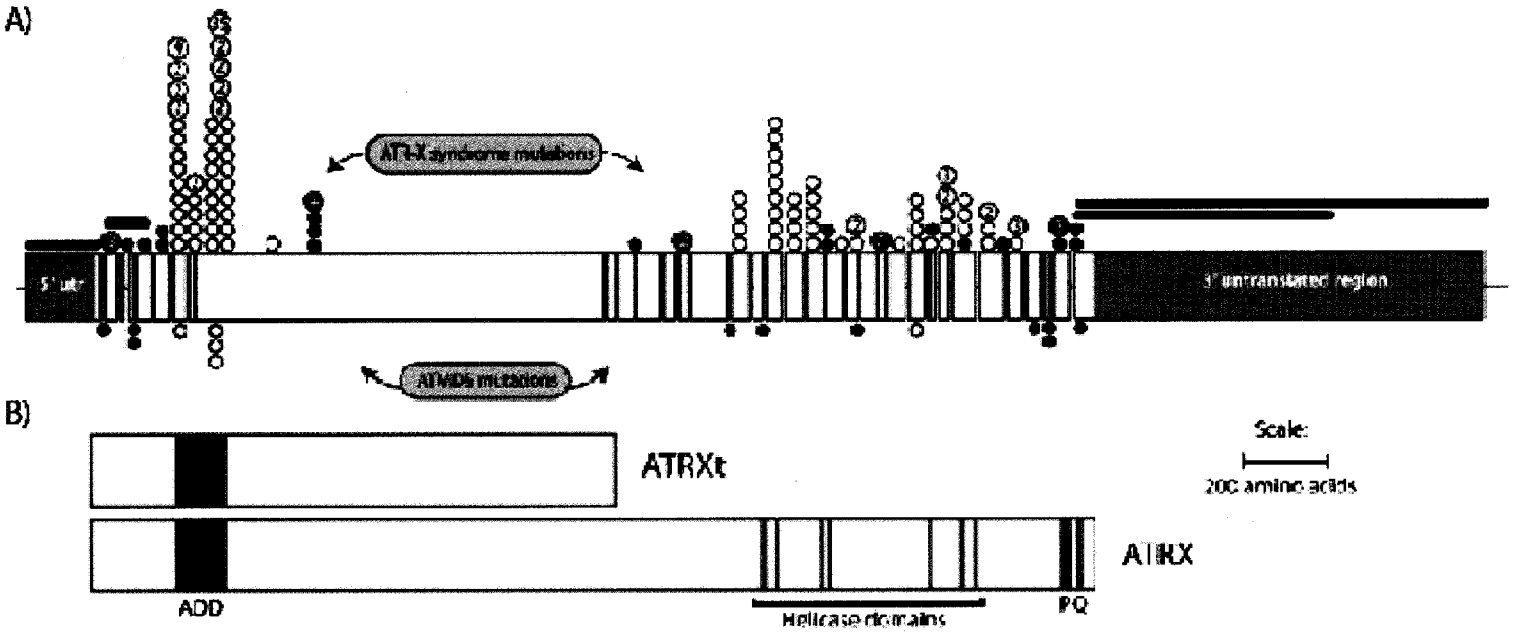
A)
ATR-X syndrome mutations
5' untranslated region
ATRXt mutations
B)
ATRXt
Scale:
200 amino acids
ATRX
ADD
Helicase domains
PQ

complex. Patient mutations, located within the ATPase/helicase domain, were found to attenuate this activity as well as alter subnuclear localization of ATRX away from PML-NBs, supporting the hypothesis that patient mutations give rise to functional hypomorphs (88, 89).

In addition to its localization to PML-NBs, both ATRX isoforms were found in mouse cells and to a lesser extent in human cells, to localize with pericentromeric heterochromatin. It is postulated that this association is mediated by the polycomb group protein enhancer of zeste 2 (EZH2) or heterochromatin protein 1 α (HP1 α), as both these proteins were shown to physically interact with ATRX (90, 91). The physical interaction between HP1 α and the N-terminal PHD domain of ATRX at heterochromatin has been further validated in mammalian cells (92, 93). Recent studies have further demonstrated that at least in mouse cells, recruitment of ATRX at heterochromatic foci also requires the interaction of MeCP2, a protein involved in the pathogenesis of another form of X-linked mental retardation, namely Rett syndrome (62, 94). This study illustrated that common Rett syndrome mutations R133C and A140V in the *MeCP2* gene impair ATRX recruitment at pericentromeric heterochromatin. Thus, it seems that at least in brain, the interaction between these proteins is crucial for appropriate ATRX localization (94).

In addition to PML and pericentromeric heterochromatin, ATRX was also found to associate at metaphase with the short arm of human acrocentric chromosomes, a region rich in ribosomal DNA repeats (92). The association of ATRX with these highly repetitive DNA repeats may offer a potential explanation as to the clinical variability between patients with identical mutations. Furthermore, ATR-X patients were found to have altered methylation patterns at these rDNA repeats, as well as at Y-specific repeats

(DYZ2) and the TelBam3.4 family of repeats, suggesting, ATRX may play a role in the modulation of chromatin structure by altering DNA methylation patterns at these repeats.

1.8 Role of ATRX in cell cycle regulation

A role for ATRX in cell cycle progression has been suggested by several lines of investigation. Changes in ATRX phosphorylation at the onset of meiosis I and II have been reported in mouse oocytes. In this regard, ablation of ATRX by RNAi had no effect on the progression of meiosis but did induce the misalignment of chromosomes at meiosis II (95). Furthermore, cell cycle dependent changes in the ATRX phosphorylation and nuclear localization have also been reported. In human cells, ATRX serine residues were found to be hyperphosphorylated at the onset of mitosis while the protein remained hypophosphorylated during interphase. Phosphorylation of ATRX was also associated with a change in subnuclear localization from the nuclear matrix to heterochromatin (93). Further emphasizing the importance of ATRX in cell cycle progression, ATRX was found to be required *in vitro* for the maintenance of a normal mitotic program (96). Upon ATRX knockdown, an increase in prometaphase to metaphase transition was observed in cultured HeLa cells (96). In addition, this study illustrated that upon ATRX ablation cells exhibited a deficiency in sister chromatid cohesion and congression at the metaphase plates albeit normal spindle checkpoint activation as determined by the expression of spindle checkpoint protein Bub1 and BubR1 (96). Yet other studies suggest ATRX has a role during S-phase, as it localizes with heterochromatin, Daxx and PML at this time (86). Taken together these results suggest that ATRX not only plays a role in the

mediation of chromatin structure but also in chromatin dynamics and cohesion. The biological complexity of these processes may help explain why mutations within the *ATRX* gene can lead to developmental abnormalities in humans. To gain a better understanding of the developmental role of ATRX, one can benefit from the use of animal models. This approach provides valuable insight as to protein function within a biologically relevant context.

1.9 ATR-X animal models

Transgenic mouse models offer an important tool in the understanding of disease pathogenesis. While recent *in vitro* reports have described a role for ATRX in the maintenance of chromatin structure and cell cycle progression, transgenic animal models have illustrated the early requirement for Atrx during embryogenesis and CNS development. During mouse development, Atrx expression is detected at E7.0 which suggests that the protein plays an important developmental role (81). This notion is further supported by the early embryonic lethality of mice lacking the full length protein (97). Global deletion of the full length *Atrx* isoform in mice resulted in embryonic lethality before E9.5 due to the abnormal differentiation of one of the first terminally differentiated lineages, the extraembryonic trophoblast (97). Embryonic lethality in mice was surprising as ATR-X patients live well into their 30's and 40's (77). This discrepancy was attributed to the complete ablation of the full length protein in mice, while some residual level (10-30%) of full length protein has been detected in all characterized ATR-X human pedigrees (75, 97).

As ATRX dosage appears to be crucial for normal development, insights into the biological function of ATRX may also be gained from overexpression studies. Transgenic mice which overexpressed the human Atrx protein were generated to further study the role of this protein during development (98). The resulting animals exhibited a range of neurodevelopmental abnormalities, including abnormal growth and organization of the neuroepithelial layer as well as disorganization of the ventricular zone. Furthermore these mice suffered from a high incidence of prenatal and perinatal lethality. The surviving transgenic animals exhibited craniofacial defects, epileptic seizures and compulsive behaviors which were reminiscent of the abnormalities observed in ATR-X patients (98).

A further understanding of the role of ATRX during neurodevelopment was brought about by recent advances in molecular biology. Over the last decade, the evolution of the Cre-loxP recombination system has revolutionized the way transgenic animal models are made. This technique allows for the generation of transgenic animals in which a gene of interest can be temporally and spatially deleted due to the use of specific Cre drivers and the insertion of targeted *loxP* sites. Thus, this method allows for tissue or organ specific ablation (99). Using this approach, conditional Atrx knockout mice were generated. In this instance, Cre recombinase expression was controlled by the *Forkhead box G1* and *Nestin* promoters, consequently confining Cre recombinase expression and full length Atrx ablation to either the forebrain or CNS neuroprogenitors, respectively (100). These animals were smaller in size and exhibited early post-natal lethality. Closer examination of these animals revealed widespread hypocellularity in the forebrain, cortex and hippocampus, albeit with normal proliferation of neuroprogenitors.

The observed reduction in cell number was attributed to an increase in neuronal apoptosis during early differentiation (100).

Based on the lessons learned both from *in vitro* models and transgenic animals, it is clear that ATRX plays a critical role in central nervous system (CNS) development, although its mode of action remains to be determined. An interesting system which may help provide insight as to the exact requirements of ATRX in CNS maturation is the retina, one of the best characterized CNS tissues.

1.10 The retina as a model of central nervous system development

1.10.1 Embryonic mouse eye development

Eye formation occurs early during vertebrate development at about 22 days post-fertilization in humans and 7 days following fertilization in mice (101). Three types of embryonic tissue will come together to form the structures of the mature eye: the retinal and pigmented epithelium will arise from the neural tube, the mesoderm of the head region will produce the components of the cornea, sclera and uvea, and the surface ectoderm will give rise to the corneal epithelium and the lens (102).

Eye development begins with the formation of the eye fields from a population of cells originating from the anterior neural plate in the presumptive forebrain (102). As depicted in Figure 4, the eye fields begin to invaginate on either side of the forebrain to form the optic vesicles and optic pits (101). The optic vesicles expand laterally into the mesoderm of the head and develop a stalk-like connection to the main portion of the

rudimentary central nervous system which will eventually give rise to the optic nerve (102). As the optic vesicles gradually expand towards the surface ectoderm, contact between the neural ectoderm of the optic vesicle and the surface ectoderm will occur by E9 to E10. Contact between the surface ectoderm and the optic vesicles will induce the thickening of the two layers in contact (103). The neuroectodermal thickening is destined to become the neuroretina, while the thickening of the surface ectoderm will induce the formation of the lens placode (103). Once the formation of the lens placode has begun, formation of a cup-shaped structure is initiated by the simultaneous invagination of the lens placode and the optic vesicle. The invaginating lens placode forms the lens vesicle that pinches off the surface ectoderm while invagination of the optic vesicle, which remains connected to the forebrain via the optic stalk, forms the bilayered optic cup. The inner half of the optic cup will form the neuroretina while the outer half is destined to become the retinal pigmented epithelium (RPE) (102). At E11, the optic stalk which connects the vesicle to the neural tube remains open and thus allows for the inclusion of a small amount of angiogenic tissue from the mesenchyme which will form the hyaloid artery and vein and, later on the central artery of the retina (103). By E13, folds in the surface ectoderm will initiate lid formation and the cornea begins to differentiate (103). The iris and cilliary body originate from the distal tip of the neuroretina where the pigmented epithelium and neuroretina meet and develop late in embryonic development and continue to mature in the postnatal period (102).

Figure 4: Schematic overview of vertebrate eye development.
In panels *A–D*, presumptive or differentiated eye tissues are color-coded in the following manner: *blue*, lens/cornea; *green*, neural retina; *yellow*, retinal pigmented epithelium (RPE); *purple*, optic stalk. (*A*) Formation of the optic vesicle is initiated by an evagination (*indicated by arrow*) of the presumptive forebrain region resulting in the formation of the optic pit (OP). The optic vesicle region is divided into dorso-distal region (*green*), which contains the presumptive neural retina (PNR) and RPE (not shown), and the proximo-ventral region, which gives rise to the presumptive ventral optic stalk (POS); PLE, presumptive lens ectoderm; M, mesenchyme; VF, ventral forebrain; PCM, prechordal mesoderm. (*B*) Continued growth of the optic vesicle culminates with a period of close contact between the lens placode (LP) and the presumptive neural retina (NR) during which important inductive signals likely exchange: RPE, presumptive retinal pigmented epithelium; VOS, ventral optic stalk; DOS, dorsal optic stalk. (*C*) Invagination of the optic vesicle results in formation of the lens vesicle (LV) and neural retina (NR) and establishes the overall structure of the eye. The point at which the neural retina and RPE meet gives rise to components of the ciliary body and iris (C/I). (*D*) Mature eye: C, cornea; LE, lens epithelium; LF, lens fiber cells; I, iris; CB, ciliary body; GCL, ganglion cell layer; INL, inner nuclear layer; ONL, outer nuclear layer; ON, optic nerve. Figure modified from Chow R,L. et al 2001 (102).

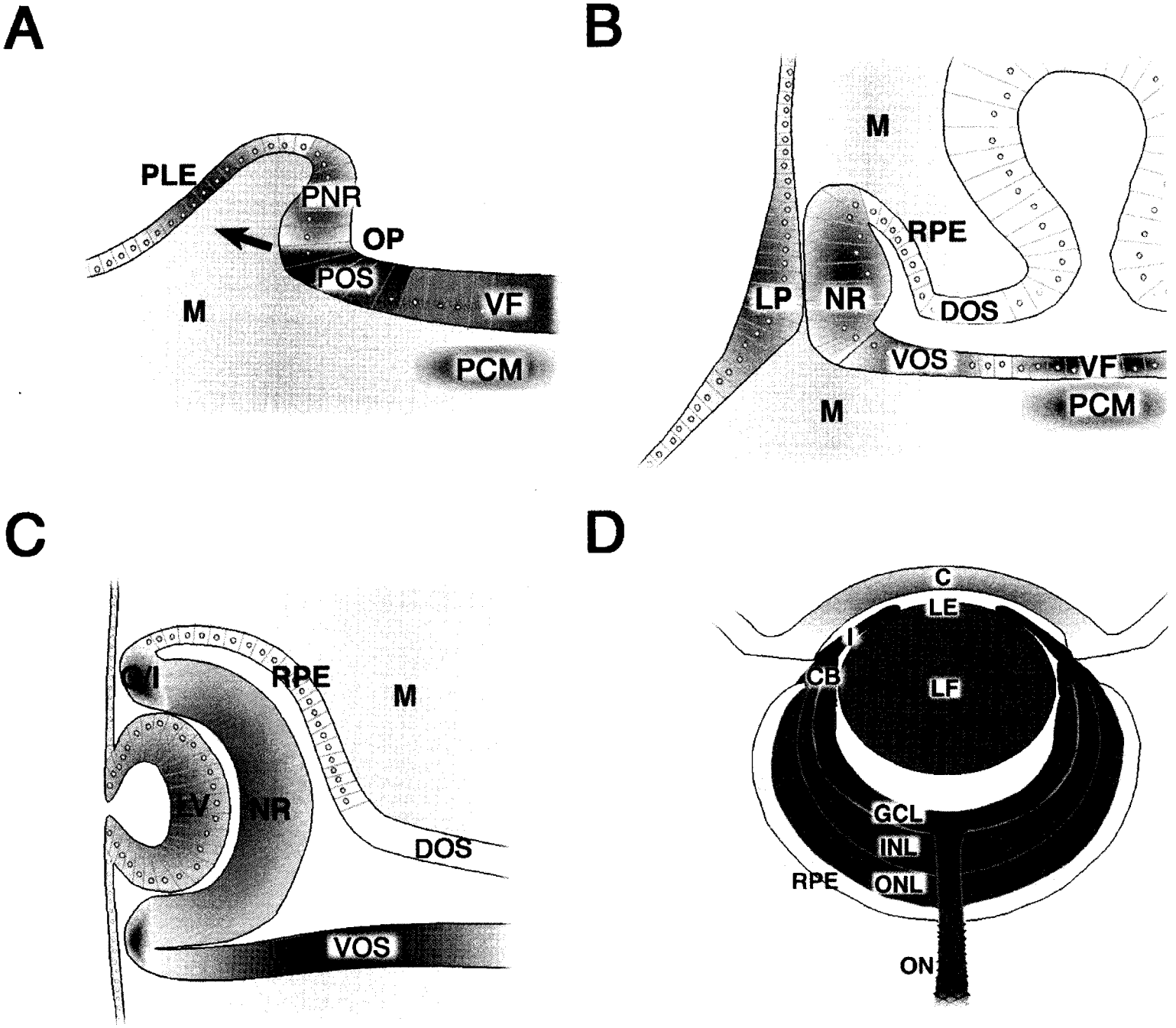
A
PLE
PNR
OP
POS
VF
M
PCM
B
M
RPE
LP
NR
DOS
VOS
VF
M
PCM
C
RPE
M
NR
DOS
VOS
D
C
LE
I
CB
LF
GCL
INL
RPE
ONL
ON

1.10.2 The neuroretina

The neuroretina is the part of the eye which is responsible for the processing and transmission of light-induced neuronal activity to the brain. Its accessibility and the well understood nature of its cellular makeup also make the retina an ideal system to investigate CNS development. The onset of differentiation in the retina occurs in the central optic cup close to the optic nerve head and progresses towards the periphery in a wave like fashion, until the mature retina, which consists of six types of neurons and one type of glia is formed (104). In vertebrates, this process occurs in a highly conserved histogenic order. More specifically, as depicted in Figure 5a, during murine development, the process occurs during a period of three weeks starting around E11. All of the seven retinal cell types arise from a common progenitor pool with ganglion cells being the first generated cell type (105). The production of ganglion cells is followed by overlapping phases of cell type generation with horizontal cells and cone photoreceptors being first generated, followed by amacrine, rod photoreceptors, bipolar cells and Müller glia (101).

The mechanism by which each of these cell fates are acquired in adequate numbers from multipotent progenitors is quite complex and involves combinational expression of a number of homeodomain and basic-helix-loop-helix (bHLH) transcription factors (106). In addition, cell extrinsic cues such as those mediated by growth factors, morphogens and Notch signaling can control the timing of cell cycle exit, proliferation

Figure 5: Birth order of retinal cell types in the rodent and wiring diagram of the adult retina.

A) Horizontal bars represent the window during which that cell type is generated in the developing retina with respect to days of mouse development (bottom bar). B) Schematic diagram illustrating the major cell types and how they are interconnected. The outer layer contains the rod (R) and cone (C) photoreceptors, which make connections to the horizontal (H) and bipolar cells (RB and CB) in the outer plexiform layer (OPL). Also located in the inner nuclear layer are the amacrine cells (A and AII) which like bipolar cells make connections in the inner plexiform layer with ganglion cells (G).

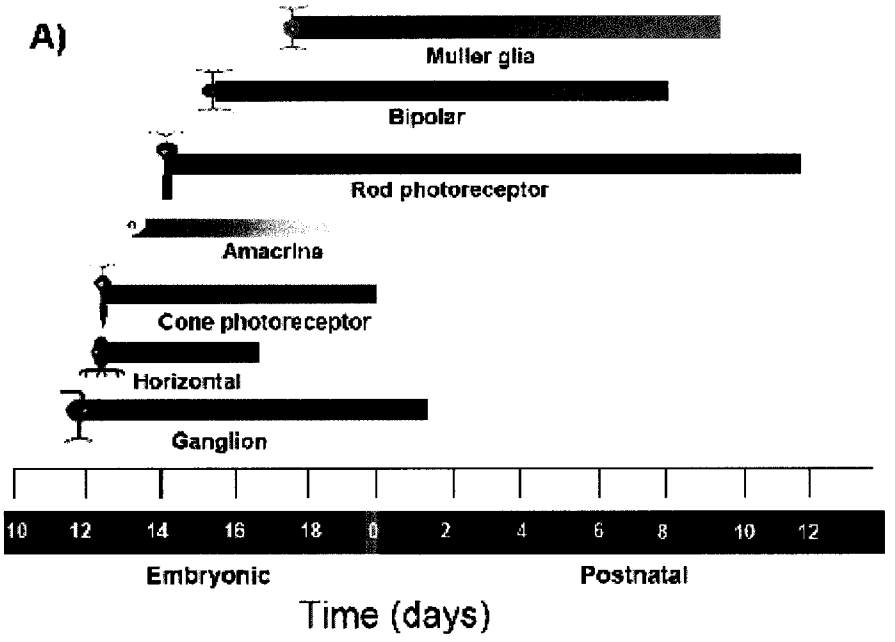
A)
Muller glia
Bipolar
Rod photoreceptor
Amacrine
Cone photoreceptor
Horizontal
Ganglion
10 12 14 16 18 0 2 4 6 8 10 12
Embryonic
Postnatal
Time (days)

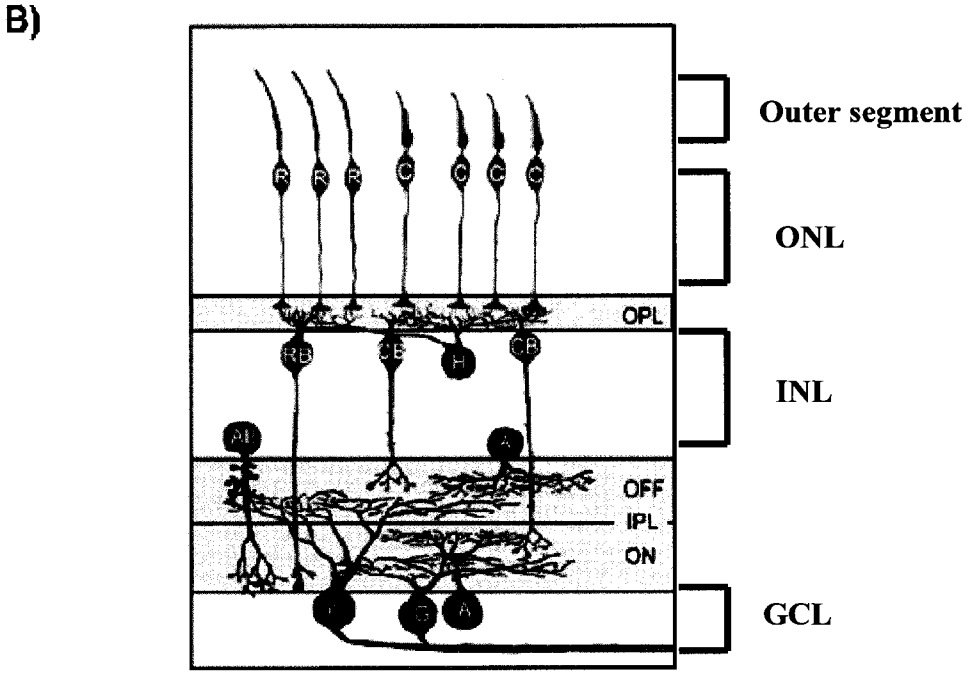
B)
Outer segment
ONL
INL
GCL
OPL
OFF
IPL
ON

and therefore contribute to the relative proportion of each cell type, without however, influencing progenitors to temporally give rise to inappropriate cell types (107). Thus retinal cell fate determination is a complex interplay of cell intrinsic and extrinsic regulators (108).

1.10.3 The visual pathway

As shown in Figure 5b, the mature vertebrate retina is a highly organized laminar structure which consists of three cellular layers. The outer nuclear layer (ONL) is composed of the cell bodies from rod and cone photoreceptors. The inner nuclear layer (INL) contains amacrine and horizontal interneurons as well as bipolar cells and Müller glia. Finally, the ganglion cell layer (GCL) consists of ganglion cells and displaced amacrine cells. Two synaptic layers, the outer and inner plexiform layer (OPL and IPL), separate these three rows of cell bodies.

Visual perception of light is first mediated by the retina, and is subsequently conducted to the brain by a set of distinct spatio-temporal pathways which stems from the different cellular and synaptic components of the retina (109). The fundamental feature of this system is that some cells are depolarized by light (ON cells) while others are hyperpolarized by light (OFF cells). Separation of the ON and OFF pathways starts as soon as a visual stimulus is detected by the rod and cone photoreceptors. In vertebrates, light stimulation results in the hyperpolarization of the membrane potentials of rod and cone photoreceptors which results in decreased glutamate secretion from these cells.

Rod photoreceptors signals are transmitted to the rod-driven bipolar cells, which synapse with AII amacrine cells and depolarize these cells in response to light. The latter then depolarizes the cone-driven OFF bipolar cells and OFF RGC by releasing glycine, an inhibitory neurotransmitter (110, 111).

On the other hand, in response to light, cone photoreceptors activate mGluR6 receptors within ON cone bipolar cells hyperpolarizing these cells. In addition, continuous release of glutamate by cone photoreceptors will depolarize the OFF bipolar cells (109). In the IPL, the ON bipolar cells synapse with the ON RGCs in sublamina *b* while OFF bipolars terminate within sublamina *a* to synapse with OFF RGCs. This RGC stratification in the IPL, maintains the separation of the ON/OFF pathways. Nevertheless, a small subset of ON-OFF RGCs do ramify in both sublamina (112). RGC subsequently transmit these signals through the optic nerve to the lateral geniculate nucleus (LGN) and visual cortex.

The two types of retinal interneurons, the amacrine and horizontal cells play a similar inhibitory role within the visual pathway. Amacrine cells with their extensive dendritic trees can inhibit the surrounding signals while horizontal cells by virtue of being connected laterally to numerous bipolar and rod/cone cells, can suppress the generation of information along some pathways and routes, while not affecting others that are adjacent to them. This selective suppression of signal transmission increases is often referred to as lateral inhibition and enables acuity of vision, movement detection and contrast enhancement (103).

1.11 Rationale and Specific Aims

Over the last sixty years, epigenetic modification of chromatin has emerged as an important regulator of cellular processes such as proliferation and differentiation. The important roles played by epigenetic regulators have made them prime targets for genes involved in the pathogenesis of human disease. An example of this includes the ATR-X syndrome, a severe form of mental retardation which arises due to mutations in the *ATRX* gene, which encodes for an ATP dependent chromatin remodeling protein.

While *in vivo* studies have shown the early requirement for ATRX during embryogenesis as well as its importance for neuronal differentiation and proper brain development, *in vitro* studies have postulated a role in cell cycle progression and survival during differentiation. The early lethality of previously generated Atrx knockout animals is a major obstacle in characterizing the post-natal effects of Atrx ablation on CNS development. Therefore, as it stems from CNS origin and is a highly accessible tissue whose cellular makeup is well understood and conserved amongst vertebrates, the retina is an ideal system to investigate the mechanisms by which Atrx may regulate CNS development. Based on previous *in vivo* and *in vitro* study, we **hypothesize that the chromatin remodeling protein Atrx is required for the terminal differentiation and subsequent neuronal survival within the mammalian retina**.

In addition, given the severity of the various developmental abnormalities described in ATR-X patients, it is likely that subtle sensory defects, such as impaired vision, have been overlooked in this population. Therefore based on the obvious requirement for ATRX in CNS development we further **hypothesize that visual defects**

are present in ATR-X patients in a much larger scale then previously reported. To address these following hypotheses three specific aims have been addressed.

-Aim 1: To determine the spatial and temporal expression of Atrx in the retina

-Aim 2: To characterize the effect of Atrx ablation on retinal development

-Aim 3: To determine the impact of Atrx inactivation in the retina on visual function in our animal model and draw parallels to the phenotypes observed in ATR-X patients.

2.0 Material and Methods

2.1 Transgenic mouse lines

The *α-Cre* transgenic mice which express Cre under control of the Pax6 promoter were obtained from Dr. P. Gruss (Max-Planck-Institute of Biophysical Chemistry, Department of Molecular Cell Biology, Göttingen, Germany) and maintained on an FVBN background (113). $Atrx^{flox/flox}$ mice which harbor loxP sites flanking exon 18 of the *Atrx* gene were maintained on a C57Bl/6 background (100). To generate α-cre;$Atrx^{f/y}$ animals, *α-Cre* transgenic mice were bred with $Atrx^{f/f}$ mice.

DNA was isolated from tail tissue by incubating a small tail fragment in 75 µl alkaline lysis buffer (25 mM NaOH, 0.2 mM EDTA) for 30 minutes at 95°C. Following the incubation, samples were cooled and neutralized with 75 µl of neutralization solution (40 mM Tris –HCl) (114). Tail DNA was genotyped using standard PCR conditions. Genotyping for the *α-Cre* transgene was done by PCR using the following primers, as

previously described: *α-Cre* 5'-ATG CTT CTG TCC GTT TGC CG -3' and 5'-GGG CGT AGA CAT CTG GGT AG -3' (113). Sex of embryos and young pups was also determined via PCR using the following primer combination: SRY 5'-TTG TCT AGA GAG CAT GGA GGG CCA TGT CAA -3' and 5'CCA CTC CTC TGT GAC ACT TTA GCC CTC CGA -3' and Fapb1 5'TGG ACA GGA CTG GAC CTC TGC TTT CCT AGA -3' and 5'CTAG AGC TTT GCC ACA TCA CAG GTC ATT CAG -3'. PCR conditions were as follows: An initial denaturation step at 96°C for 2 minutes followed by 35 cycles of: 95°C for 20 seconds, 57°C for 20 seconds, 72°C for 40 seconds. A final elongation at 72°C for 5 minutes ensued. Results were visualized after electrophoresis on a 1.5% agarose (Sigma) gel in TAE buffer (40 mM Tris acetate and 1 mM EDTA) containing 0.5 μg/mL ethidium bromide.

SNF2L KO animals were obtained by crossing SNF2L f/f mice to the ubiquitously expressing *Gata- 1 Cre* transgenic line on a CD-1 background which was kindly provided by Dr. S. Orkin (Howard Hughes Medical Institute, Chevy Chase MD, USA). Mice heterozygous for the floxed exon 6 *Snf2l* allele ($Snf2l^{f/x}$) (DJP unpublished) were bred to males heterozygous for *Gata-1* $Cre^{+/-}$ to generate the Ex6DEL line ($Snf2l^{-/x}$ or $Snf2l^{-/y}$).

2.2 Tissue preparation

For timed mating purposes, the day of vaginal plug detection was counted as embryonic day 0.5 (E0.5). At scheduled times, animals were anesthetized by CO_2 and sacrificed by cervical dislocation. Uteri were removed from pregnant females and embryos were freed from their embryonic sac and placental structures. The head was

removed from the embryos and nasal structures were removed to allow fixative to penetrate. After birth, eyes and optic nerve were enucleated from animals. A hole in the cornea was made and the lens was scratched to allow for proper fixation of tissue. Lens structure was completely removed in animals older than P10 again to optimize the fixation conditions.

Whole heads from embryos and dissected eyes plus optic nerves from animals younger than P7 were fixed in 4% paraformaldehyde (PFA) overnight in 0.1M phosphate buffered saline (PBS) (0.14 M NaCl, 2.5 mM KCl, 0.2M Na_2HPO_4 and 0.2M KH_2HPO_4 at pH 7.4). Older animals were transcardially perfused with 4% PFA prior to eyes being enucleated and overnight incubation. Following three 10 minute PBS washes, samples were cryoprotected overnight in a 30% sucrose/PBS solution. Tissues were embedded in 1:1 mix of 30% sucrose and OCT (Tissue-Tek, Japan) and frozen on liquid nitrogen.

For preparation of retinal whole mounts, following cardiac perfusion of animals the eyes were enucleated and a hole was made in the cornea to allow for the removal of the RPE sclera and cornea. Retinas were fixed for 2 hours in 4% PFA and washed with PBS for 1 hour. PBS was changed every 10 minutes. Whole mount staining procedures are indicated below.

All experiments were approved by the University of Ottawa's Animal Care ethics committee adhering to the guidelines of the Canadian Council on Animal Care.

2.3 Birthdating experiments

For birthdating experiments, cells in S phase were labeled in vivo by injecting time-mated females with two intraperitoneal injections 2 hours apart of BrdU at a concentration of 0.1 mg/g body weight resuspended in DMEM (Gibco). Pups were harvested on the day of birth and BrdU positive cells were detected by immunohistochemistry (see below).

2.4 Immunohistochemistry and in situ hybridization

Embedded tissues were sectioned on a Leica 1850 cryostat at 12 μm. Sections were transferred onto Superfrost Plus coated slides (Fisher Scientific, USA), air dried for 2-6 hours at room temperature and stored with dessicant at -20°C. For more reliable comparisons wild-type and mutant tissues were processed on the same slide.

For immunofluorescence studies, cryosections were dehydrated in 70% ethanol for 5 minutes and re-hydrated in PBS using three 10 minute washes. Cryosections were blocked in 20% bovine calf serum (Sigma)/0.03% Triton-X 100 in PBS for 1 hour and incubated overnight at 4°C in a humidified box with the following primary antibodies diluted in blocking solution: goat polyclonal anti-Brn3b (1/100, Santa Cruz Biotechnology), sheep polyclonal anti-CHX10 (1/2000, gift from Dr. Rod Bremner, University of Toronto), rabbit polyclonals anti-ATRX (1/100, Santa Cruz Biotechnology) anti-calretinin (1/2000, Swant), anti-cone arrestin (1/500; gift from Dr. Xuemei Zhu and Cheryl Craft from the Mary D. Allen Laboratory) anti-CRALBP (1/2000, gift from Dr. Gregory Garwin University of Washington), anti-PKC (1/100, BD Pharmingen), anti-tyrosine-hydroxylase (1/500, Chemicon International) anti-Prox1 (1/3000, Chemicon

International) and the mouse monoclonals anti-B630 (1/3; Developmental Studies Hybridoma Bank), anti-Pax6 (1/3; Developmental Studies Hybridoma Bank) anti-BrdU (1/100,BD Bioscience), anti-Ki67 (1/200, BD Pharmingen), anti-calbindin (1/500, SIGMA), anti-rhodopsin (1/3;), anti-syntaxin (1/1000, Sigma), anti-GFP (1/500, Molecular Probes), anti-glutamine synthetase (1/500, BD Bioscience). The rabbit polyclonal anti-ChAT (1/500, Chemicon International) was incubated for 24 hours at room temperature. Prior to the incubation in blocking solution the following antibodies required antigen retrieval: the goat polyclonal anti-Brn3b, the rabbit polyclonal anti-PKC, -ChAT, -tyrosine hydroxylase and -BrdU as well as the mouse monoclonal Ki67. Antigen retrieval consisted of a 10 minute microwave treatment in a 1X sodium citrate solution (0.01 M citric acid, 0.025 M NaOH) pH 6.0 followed by two 10 minute PBS wash. In addition to antigen retrieval visualization of BrdU required a 15 minute treatment in 2N HCL at 37°C followed by a 10 minute permeabilization step in 0.1M Tris pH 8.8 + 0.01% Tween 20. Antibodies were visualized with the following secondary antibodies diluted in TBLS (0.05 M Tris-HCl pH 7.4, 0.15 M NaCl, 10 g/ L BSA, 9 g/L L-Lysine, 2 g/L Sodium Azide) Alexa 594 Red-conjugated donkey anti-rabbit-IgG (1/1000, Molecular Probes) Alexa 594 Red-conjugated donkey anti-mouse-IgG (1/1000, Molecular Probes), Alexa 488 Green-conjugated donkey anti-mouse-IgG (1/1000, Molecular Probes), Alexa 588 Red conjugated donkey anti-goat-IgG. Cell nuclei were counterstained with DAPI for 5 minutes (10 μg/mL). Sections were mounted with DAKO fluorescence protector.

For Brn3b immunoreactivity, some sections were processed using 3,3'-diaminobenzidine (DAB) as a substrate as previously described (115). Briefly sections were fixed and

processed for antigen retrieval as described. Slides were then treated with 0.3% H2O2, for 10 minutes, washed for 10 minutes in PBS and blocked in 20% sheep serum in 0.5% Triton X-100 before overnight incubation with primary Brn3b antibody (1/100, Santa Cruz Biotechnology). Following three 10 minute PBS washes, slides were incubated with biotinylated anti-goat antibody (1:200 Amersham Bioscience). Following three more 10 minute PBS washes, antibody detection was performed using DAB as a substrate. Conjugated antibodies were detected with the Vectorstain ABC Elite avidin/biotin/peroxidase kit as per manufacturer's instruction (Vector Laboratories, Burlingame, California). In brief, slides were incubated in ABC solution for 40 minutes and washed with PBS three times. Colour was developed in DAB/PBS (27 mL PBS, 3 mL of 3% H2O2, 0.5 mL 2.5% DAB) for 5 minutes. Slides were run under tap water for 10 minutes and mounted with coverslips using a 1:1 mixture of PBS and 30% glycerol.

For flat mount staining, retinas were blocked in 20% bovine calf serum (Sigma)/0.03% Triton-X 100 in PBS overnight at 4°C and incubated again at 4°C for 24 hours with the anti-tyrosine-hydroxylase (1/500, Chemicon International) primary antibody. Following 10 PBS washes of 10 minutes each, retinas were incubated with the Alexa 594 Red-conjugated donkey anti-rabbit-IgG (1/1000, Molecular Probes) secondary antibody diluted in TBLS for 2 hours. Following 10-15 PBS washes of 10 minutes each, nuclei were counterstained with DAPI for 5 minutes (10 μg/mL). Retinas were flattened onto Superfrost Plus coated slides (Fisher Scientific, USA) and mounted with DAKO fluorescence protector.

Sections and whole mounts were analyzed on a Zeiss Axioplan microscope and digital images were captured using an AxioVision 6.05 (Zeiss) camera and processed with Adobe® Photoshop.

In situ hybridization was performed as previously described. (116) Briefly DIG-labelled RNA probes were diluted 1/1000 in hybridization buffer (50% formamide, 10% dextran sulfate, 1 mg/mL yeast RNA, 1xDenhardt's and 1x salt) and denatured for 10 minutes at 70°C. Probes were allowed to hybridize overnight at 65°C in a humidified box. The slides were then washed twice for 30 minutes with wash buffer solution (50% formamide 1x SSC, 0.1% Tween-20) at 65°C. Slides were then washed three times for 20 minutes at room temperature with MABT (100 mM maleic acid, 150 mM NaCl, pH 7.5, 0.1% Tween-20). Sections were blocked for two hours with blocking solution which consisted of 20% sheep serum (Sigma) and 2% blocking solution (Boehringer Mannheim) in MABT. Alkaline-phosphatase-conjugated Fab fragments of sheep anti-DIG diluted 1/1000 in blocking solution were then allowed to hybridize at 4°C overnight in a humidified box. The following day, slides were washed four times for 20 minutes in MABT at room temperature followed by two 10 minute washes in pre-staining buffer (100 mM NaCl, 50 mM MgCl2, 100 mM Tris pH 9.5 and 0.1%-Tween 20). Color reaction was allowed to develop for 2-24 hours in staining buffer which consisted of 100 mM NaCl, 50 mM MgCl2, 100 mM Tris pH 9.5 and 0.1%-Tween 20ml 4.5 µl/mL 4-Nitro blue tetrazolium chloride (Roche) and 3.5 µl /mL 5-bromo-4chloro-3indolyl-phosphate (Roche). Slides were rinsed in PBS before being mounted using a 1:1 mixture of PBS and 30% glycerol.

Sections were analyzed on a Zeiss Axioplan microscope and digital images were captured using an AxioVision 2.05 (Zeiss) camera and processed with Adobe® Photoshop.

2.5 TUNEL assay

Terminal uridine deoxynucleotidyl transferase dUTP nick end labeling TUNEL assay was performed using the In Situ Cell Death Detection Kit (Roche Diagnostics) according to the manufacturer's instructions. In summary, sections were hydrated in PBS for 30 minutes and incubated in permeabilisation solution (0.01% Triton-X, 0.1% Sodium citrate (Sigma)) at room temperature. Slides were washed for 10 minutes with PBS and incubated in a mixture of 10 µl of enzyme solution and 90 µl labeling solution for 1 hour at 37°C. After three 10 minute PBS washes, cell nuclei were counterstained with DAPI for 5 minutes (10 µg/mL). Sections were mounted with DAKO fluorescence protector.

2.6 Q-RT-PCR analysis

Total RNA was isolated from two different retinas harvested from the same animal using Trizol reagent (Invitrogen) followed by RNase free DNAse I (Sigma) to remove DNA contamination. Using 1-2ug of total RNA first strand cDNA was synthesized using random primers and a reverse transcription cocktail containing 5x first strand buffer, 100 mM DTT, 25 mM dNTPs and Superscript II RT (Invitrogen). Q-RT PCR was performed using a Stratagene Mx 3000 with Absolute SYBR Green Q-PCR Master Mix (Abgene) under the following conditions: 10 minutes at 95°C followed by 40 cycles of 30 seconds at 95°C, 30 seconds at 59°C and 30 seconds at 72 °C. A final

elongation step of 1 minute at 95°C, 30 seconds at 55°C and 30 seconds at 95°C ensued. The primers used for Q-RT-PCR are indicated in Appendix A. Using the standard curve corresponding threshold method of quantification, PCR product formation was monitored in real time (Mx4000 multiplex quantitative PCR system; Stratagene) and the threshold cycles were determined using the Mx4000 software. All data was normalized to GAPDH and 18S RNA expression levels. Threshold cycle variance in seven biological replicates was tested for significance using a two-sample Student's *t*-test with equal variance.

2.7 Electroretinography

Electoretinograms were generated using the ESPION system (Diagnosys LLC, Littleton, MA) as previously described (117). Briefly, prior to ERG analysis, mice which had been dark-adapted overnight were anaesthetized under safe light conditions using intraperitoneal injection of avertin. Eyes were dilated with administration of 1% tropicamide and 2.5% phenylephrine hydrochloride drops (Alcon Canada). Silver wire loop electrodes were placed on both corneas with a drop of 0.3% hypromellose (Novartis) to maintain corneal hydration. A gold minidisc reference electrode was placed on the tongue and a ground needle electrode was placed subcutaneously in the tail. The animal's head was positioned under the center of the Ganzfeld dome. Single flash stimuli (4 ms duration) were presented at eleven increasing intensities ranging from 0.001 cd.s/m^2 to 25 cd.s/m^2. Five ERG traces were obtained and averaged for each luminance step. Differences during ERG analyses were determined on at least 11 different animals of each genotype. Each eye was considered as a biological replicate and differences were determined using ANOVA analysis.

3.0 Results

3.1 Characterization of Atrx expression in the retina

3.1.2 Temporal and spatial expression of Atrx in the developing and adult retina

Based on the widespread expression of Atrx in the CNS, we suspected that Atrx was abundantly expressed within the retina. To identify the Atrx-expressing cells in the developing mouse retina we stained embryonic and perinatal cryosections with a polyclonal ATRX antibody which recognizes the full length protein. As illustrated in Figure 6A-C, Atrx was found to be abundantly expressed in progenitor cells throughout the retina at E13.5 as shown by co-localization of Atrx and the cell cycle marker Ki67. In E15.5 embryos, the developing retina is divided into two discrete zones: the outer neuroblast layer which contains actively dividing cells and the retinal ganglion cell layer (GCL) where newly post-mitotic cells reside. Similarly, two discrete populations of Atrx positive cells could be distinguished. At this stage, Atrx is expressed at low levels in progenitors in the outer region of the neuroblast layer (Fig. 6D-F) and at higher levels in cells located in the inner region of the neuroblast layer and in the ganglion cell layer (arrow in Fig. 6 F). This second population is post-mitotic as they do not co-localize with Ki67 (Fig 6 F). At P0, Atrx expression persists in progenitor cells at low levels as indicated by Ki67 colocalization with Atrx+ cells in the outer region of the neuroblast layer (Fig 6 G-I). Again, a strong Atrx signal is detected in post-mitotic cells in the developing inner region of the neuroblast layer and in the GCL.

Figure 6: Temporal expression of Atrx in the retina.
Retinal sections from the indicated embryonic stages were double-labeled with an anti-ATRX antibody (red) and an antibody against the proliferation marker Ki67 (green). (A-C) At E13.5, Atrx expression corresponds almost exclusively to that of progenitors. Inset in (C) is a higher magnification view of AtrxKi67+ cells. (D-F) at E15.5 Atrx continues to be expressed in cycling progenitors while a sub-population of Atrx+ cells which have exited the cells cycle (Ki67-) is evident in the inner retina and is indicated with an arrow in F. Inset in (F) is a higher magnification view of double Atrx+Ki67+ cells in the ONBL. Atrx+Ki67- cells which are post-mitotic are evident in the inner half of the ONBL and the GCL and are indicated with the arrow. (G-I) at P0 Atrx continues to be expressed in cycling progenitors, particularly in the peripheral retina, which corresponds to the least differentiated region at this stage of development. The post-mitotic pool of ATRX+cells is located in the GCL and the developing inner nuclear layer. Inset in (I) shows a higher magnification of double ATRX+Ki67+ progenitor cells and ATRX+Ki67- post-mitotic cells. Boxes in C, F and I are representative of the areas where the magnified inset was taken.

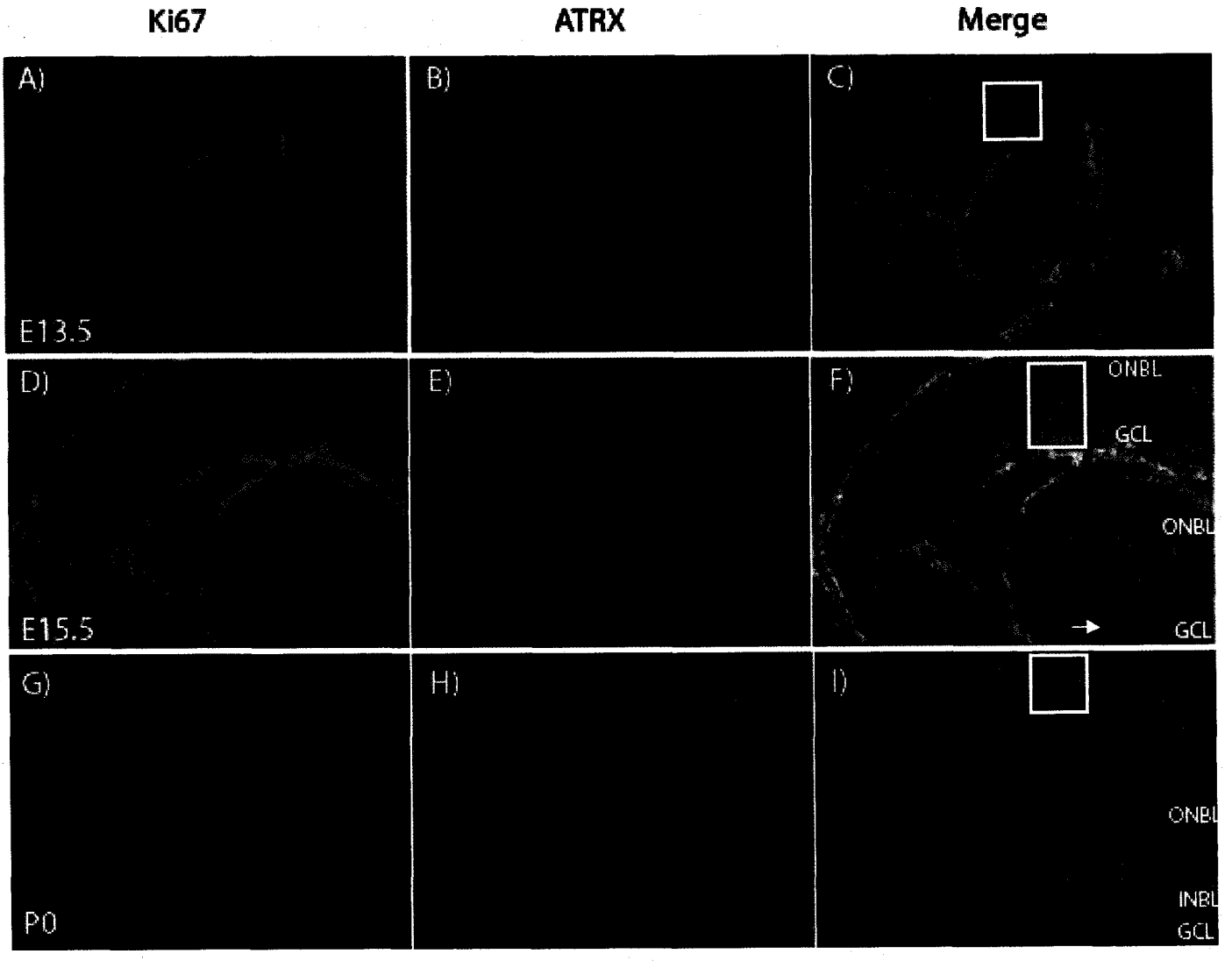
Ki67
ATRX
Merge
A)
B)
C)
E13.5
D)
E)
F)
ONBL
GCL
ONBL
E15.5
GCL
G)
H)
I)
ONBL
INBL
GCL
P0

Figure 7: Atrx localization in the adult retina.
(A) Transverse cryosections of adult (6-8 weeks) retina immunostained for Atrx(red) and DAPI to reveal nuclei (blue). Note that ATRX+ cells are located in the retinal ganglion cell layer (RGC) and the inner nuclear layer (INL). At this exposure Atrx staining is not discernable in the outer nuclear layer (ONL). (B-E) Adult retina sections double-labeled for Atrx(red) and cell type specific markers for (B) Müller glia (glutamine synthetase, GS), (C) bipolar cells (Chx10), (D) horizontal and amacrine cells (calbindin), (E) amacrine cells (syntaxin). Inset in (E) shows a higher magnification view of Atrx and syntaxin expression. (F) Double-labeled sections for (green) and RGC (Brn3b) in red. (G) A longer exposure of an adult (6-8 weeks) retina, reveals Atrx staining in the apical region of the ONL where cone photoreceptors are located. (H) Immunostaining for Atrx in the NRL-/- retina confirms the Atrx expression in cone photoreceptors in the ONL.

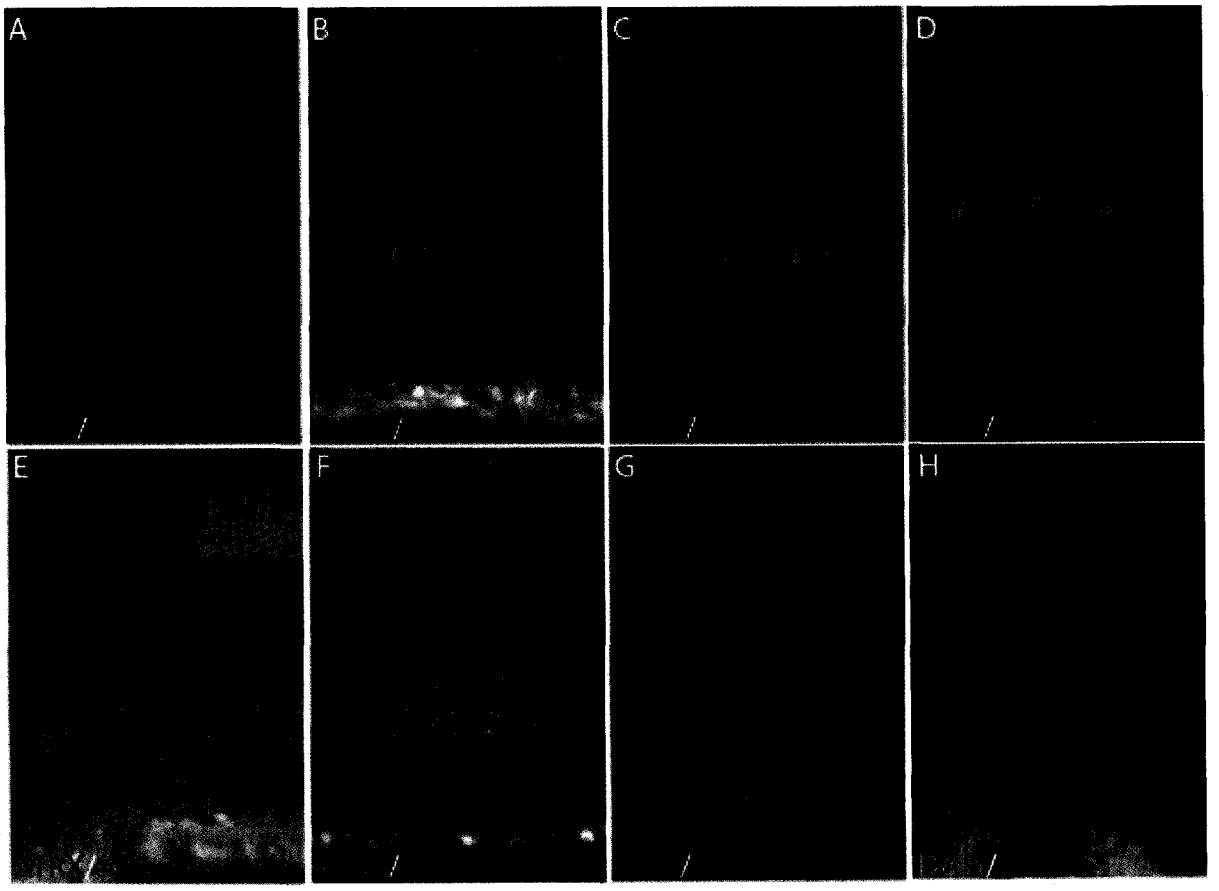
A
B
C
D
E
F
G
H

Elevated Atrx expression in differentiated cells and lower protein levels in the progenitor pool is consistent with previously published observations in the mouse cortex and hippocampus (100).

Immunohistochemistry for Atrx on retinal sections from late postnatal stages and in the adult retina, revealed that high levels of Atrx are found in the inner nuclear layer (INL) and ganglion cell layer, while fainter Atrx staining is also present in the apical region of the outer nuclear layer (Figure 7A and G) . To identify ATRX-expressing cells in the adult retina we performed double-labeling IHC using an ATRX antibody and retinal cell type specific antibodies: glutamine synthetase (Müller glia), CHX 10 (bipolar cells), syntaxin (amacrine cells), calbindin (horizontal cells) and Brn3b (ganglion cells). We obseved that Atrx is expressed in all cell types of the INL (Müller, amacrine, bipolar and horizontal) as well as in ganglion cells and displaced amacrine cells in the GCL (Figure 7B-E). A weak and infrequent perinuclear Atrx signal was detected in the apical region of the outer nuclear layer (ONL) in a distribution pattern reminiscent of cone photoreceptors (Figure 7G). In the ONL of the mature retina, rods greatly outnumber cone photoreceptors, the latter accounting only for 3% of the cellular makeup of the ONL. To confirm that these Atrx immunopositive cells in the ONL were indeed cone photoreceptors, we immunostained sections of a cone-dominant retina harvested from $NRL^{-/-}$ mice (118). In these mice, ablation of *NRL* results in a cone-only retina due to the generation of cones at the expense of rod photoreceptors (118). As shown in Figure 7H, all of the cells in the ONL of $NRL^{-/-}$ retinas exhibit perinuclear Atrx staining thus confirming the expression of Atrx in cone photoreceptors. Based on our immunolocalization study we can conclude that Atrx is expressed in progenitor cells

throughout retinal development. Moreover, beginning at E15.5 higher intensity of Atrx staining was detected in post-mitotic cells than in progenitor cells. In the mature retina Atrx expression persists in all differentiated cell types with the exception of rod photoreceptors.

3.2 Generation and characterization of conditional Atrx knockout mice

3.2.1 Conditional deletion of Atrx results in retinal dysplasia.

To study the biological function of *Atrx* during retinal development the use of a conditional gene inactivation system is required, as complete Atrx inactivation results in early embryonic lethality (97). Therefore, we used a Cre-recombination system to target Atrx inactivation to the retina. Atrx floxed mice were bred to mice expressing Cre under the control of a regulatory element of the murine Pax6 promoter (α-Cre) (113). This α-Cre mouse line has been used on numerous occasions to target gene inactivation (119-123). This α-Cre mouse line is characterized by significant Cre expression in the mid-peripheral and peripheral retina, while in the central retina Cre expression is minimal (113).

Crossing of the α-Cre mice with Atrx floxed mice generated α-cre;$ATRX^{f/y}$ animals which should inactivate for Atrx around E10.5 in the peripheral retina (113). For simplicity, these animals will be referred to subsequently as Atrx KO throughout the text. Pax6αCre mice express GFP and Cre from a bicistronic mRNA which allowed us to use GFP staining as a surrogate marker to monitor Cre expression and inactivation

Figure 8: Atrx expression in the retinas of Atrx KO mice.
Conditional inactivation of *Atrx* in the retina was achieved by crossing αCre mice with floxed Atrx mice to generate *αCre;ATRXf/y* animals (Atrx KO). αCre activity is restricted to the peripheral regions of the retina and the GFP reporter in the αCre transgenic construct is used to monitor the location of Cre-expressing cells. Horizontal sections of the peripheral (A-R) or central (S-X) retinas from wildtype and Atrx KO retinas at the indicated ages were stained with DAPI (blue) or with antibodies specific for Atrx (red) and GFP (green). (A-F) Note the absence of ATRX+ cells in the neuroblast layer of the Atrx KO retina at E13.5 (bracket in D). ATRX+ cells are present in the ciliary margin (most distal region of the eyecup, arrow in D) in the Atrx KO mice. (G-L) P7 and (M-R) adult retinas exhibit Atrx staining in sporadic cells in the peripheral retina of the Atrx KO mice that does not co-localize with GFP staining in the INL and GCL (higher magnification inset in L). The residual Atrx staining is an indication that some cells in the peripheral retina of the αCre mice escape recombination. (S-X) Atrx expression is abundant in the central retina due to poor αCre activity in this region.

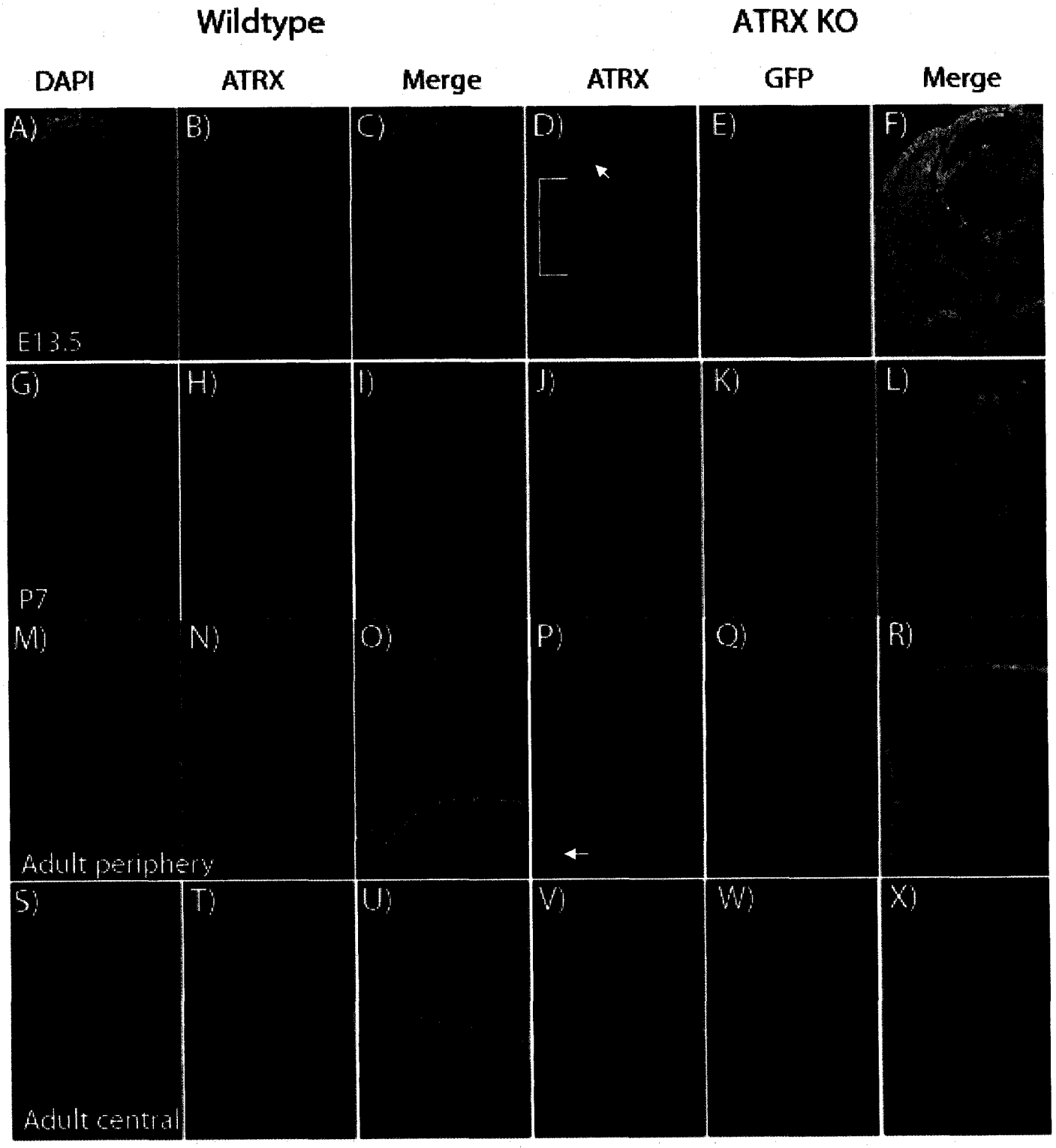
Wildtype
ATRX KO
DAPI
ATRX
Merge
ATRX
GFP
Merge
A)
B)
C)
D)
E)
F)
E13.5
G)
H)
I)
J)
K)
L)
P7
M)
N)
O)
P)
Q)
R)
Adult periphery
S)
T)
U)
V)
W)
X)
Adult central

of the full length Atrx protein via IHC. At all time points observed, E13.5, P7 and adults GFP expression in the peripheral retina was correlated with the absence of Atrx protein (Figure 8). Consistent with previous reports, we did note however, that the peripheral retinas of Atrx KO mice contained sporadic ATRX+ cells, indicating that some cells escape Cre recombination in this model (Figure 8, arrow in P) (113). Moreover, abundant Atrx expression could be found in the central retina supporting previous reports of low α-Cre activity in the central retina in this transgenic mouse line (113, 120). Indeed, our results illustrate that there is almost complete ablation of Atrx in the peripheral retina of hemizygous male progeny.

To characterize the impact of Atrx ablation on retinal development we performed immunohistochemical studies on the retinas of adult (6-8 weeks) Atrx KO mice. Upon initial observation, the gross morphology and organization of Atrx KO retinas did not differ from their wildtype counterparts (Figure 9 A). As shown in Figure 9 immunohistochemical analysis with a panel of cell type specific markers revealed no obvious deficiencies in the morphology and number of rod (B630+) and cone (cone-arrestin+) photoreceptors, RGCs (Brn3b+), rod bipolar cells (PKCα) and Müller glia (CRALBP+) (Figure 9B-J). However, we did observe striking differences in the expression of the horizontal cell marker calbindin (compare arrows in Fig 9 K and O), the pan-amacrine marker syntaxin and the width of the IPL, where amacrine, bipolar and RGC processes are located (Fig 9 P). Cell counting confirmed a 37% reduction in horizontal cells (calbindin+) and a 25% reduction in amacrine cells in the INL (Pax6+) in the peripheral retina of Atrx KO mice. To determine if the reduction in Pax6 and

Figure 9: Characterization of the cell type specific marker expression in Atrx KO retinas.

Retinal sections from adult (6-8week) mice were immunostained for retinal cell-specific markers (red) and DAPI (blue) to reveal nuclei. (A and E) DAPI staining revealed no gross lamination or morphological defects in Atrx KO retinas. Rod (B630) and cone photoreceptors (cone-arrestin), RGC (Brn3b), rod bipolar (PKC) and Müller glia (CRALBP) appeared to be unaffected in the Atrx KO mice (B-D and F-J, M, N), compared with wildtype littermates. However there is a reduction in calbindin+ horizontal cells located at the border of the outer plexiform layer (arrow in K compared to arrow in O) and in syntaxin+ cells (L and P) in the inner nuclear layer (inset in L as compared to inset in P) and the width of the inner plexiform layer indicated by syntaxin staining (L vs P).

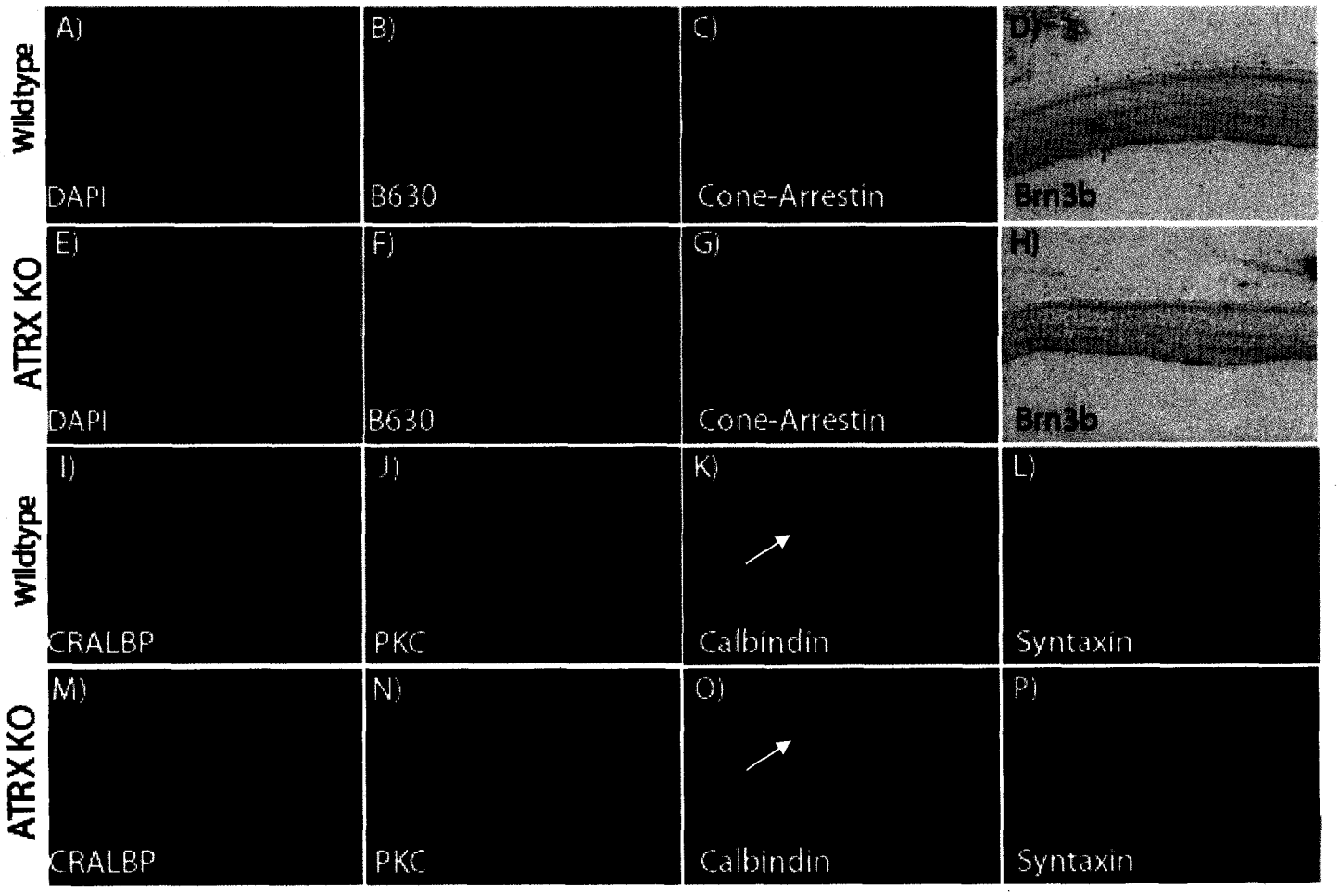
Wildtype
A)
DAPI
B)
B630
C)
Cone-Arrestin
D)
Brn3b
ATRX KO
E)
DAPI
F)
B630
G)
Cone-Arrestin
H)
Brn3b
Wildtype
I)
CRALBP
J)
PKC
K)
Calbindin
L)
Syntaxin
ATRX KO
M)
CRALBP
N)
PKC
O)
Calbindin
P)
Syntaxin

syntaxin immunoreactivity in Atrx KO retinas was due to the aberrant differentiation, a cell fate change of amacrine cells or the absence of these cells, we quantified cell numbers in the three layers of the adult Atrx KO and wildtype retina. As shown in Figure 10A and 10B, we observed a ~15% and 25% reduction in the number of cell bodies residing in the GCL and INL of Atrx KO animals, respectively. The reduction in the INL was attributed to the loss of amacrine cells as indicated by Pax6 staining and horizontal cells identified by calbindin immunoreactivity (Figure 10C). The other neuronal INL subtype, bipolar cells, was not significantly altered in Atrx KO retinas (Figure 10C). In addition, no compensating changes in the ONL including in cone photoreceptors was detected (Figure 10A-C). Moreover, the reduction in the GCL was not attributed to a reduction in the number of ganglion cells as equal numbers of Brn3b+ cells were present in both Atrx KO and wildtype littermates (Figure10C). Taken together these results suggest that Atrx may play a potential role in the development or survival of amacrine and horizontal cells.

To further examine whether the amacrine cell phenotype observed in Atrx KO retinas was due to the selective loss of a specific amacrine subtype or a uniform loss of the amacrine cell class, we again performed an immunohistochemical analysis of adult retinas using subtype specific markers. Morphological studies of the mammalian retina have identified close to 30 distinct subtypes of amacrine cells, all of which are present in defined ratios and with discrete roles in the processing of information through the INL (124). As a result of their extreme heterogeneity, to date only a handful of molecular markers for distinct amacrine subtypes have been identified. A list of some of these

Figure 10: Decreased cell numbers in the INL and GCL of Atrx KO retina is due to the absence of amacrine and horizontal cells

A) The number of DAPI positive nuclei in 700μm^2 found in the three retinal layers were quantified in transverse sections of the retinas from adult Atrx KO and wildtype littermates. Atrx KO animals exhibit a reduction of approximately 25% and 17% in the number of cell bodies in the INL and GCL respectively, but there is no significant reduction in cell number in the ONL. B) Graphical representation of the number of DAPI positive nuclei in the three retinal layers. C) Quantification of marker+ cells in Atrx KO and wildtype adult retinas per 700μm^2. There is no reduction in the number of RGC (Brn3b), cone photoreceptors (cone arrestin) and bipolar cells (Chx10). There is a ~37% reduction in the number of cabindin+ horizontal cells in the outer plexiform layer and a ~25% reduction in the number of Pax6+ cells in the inner nuclear layer in the Atrx KO compared with wildtype littermates (*$p \leq 0.01$;**$p \leq 0.05$ $n \geq 3$,Student T-TEST).

A)

	GCL	INL	ONL
Wildtype	75.4±2.3	529.3±45.5	1142.361.9
ATRX KO	62.9±5.0	400.9±16.3	1150.7±105.5

B)

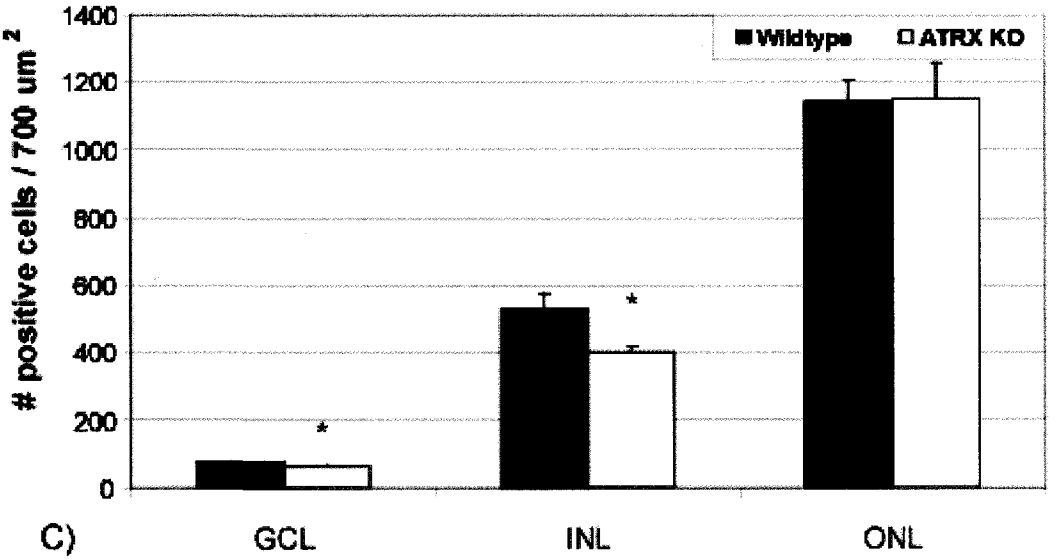

C)

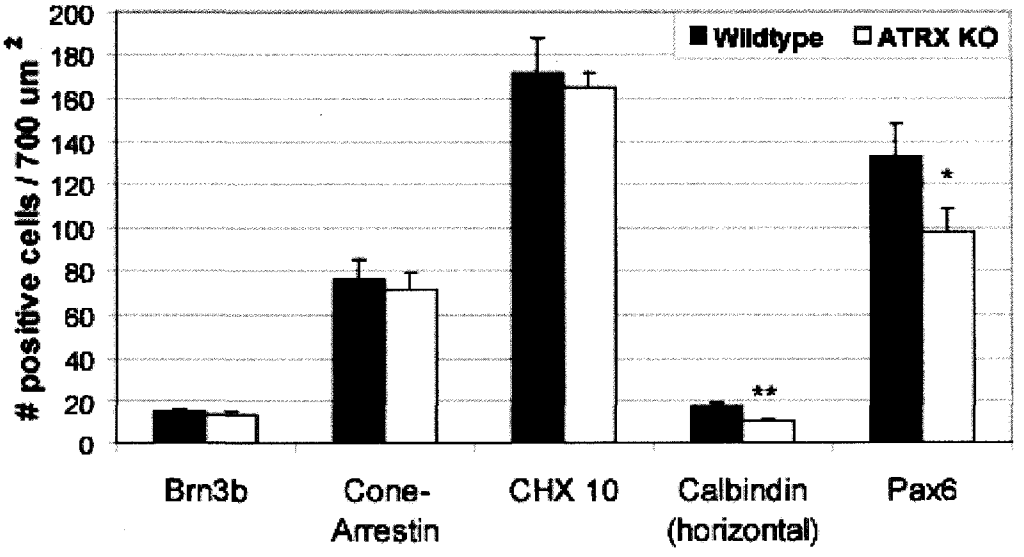

markers is appended in Appendix B. Immunohistochemical analysis revealed a reduction in all amacrine subtype specific markers tested in Atrx KO retinas. As illustrated in Figure 11, Glyt1, Calretinin, ChAT, Prox1 and TH staining was reduced in the retinas of Atrx KO animals. Cell scoring confirmed a significant reduction in the number of Glyt1+, Calretinin+ and Prox1+ amacrine cells in the Atrx KO compared with the control (Figure 11 M). The number of ChAT+ and TH+ cells in retinal sections was not significantly different between wildtype and Atrx KO, however, the expression of these markers in amacrine cell processes was abnormal and reduced (Figure11 H and K, I and L).

As TH+ cell processes were drastically less intense in our Atrx KO we took a closer look at these processes using retinal flat mount staining. One of the peculiar characteristic of adult dopaminergic innervation, which can be observed in whole mounts, is its organization into pericellular baskets surrounding the somata of glycernergic and AII amacrine neurons (125). As illustrated in Figure 12 these pericellular varicosities were significantly reduced in Atrx KO mice, thereby illustrating the disturbance of the dopaminergic network.

To confirm that our phenotype was indeed due to reduced Atrx expression we analyzed the expression of these same markers by IHC in the central retina where Atrx expression is abundant. Similar calretinin, ChAT, Prox1 and TH staining was observed in both ATRK KO and wildtype retina (Figure 13). The specificity of amacrine and horizontal cell loss to the absence of the chromatin remodeling protein Atrx was further examined by looking at another chromatin remodeling protein conditional knockout. Deletion of SNF2L, one of the two mammalian ISWI homologs, revealed no gross changes in any horizontal and amacrine cells markers as determined by immunohistochemistry (Figure 14).

Figure 11: Impact of Atrx inactivation on amacrine cell subtypes.
A-L) A panel of amacrine subtype specific makers was used to characterize the amacrine cell phenotype in the Atrx KO retina. The following changes were noted in the Atrx KO retinas, compared with wildtype littermates. Syntaxin staining is reduced in the inner plexiform and inner nuclear layers (A vs D). Glycinergic amacrine cells were reduced in number (B vs E). Prox 1 staining identifies horizontal, bipolar and amacrine cells. Prox1+ amacrine cells are located in the inner region of the INL and are reduced in the Atrx KO retina (C vs F, see arrow heads). Calretinin+ tracks in the inner plexiform layer are disorganized and the number of calretinin+ cells is reduced in the INL and GCL (G vs J). ChAT+ tracks in the inner plexiform layer are disorganized (H vs K) and TH+ tracks are discontinuous (I vs L). M) Pax6+, GlyT1+, Prox1+ and Calretinin+ cell bodies in the INL and GCL are reduced in number. In summary we find a reduction in amacrine and horizontal cells. The amacrine cell phenotype affects at least three subclasses: cholinergic (ChAT+), AII (Prox1+) and domapinergic (TH). Quantification of marker+ cells in Atrx KO and wildtype retinas (*$p \leq 0.05$; $n \geq 3$ Student T-TEST)

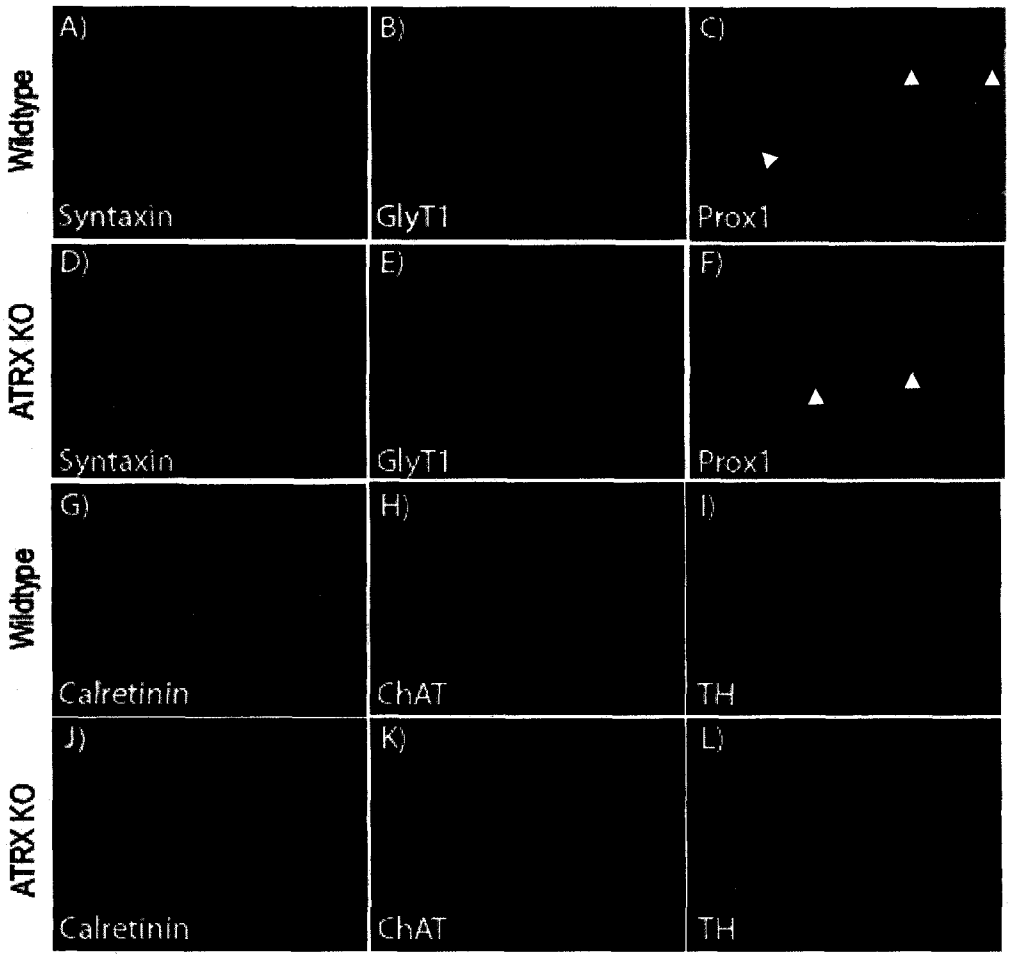
Wildtype
ATRX KO
Wildtype
ATRX KO
A)
Syntaxin
B)
GlyT1
C)
Prox1
D)
Syntaxin
E)
GlyT1
F)
Prox1
G)
Calretinin
H)
ChAT
I)
TH
J)
Calretinin
K)
ChAT
L)
TH

M)

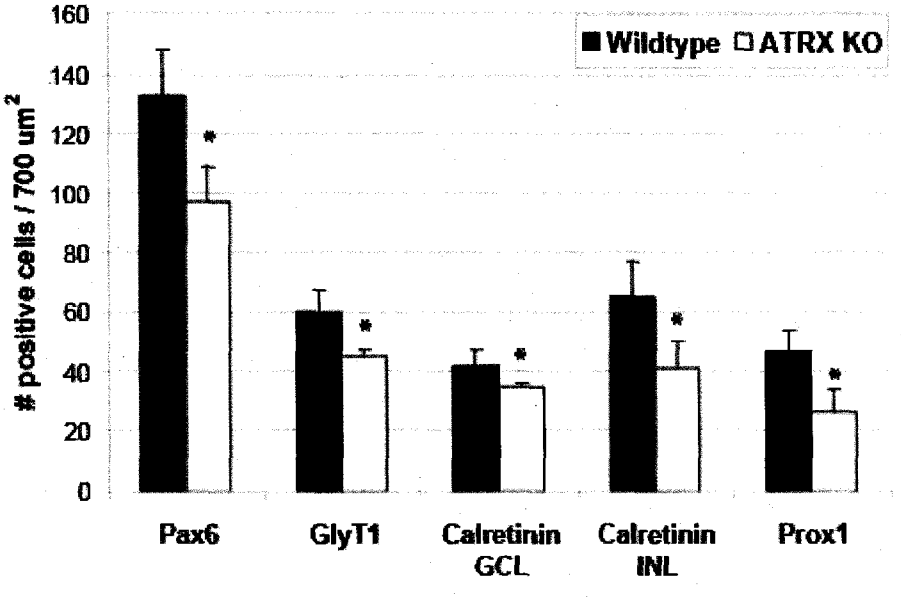
Wildtype
ATRX KO
positive cells / 700 um2
160
140
120
100
80
60
40
20
0
Pax6
GlyT1
Calretinin GCL
Calretinin INL
Prox1

Figure 12: Dopaminergic network in wildtype and Atrx KO retinas
Flat mount retinal preparation reveals a reduced density of TH+ cell bodies in Atrx KO retinas as compared to wildtype littermates (A vs C). Higher magnification reveals the presence of an altered dopaminergic network in Atrx KO as shown by the near absence of pericellular varicosities in flat mount preparations (D vs B).

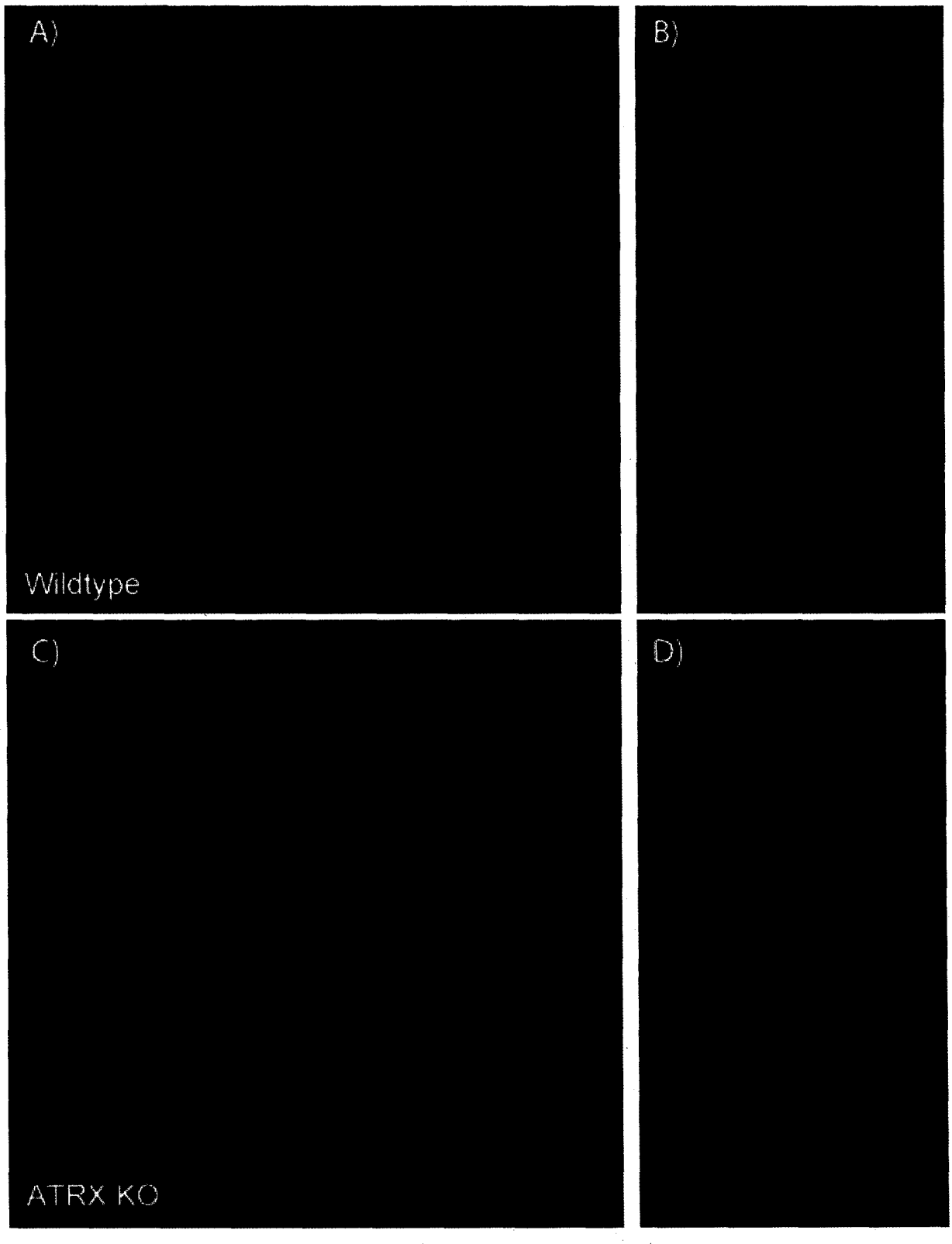
A)
B)
Wildtype
C)
D)
ATRX KO

Figure 13: The amacrine and horizontal cell phenotype is diminished in the central retina where Atrx expression is abundant.
Immunohistochemical analysis of the central region did not reveal a reduction in calbindin+ horizontal cells and syntaxin+ cells amacrine cells or in the width of the inner plexiform layer, revealed here by syntaxin staining (A vs F and B vs G). IHC for horizontal and amacrine markers in wildtype and Atrx KO retinas did not reveal any gross abnormalities in the morphology or number of these cells: Calretinin+ tracks in the inner plexiform layer retain a similar organization in Atrx KO and wildtype (C and H) Prox 1+ amacrine cells are located in the inner region of the INL (arrows in D and I) are present in similar numbers in the central retina in both wildtype and Atrx KO retinas. TH+ tracks (E and J), which are irregular in the periphery, become continuous in the central retina of Atrx KO.

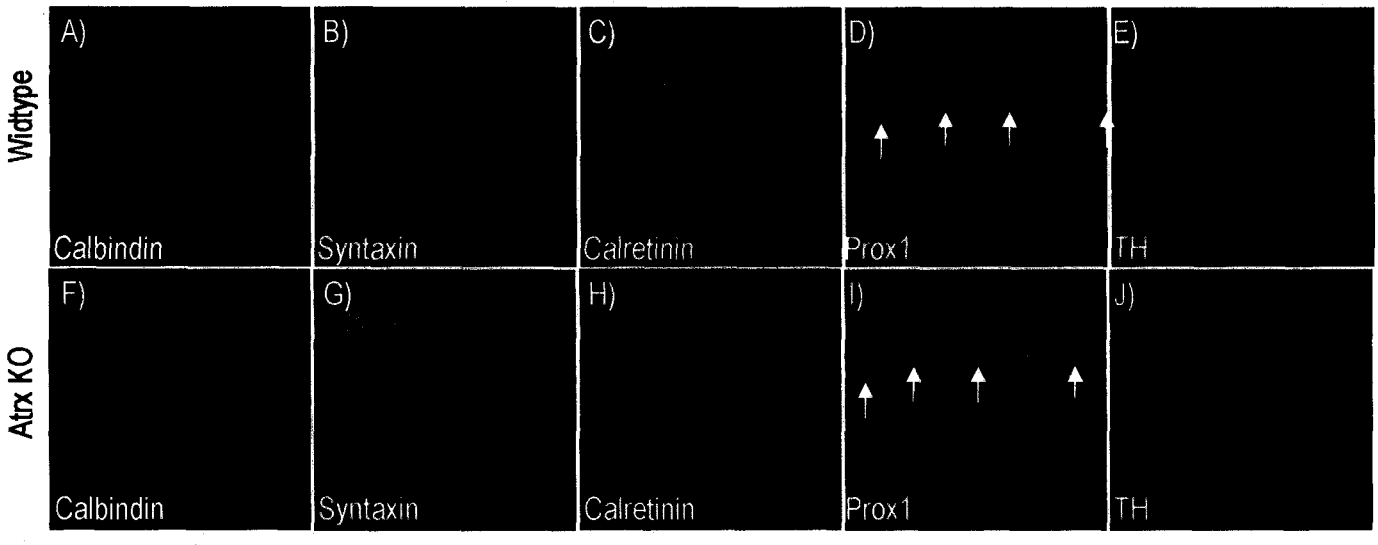
Widtype
Atrx KO
A)
Calbindin
B)
Syntaxin
C)
Calretinin
D)
Prox1
E)
TH
F)
Calbindin
G)
Syntaxin
H)
Calretinin
I)
Prox1
J)
TH

Figure 14: Cell type specific characterization of SNF2L KO retinas.
Retinal sections from adult (6-8 weeks) mice were immunostained for retinal cell-specific markers (red) and DAPI (blue) to reveal nuclei. DAPI staining revealed no gross lamination or lamination defects in SNF2L KO retinas. Cone photoreceptors (cone-arrestin+), RGC (Brn3b+), rod bipolar (CHX10+) and Müller glia (GFAP+) reactivity was comparable in both SNF2L KO mice, and wildtype littermates (A-F and I, L). Furthermore, unlike Atrx KO animals, no changes in horizontal (calbindin) or amacrine cells (syntaxin) immunoreactivity was observed in SNF2L KO, suggesting that not all mammalian chromatin remodeling proteins are essential for the proper development of amacrine and horizontal cells.

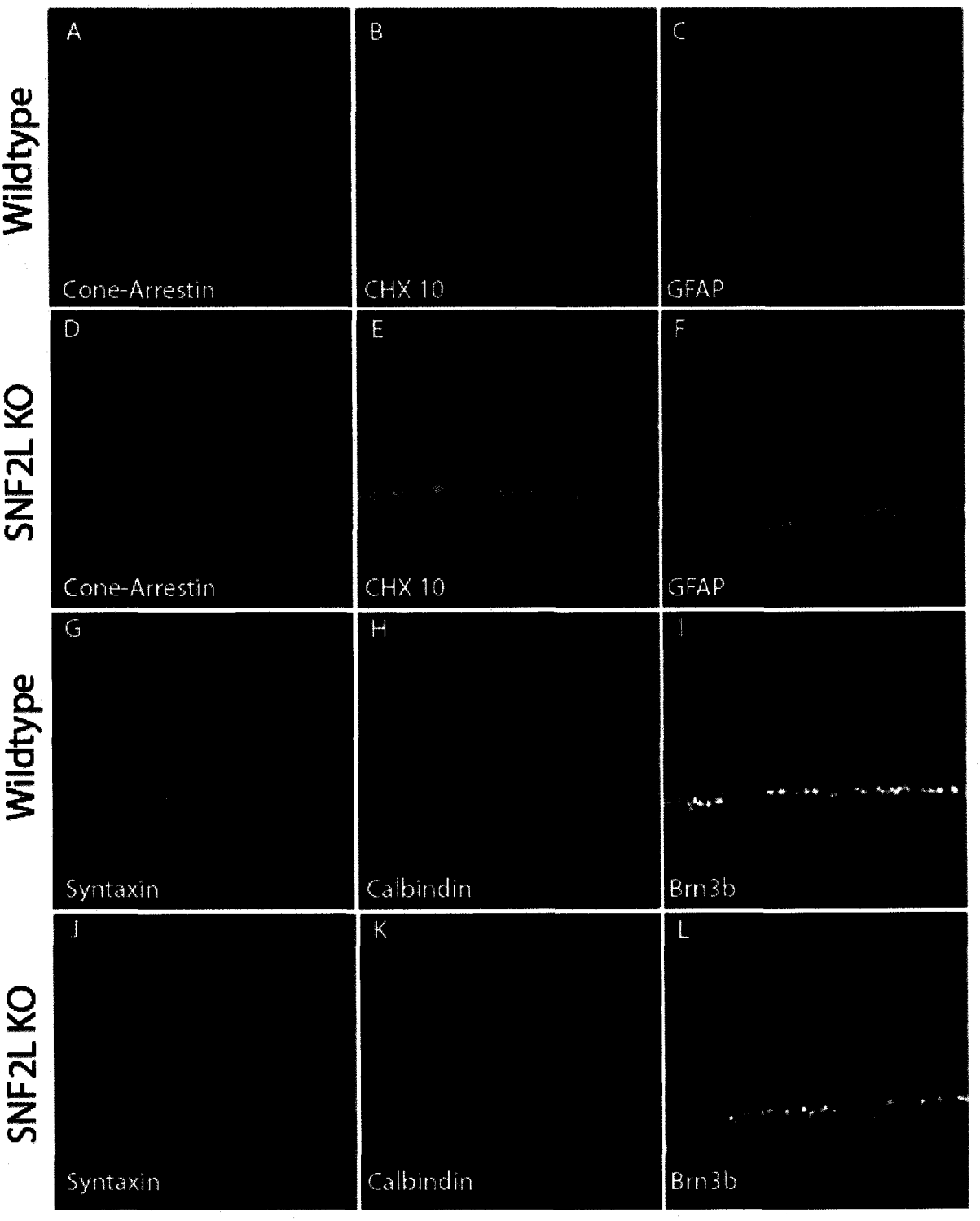
Wildtype
SNF2L KO
Wildtype
SNF2L KO
A
B
C
Cone-Arrestin
CHX 10
GFAP
D
E
F
Cone-Arrestin
CHX 10
GFAP
G
H
I
Syntaxin
Calbindin
Brn3b
J
K
L
Syntaxin
Calbindin
Brn3b

Thus, our data suggests that Atrx inactivation specifically results in a significant reduction in horizontal cells and in multiple subtypes of amacrine neurons.

3.3 Characterization of amacrine cell embryonic development in conditional Atrx knockout

3.3.1 Embryonic gene expression profile is unaltered in Atrx KO

ATRX is a chromatin remodeling protein thought to regulate the transcription of specific target genes, thus we reasoned that it might regulate genes necessary for the proper development of amacrine and horizontal cells. We therefore examined the expression pattern of basic helix loop helix (bHLH) and homeodomain (HD) transcription factors necessary for the generation of these cell types. To this effect, previous studies have shown that the bHLH factor *Pax6* is required for retinal progenitor multipotency as upon its inactivation, retinal progenitors become restricted to the amacrine cell fate (113). Furthermore, the winged-helix-loop-helix transcription factor *Foxn4* has been shown to play a critical role in the specification of horizontal and amacrine cell fate as ablation of this factor in the retina results in the complete absence of horizontal and amacrine cells due to the mysregulation of the bHLH factors *NeuroD1*, *Math 3* and *Prox 1* (126-128). Moreover, recent studies have illustrated that the bHLH factor Ptf1a acts downstream of *Foxn 4* to control amacrine and horizontal cell development by regulating other terminal differentiation factors such as the horizontal cell specific factor *Lim-1* (129, 130).

In the mouse retina horizontal cells become postmitotic between E11 and E16 while the generation of amacrine cells spans a period of two weeks beginning at E11 and

Figure 15: RNA *in situ hybridization* analysis of gene expression in the developing retina of Atrx KO mice.

RNA in situ hybridization for bHLH and homeodomain transcription factors implicated in amacrine and horizontal cell development in the retinas of Atrx KO and wildtype littermates at E13.5, E15.5 and P0. Altered expression of *Foxn4, Math3* and *Prox1* was noted at E15.5 and P0 in the Atrx KO retina. *Pax6* expression was unaltered as was the expression of *Math5* an important regulator of ganglion cell fate.

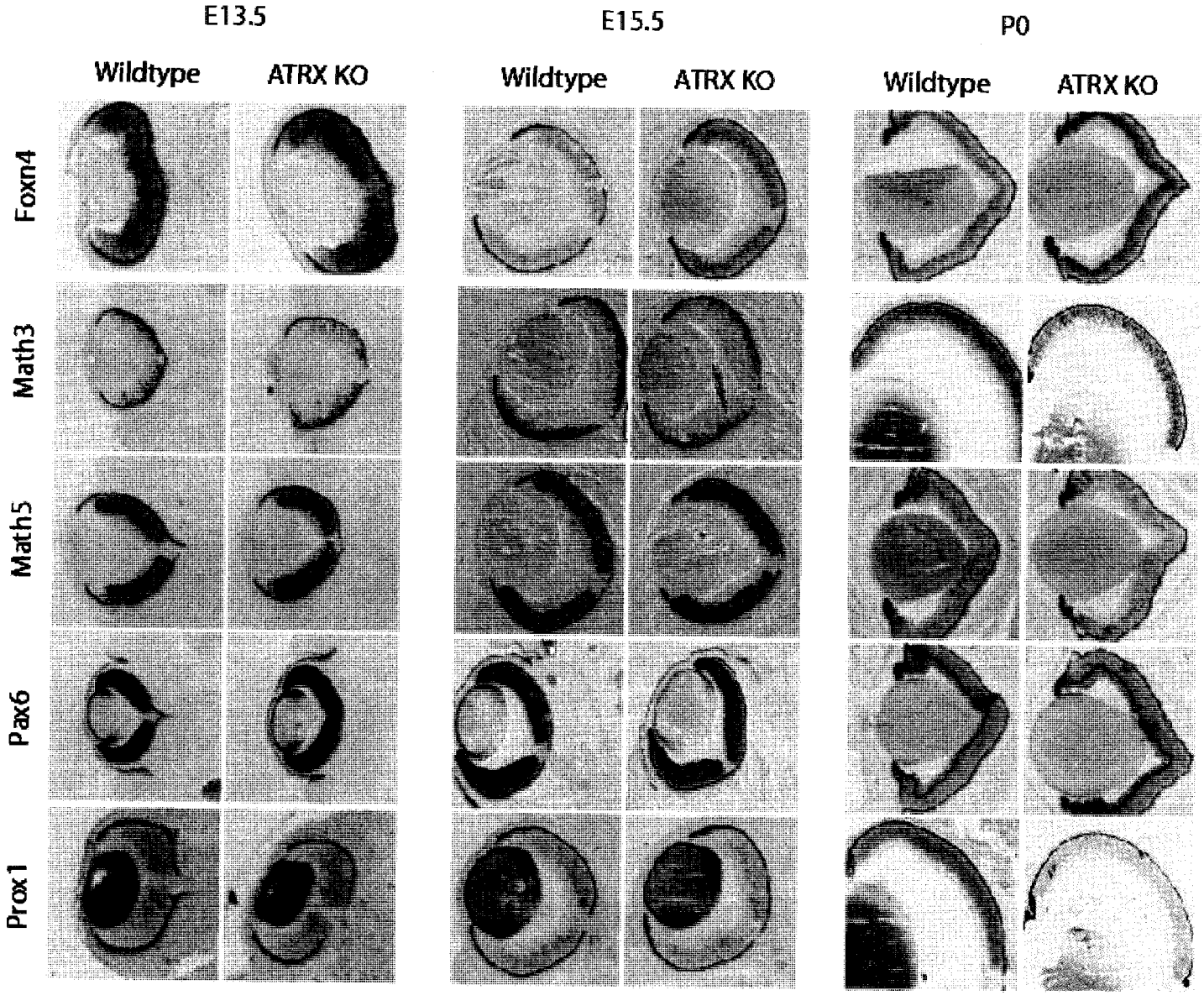
E13.5
E15.5
P0
Wildtype
ATRX KO
Wildtype
ATRX KO
Wildtype
ATRX KO
Foxn4
Math3
Math5
Pax6
Prox1

ending at postnatal day 3 (P3) (131). We therefore examined via RNA *in situ* hybridization analysis, the expression of transcription factors important for amacrine and horizontal cell fate between E13.5 and P0. As illustrated in Figure 15, at E13.5 RNA in situ hybridization analysis revealed no changes in the expression of the bHLH genes *Math 3* and *Math5* or in the HD gene *Pax6* and *Prox1* and the winged helix loop helix transcription *Foxn4*. The expression of the bHLH genes *Math5* as well as the HD gene *Pax6* remained similar in both wildtype and Atrx KO retinas at E15.5 and at birth. However, on two separate occasions, notably differential gene expression levels starting at E15.5 was observed in mutant retinas for some of these factors. A decrease in *Math3* and P*rox1* expression was observed at E15.5 and persisted until birth while Fo*xn4* appeared to be increased in the retinas of conditional KO at the same time points (Figure 15). To confirm these changes we carried out real time RT-PCR analysis on the retinas of E17.5 animals. Albeit a greater than 2-fold decrease in Atrx expression in Atrx KO retinas, no changes in expression of key regulators of amacrine and horizontal cell fate was observed (Figure 16). As illustrated in Figure 16, Chx 10, Foxn 4, NeuroD1, Math3, Pax6, Prox1, Ptf1a and the terminal horizontal differentiation marker Lim1 were expressed at similar levels in both wildtype and Atrx KO retinas.

3.3.2 Loss of Atrx has no impact on embryonic amacrine cell birth

Although we were unable to quantify changes in the embryonic gene expression profile of Atrx KO retinas, it remained a possibility that the phenotype observed in Atrx KO animals reflected a failure to generate amacrine neurons. Therefore, we

Figure 16: Genes involved in the specification of amacrine and horizontal cells are expressed normally in Atrx KO

Quantitative RT-PCR analysis on RNA isolated from whole retina at E17.5 for the indicated genes. The results are presented as the expression of each gene relative to wildtype levels ± s.e.m. All levels were standardized to GAPDH and 18S expression. Note that Atrx expression is significantly decreased by 2.3-fold in Atrx KO retinas. No other significant changes in key regulators of amacrine and horizontal cell fate such as *Foxn 4, NeuroD1, Neuro D4, Pax6, Prox1, Ptf1a* and *Lim1* was observed. *Chx10* expression served as an internal control and was also unaltered in ATRX KO retinas. (*$p \leq 0.008$; n=7 Student T-TEST)

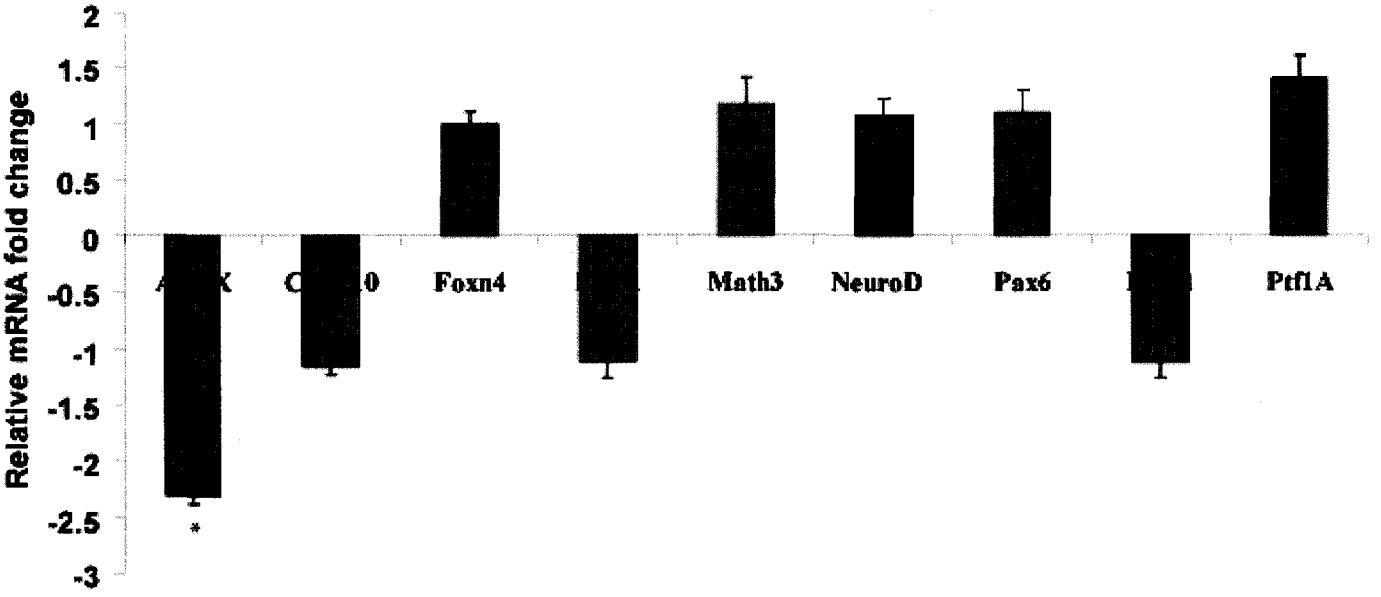
Relative mRNA fold change
2
1.5
1
0.5
0
-0.5
-1
-1.5
-2
-2.5
-3
Foxn4
Math3
NeuroD
Pax6
Ptf1A
*

performed BrdU birthdating experiments to address whether the reduction in amacrine cell number resulted from impaired embryonic development.

Pregnant females were injected with two doses of BrdU, at a two hour interval, to label cells in S-phase at three embryonic stages (E13.5, E15.5 and E17.5) and pups were harvested at birth. Retinas were stained with anti-BrdU antibodies and cells with intense BrdU labeling were scored as birthdated on the day of BrdU injection. The number of intensely labeled cells located in the inner half of the INBL (amacrine cells) or the GCL (displaced amacrine cells and RGC) were quantified. As shown in Figure 17, similar numbers of BrdU positive cells were found in both the INBL and GCL of wildtype and Atrx KO retinas. Thus it appears that Atrx is not required during embryonic development for the generation of amacrine cells and RGCs but may have an important role later on during differentiation.

3.4 Postnatal amacrine and horizontal cell survival is compromised in Atrx KO retinas

As the generation of amacrine cells at embryonic stages was unaltered in our mutant animals, this prompted us to look at the status of amacrine cells at different stages in the post-natal retina. The number of Pax6 positive amacrine cells was not significantly different at P7 and P10 in both wildtype and mutant retinas (Figure 18 C). By P14, the number of amacrine cells was reduced, albeit not significantly. However, by P17 there was a significant reduction in amacrine cell number in the KO retina. Loss of amacrine cells was not progressive after P17, as the reduction in amacrine cell number was equivalent in the adult KO retina. Amacrine cell loss was not associated with an increase

Figure 17: Amacrine cell reduction in Atrx KO retinas is not secondary to impaired generation of this cell type.
Pregnant females were injected with BrdU at E13.5, E15.5 or E17.5. Pups were harvested at P0 and immunostained with anti-BrdU antibodies. Cells with intense BrdU staining were considered to have exited the cell cycle on the day that they incorporated the label and were scored as "born". The number of heavily labeled cells in the (A) GCL and (B) inner neuroblast layer (INBL) from animals receiving a 2 hour pulse of BrdU on the indicated days was scored. The cells located in the lower half of the INBL are amacrine cells, cells in the GCL layer could be amacrine or RGC cells. No significant difference in the number of birthdated cells in the GCL or INBL was observed in the retinas of Atrx KO compared with wildtype littermates.

A)

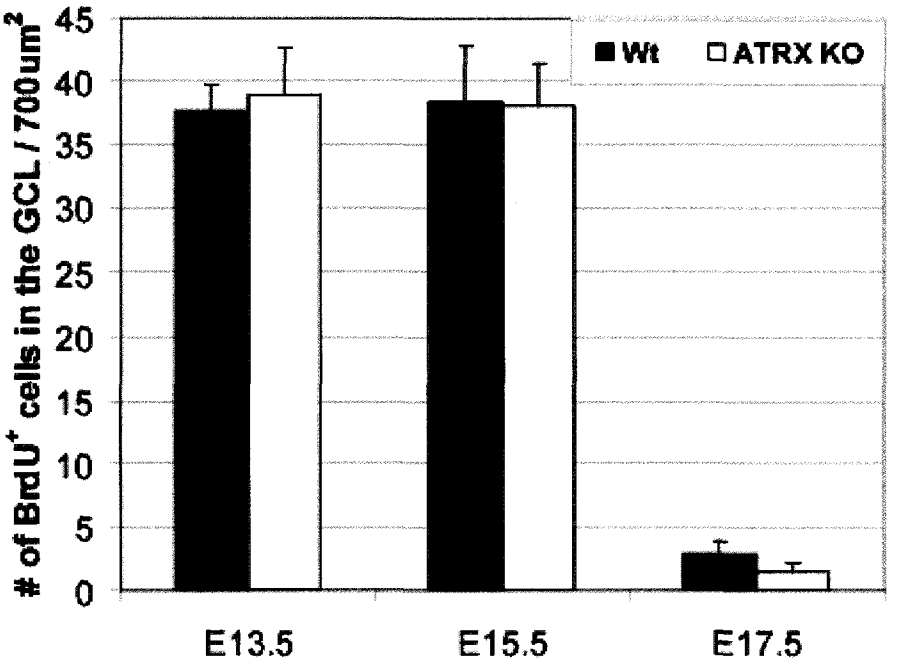
# of BrdU+ cells in the GCL / 700um2
45
40
35
30
25
20
15
10
5
0
Wt
ATRX KO
E13.5
E15.5
E17.5

B)

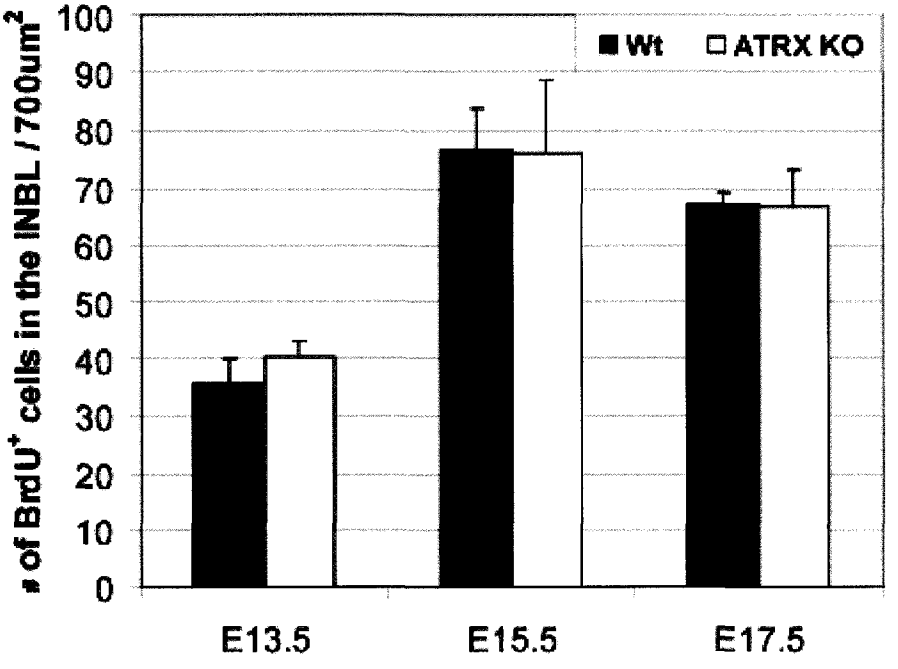
# of BrdU+ cells in the INBL / 700um2
100
90
80
70
60
50
40
30
20
10
0
Wt
ATRX KO
E13.5
E15.5
E17.5

Figure 18: Loss of horizontal cells occurs before P7 while gradual loss of amacrine cells occurs between P10 and P17 in Atrx KO retinas

A) Calbindin immunoreactive horizontal cells were reduced as early as P7 in Atrx KO retinas. B) In wildtype animals, the timing of horizontal cell death coincides with a change in Atrx subnuclear localization in horizontal cells from heterochromatin to homogenous nuclear as shown by calbindin-Atrx colocalization. C) The number of Pax6 positive cells in the INL of wildtype or Atrx KO was quantified at the indicated times. A small but non-significant reduction in the number of Pax6+ cells was observed in Atrx KO retinas at P14. A significant reduction in the number of Pax6+ cells was observed by P17 and in adult retinas. D) Immunohistochemistry for Atrx shows that in wildtype mice, the period of amacrine cell loss also coincides with a change in Atrx nuclear localization in amacrine cells. E) No significant increase in TUNEL positive nuclei in the INL was detected at P10, P14 or P17 in Atrx KO retinal section counterstained with DAPI. (*$p \leq 0.01$;**$p \leq 0.05$ $n \geq 3$ Student T-TEST)

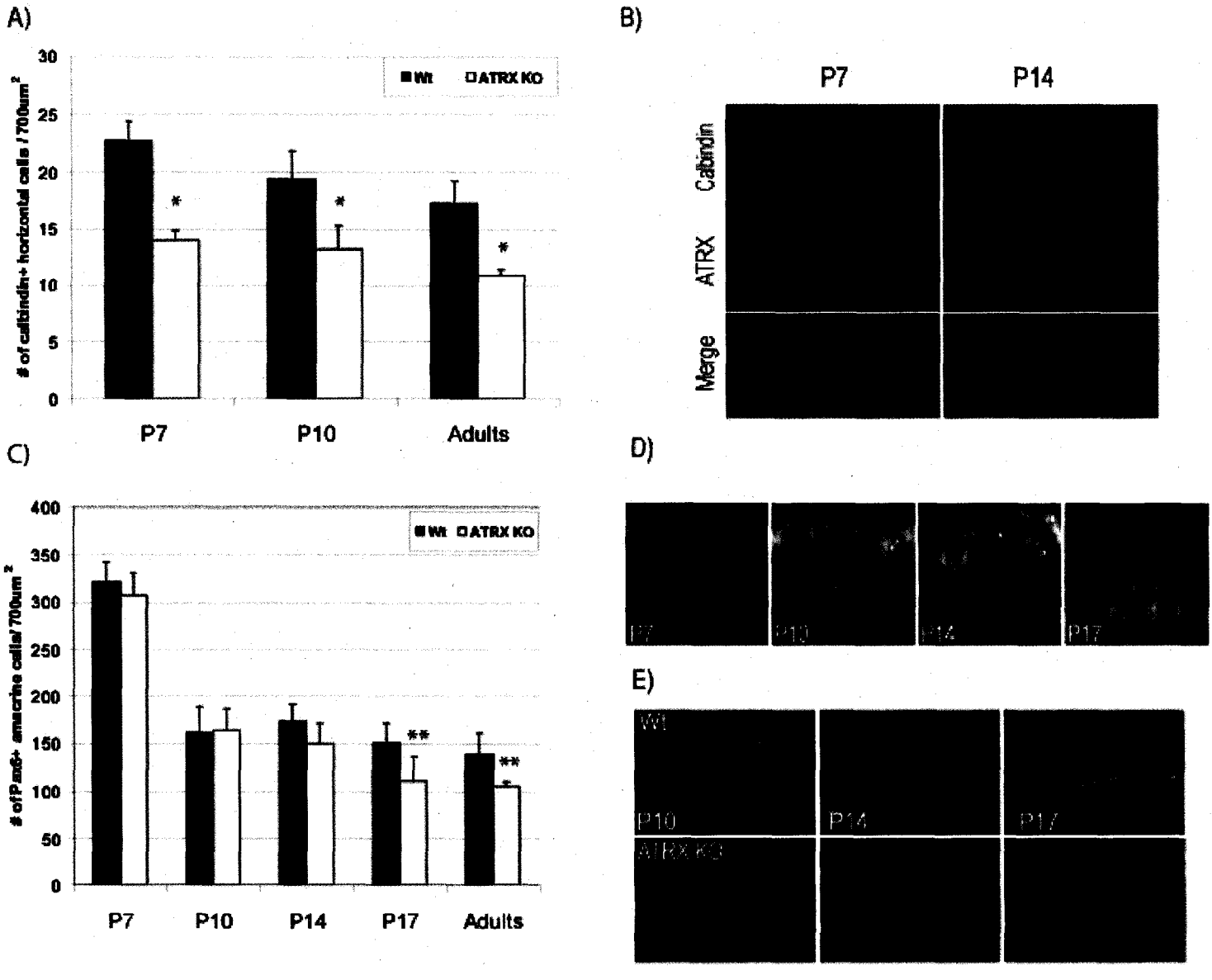
A)
B)
C)
D)
E)
Wt
ATRX KO
# of calbindin+ horizontal cells / 700um²
P7
P10
Adults
P7
P14
Calbindin
ATRX
Merge
# of Pax6+ amacrine cells/ 700um²
P14
P17
P10
P17
ATRX KO

in TUNEL staining in retinal sections of KO retina (Figure 18 E and data not shown). Interestingly, the loss of amacrine cells coincides with a change in Atrx subnuclear localization. At P7, Atrx staining in the inner half of the INL and GCL gives rise to a nuclear speckle staining which colocalizes with regions of intense DAPI staining, a pattern consistent with the heterochromatin colocalization of Atrx previously reported in murine cells (92). This nuclear speckle staining pattern gradually changes to a homogenous Atrx nuclear staining pattern by P17 (Figure 18 D). This change in Atrx nuclear localization does not reflect a change in the status of pericentromeric heterochromatin as intense DAPI staining persists in all cells of the INL in the murine retina.

Horizontal cells are also decreased by ~37% in Atrx KO animals. For this cell type we observed a decreased number of calbindin+ horizontal cells by P7 in our mutant retinas. As illustrated in Figure 18 A, the decline in the number of horizontal cells did not significantly progress after P7 as a similar reduction in calbindin positive horizontal cells was found in both P7 and adult retina (33% vs 37%). Similar to amacrine cells, subnuclear localization of Atrx is altered in horizontal cells around P7 when presumably these cells are lost. Taken together our results illustrate that disruption of Atrx expression in the retina results in the gradual loss of amacrine cells in the post-natal retina between P10 and P17 and correlates with a switch in Atrx staining pattern. Furthermore, loss of Atrx impairs horizontal cell generation or survival prior to P7.

3.5 Characterization of visual system phenotype of Atrx KO mice and ATR-X patients

3.5.1 ATRX KO mice have impaired visual function

To investigate if the amacrine and horizontal cell phenotype in Atrx KO animals resulted in impaired retinal function, we performed electroretinograms (ERGs) on dark-adapted adult wildtype and Atrx KO animals. ERGs measure the electrical response of the various components of retina to photic stimulation. These tests are normally divided into a hyperpolarizing a-wave and a depolarizing b-wave that assays photoreceptor and inner layer function respectively. ERG recordings revealed comparable a-wave amplitude in both Atrx KO and wildtype littermates (Figure 19A). Latency times were also unaffected in Atrx KO (Figure 19B). However, there was a 30-35% reduction in b-wave amplitude in Atrx KO at the five highest light intensities tested (Figure 19C). As the b-wave is indicative of INL function, it is likely that the amacrine and horizontal cell phenotype exhibited by Atrx KO contributes to the attenuated ERG reading observed.

3.5.2 ATR-X patients exhibit a variety of visual defects

To determine if the observation noted in our animal model was relevant to the clinical manifestation of ATR-X syndrome, we surveyed the clinical findings of ATR-X patients to determine if the severe phenotype exhibited by these patients may have overshadowed subtle sensory defects, such as impaired vision.

Figure 19: Impaired retinal function in Atrx KO animals
ERGs were recorded from 6-8 weeks old wildtype and Atrx KO littermates under dark-adapted (scotopic) conditions. Average amplitude ± standard error of the mean for the a-wave (A), the latency time (B) and the b-wave amplitude (C) at the 7th to 11th steps are graphed. A 30-35% decrease in b-wave amplitude was observed in Atrx KO animals (*$p \leq 0.0004$; n=22, ANOVA analysis)

A)

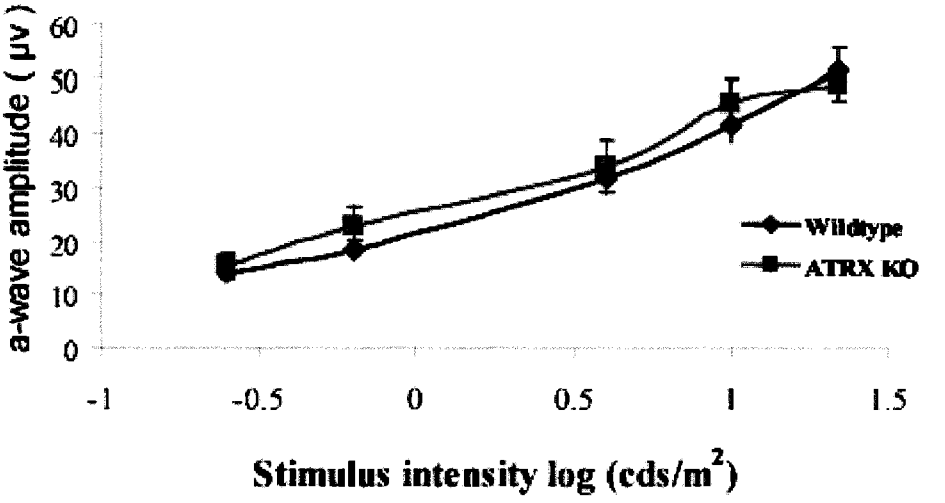
a-wave amplitude (µv)
60
50
40
30
20
10
0
-1
-0.5
0
0.5
1
1.5
Wildtype
ATRX KO
Stimulus intensity log (cds/m2)

B)

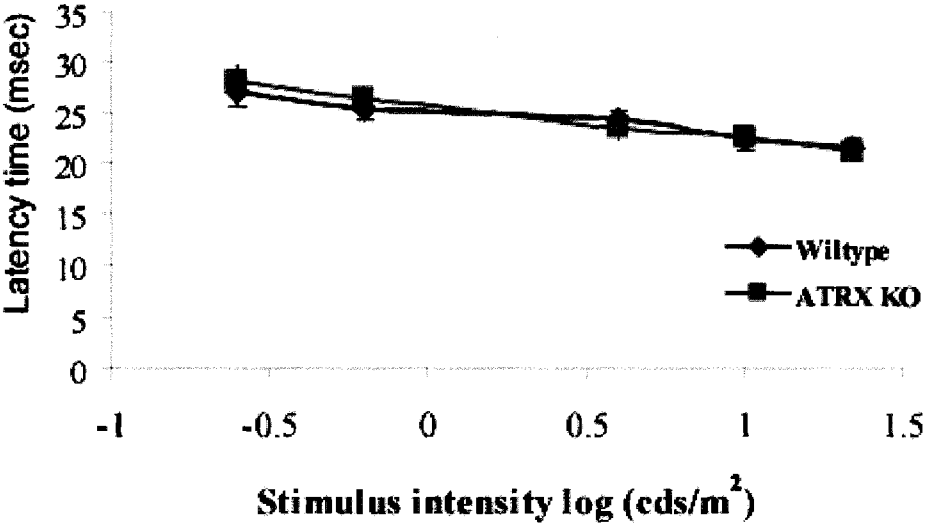
Latency time (msec)
35
30
25
20
15
10
5
0
-1
-0.5
0
0.5
1
1.5
Wiltype
ATRX KO
Stimulus intensity log (cds/m2)

C)

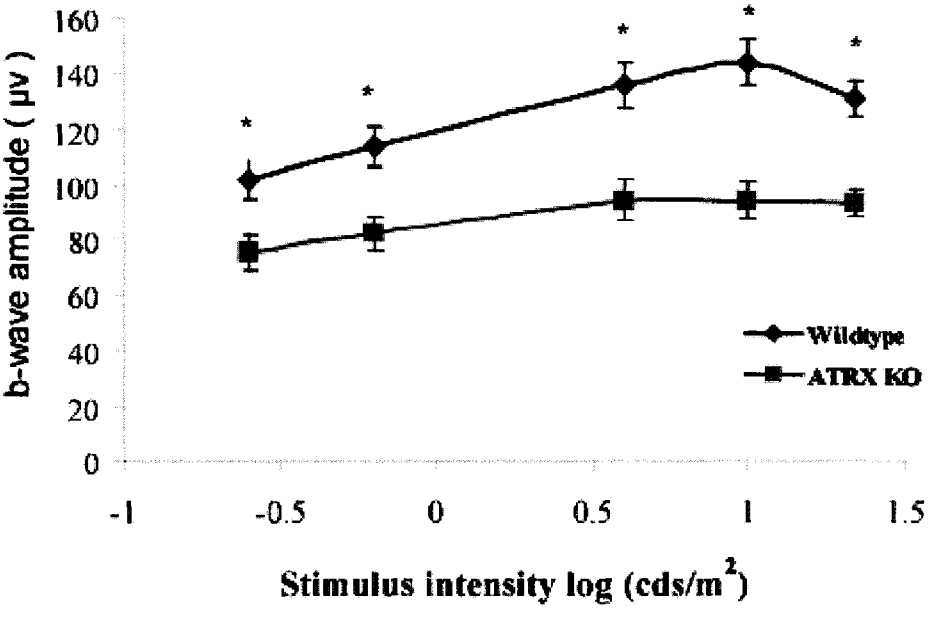
b-wave amplitude (µv)
160
140
120
100
80
60
40
20
0
-1
-0.5
0
0.5
1
1.5
*
Wildtype
ATRX KO
Stimulus intensity log (cds/m2)

After surveying the clinical findings of 202 patients, which are currently or had previously been under the care of a physician, we observed that in 23% (47 out of the 202) patients, visual anomaly had been previously annotated. These are summarized in Table 3. Strabismus, myopia, pale disc and optic nerve atrophy or hypoplasia were the most common visual deficiency observed amongst ATR-X patients. Two ERG recordings from two distinct ATR-X patients were obtained. The first which had been performed on an infant had high background noise and was deemed un-interpretable. The other ERG recording we obtained had been performed many years ago on a now deceased patient. This patient had been diagnosed with strabismus and optic nerve atrophy. ERG recording had a reduced response characterized by a delay in peak latency. Nevertheless, in most instances there appeared to be no follow up to the original diagnosis. This may reflect the minimal significance of the eye defect as compared to their other symptoms. Moreover, this also suggests that visual defects may be significantly under-reported in ATR-X patients. Nonetheless, the clinical data suggests a role for ATRX in the developing visual system and therefore warrants further study.

4.0 Discussion

In recent years, advances in genetics have allowed for the rapid identification of many disease causing genes. These studies have brought to light the involvement of many epigenetic regulators in the development and pathogenesis of human disorders. Of particular interest have been the mediators of chromatin structure which are located on the X chromosome. Studies to date have illustrated that a number of these genes are

Table 3: Prevalence of visual anomaly in ATR-X patients
Noted is the prevalence of different visual phenotypes annotated in 47 ATR-X patients. A total of 47 patients of a total of 202 surveyed were found to have clinical annotation of visual system anomaly.

Phenotype	% of ATR-X patients affected (N=47)
Strabismus	34%
Myopia	26%
Pale disc	19%
Optic atrophy or hypoplasia	15%
Squint (convergent and divergent)	15%
Nystagmus	11%
Coloboma	4%
Blindness	4%
Astigmatism	4%

implicated in severe developmental and cognitive delay. Examples of these include, *MECP2*, *PHF6* and *ATRX* which lead to Rett Syndrome, BFLS, and ATR-X syndrome respectively.

Although the causative gene for many diseases have been identified, the functional role of the encoded protein often remains ambiguous at best. In this regard, ATRX is a prime example. The undefined role of proteins such as ATRX is a major obstacle in the development of effective treatment options. In the present study, we sought to better comprehend the biological function of ATRX to gain a better understanding of the molecular basis for the phenotype observed in patients.

Its chromatin remodeling activity as well as the early requirement for Atrx during embryogenesis has led us to propose that it may be involved in the modulation of genes that are critical for the maturation of the central nervous system. As studies of the CNS can pose quite an obstacle due to its overwhelming complexity, we utilized the retina as our model. The use of the retina as a model of CNS development is quite advantageous as tissues are easily accessible and neuronal cell genesis in this system is well defined and highly conserved. In addition, the use of the retina enabled us to explore the possible visual system deficit in ATR-X patients, which to date, has been mostly disregarded.

4.1 Atrx is widely expressed in the developing and mature retina

Consistent with previous observations in the developing cortex, Atrx expression was found to be ubiquitous in all retinal progenitors as of E13.5. Atrx expression within the neuroprogenitor pool persisted throughout retinal development (Figure 6) (100). As

previously reported in murine cells, within retinal progenitors Atrx expression was nuclear and coincided with heterochromatin as identified by regions of intense DAPI staining (92, 100). Again, similar to what has been observed during murine cortical development, upon retinal differentiation more intense Atrx staining was detected in post-mitotic cells, as compared to the progenitor population. This may reflect higher levels of protein in differentiated retinal cells (Figure 6 D-I) (100). In the mature retina Atrx expression was maintained in all cell types with the exception of rod photoreceptors (Figure 7A-F). Albeit still nuclear, Atrx expression in ganglion, amacrine, horizontal, bipolar and Müller cells was diffuse and no longer coincided with DAPI bright spots and heterochromatic regions. However, in cone photoreceptors, Atrx staining was found to be weak and perinuclear (Figure 7 G and H).

The change in Atrx expression patterns from pericentromeric heterochromatin to a diffuse nuclear staining pattern may indicate a shift in the set of target genes modulated by Atrx during retinal development. In support of this, disease causing mutations have been shown to alter the nuclear localization of ATRX away from PML nuclear bodies where it is normally found, thus suggesting that proper Atrx localization is essential for proper CNS development (89). As Atrx expression is absent from rod photoreceptors and is perinuclear in cone photoreceptors this seems to suggest that mature photoreceptors do not require the chromatin remodeling activity of Atrx for their maintenance and survival.

4.2 Ablation of Atrx results in retina dysplasia

As we found Atrx to be abundantly expressed in the retina, we determined it would be an appropriate model to study the impact of Atrx ablation on CNS development. To gain a better understanding of the molecular basis for the clinical phenotype observed in ATR-X patients and to further elucidate the function of Atrx in neuronal development, we generated a murine model in which Atrx inactivation is confined to the peripheral retina. At the age of maturity, these α-cre;$Atrx^{f/y}$ (Atrx KO) mice exhibited retinal dysplasia characterized by a reduction in the thickness of the INL and IPL (Figure 9). Thinning of the INL was attributed to a reduction in cell number; more specifically a reduction in horizontal and amacrine interneurons while the observed reduction in the IPL was credited to the loss of amacrine cell processes which form synapses with ganglion cells in this region (Figure 9 K and L vs O and P, Figure 10 A and B). With the exception of horizontal cells and amacrine cells which were reduced by 37% and 25%, respectively, immunohistochemical analysis revealed that no other retinal neuronal cell types including ganglion, bipolar and cone photoreceptor cells were altered in Atrx KO retinas (Figure 10 C). The phenotype observed was specific to the regions of *Atrx* ablation, as an attenuated mutant phenotype was observed in the central retina where Atrx expression was abundant (Figure 13). In addition, a similar phenotype was not observed in mice which did not express SNF2L, a chromatin remodeling protein of the ISWI family, thus indicating the specificity of our phenotype to a loss of Atrx (Figure 14).

Morphological studies of the mammalian retina have identified close to 30 distinct subtypes of amacrine cells (124). Most of these amacrine subtypes were found to be positive either for the neurotransmitter gamma-aminobutyric acid (GABA) or glycine

(GLY). Together these two neurotransmitters account for about 70% of the amacrine cells, with GABA+ and GLY+ accounting for 40% and 30% respectively (132). Interestingly, all amacrine subtypes which were analyzed were found to be reduced (Figure 11 A-M). The glycinergic amacrine cell population was globally reduced by 25% as indicated by the decrease in glycine transporter 1 immunoreactivity. The most characterized glycinergic amacrine subtype, AII amacrine cells, was also reduced by 43 % as indicated by Prox1 staining. Calretinin, another marker which can be used to identify AII amacrine cells was also significantly reduced. Starburst amacrine cells are one of the most characterized GABAergic amacrine subtype and are identified by ChAT immunoreactivity (133). Although we could not conclusively demonstrate a reduction in ChAT+ cell number in retinal sections, ChAT immunoreactivity was obviously altered in Atrx KO retinas. ChAT staining usually reveals two outer tracks in the IPL which corresponds to starburst amacrine processes which synapse in both the OFF and ON sublamina (109, 123). This pattern was significantly disturbed in Atrx KO mice and ChAT+ processes appeared drastically disorganized (Figure 11 H vs K). Thus our data suggests that Atrx is an epigenetic regulator essential for the specification of all amacrine and horizontal cells in the mouse retina.

A18 amacrine cells are a glycinergic amacrine subtype which can be identified by tyrosine hydroxylase immunoreactivity. A reduction in TH+ positive cell bodies could not be identified in retinal sections due to the low density of this cell type in the murine retina (450/retina) (134). Nevertheless, the amacrine dopaminergic network was obviously disturbed in Atrx KO mice as shown by the reduction in the density of TH positive cell bodies and varicosities in flat mount preparation (Figure 12). A similar

alteration of the dopaminergic system has been observed in mice deficient for the neurotrophins brain-derived neurotrophic factor (BDNF) and neurotrophin- 4 (NT-4) (133, 135, 136). Interestingly, a known ATRX interacting protein MeCP2 has been recognized as an important transcriptional regulator of BDNF expression (137, 138). As in the case of MeCP2 deficient mice and Rett syndrome, it is plausible that diminished neurotrophin expression may contribute to the phenotype observed in Atrx KO mice (139, 140).

As shown in retinal sections, changes in the lamina-specific distribution of calretinin and ChAT immunoreactive processes in the IPL were also evident in Atrx KO retinas (Figure 11 H vs K). Such changes cannot be explained by misregulation of BDNF or other neurotrophins as these two markers are unaffected in BDNF or NT-4 knockout animals or by injection of neurotrophins (135, 136). Other molecules, such as cell adhesion molecules are also known to impact the dendritic morphology within the CNS including proper retinal lamination of amacrine and horizontal cell processes (141, 142). More specifically, loss of N-cadherin, a member of the cadherin adhesion molecule family, has been shown to be essential to mediate neurite outgrowth and targeting of amacrine cells in zebrafish. Similarly, in the chick retina, N-cadherin mediates dendritic outgrowth of horizontal cells as well as proper dendritic targeting onto photoreceptor synapses (142, 143). In support of the idea that Atrx is involved in mediating the expression of one of the cadherin family members, the N-terminal domain of Dnmt3b which shares considerable homology to Atrx has been shown to negatively regulate T-Cadherin by suppressing the T-cadherin promoter (144). Consequently, T-Cadherin was found to impede NGF-induced neurite outgrowth in PC12 cells (144).

Recent studies have also shown that molecules such as DSCAM, DSCAM- like1 and Sidekick are required for proper targeting of neurite arborization of different amacrine subtypes (145, 146). Because our amacrine phenotype targets all amacrine subtypes tested, and targeting of different amacrine and horizontal cell stratification is mediated by different molecules, it is possible that the chromatin remodeling activity of Atrx is required at all of these distinct target genes.

Whether the apparent altered dendritic morphology in Atrx KO retinas is the result of abnormal cell number or is the result of inappropriate synaptic connections due to misexpression of one or more Atrx target genes remains to be determined.

4.3 Normal embryonic amacrine cell development in Atrx KO

We have shown previously that loss of Atrx in the forebrain and cortex results in widespread hypocellularity due to increased apoptosis during the first wave of differentiation (100). In contrast to the forebrain knockout, our birthdating analysis reveals that amacrine cell generation is normal in α-cre;$Atrx^{f/y}$ animals and that early retinal lamination is unaffected by early cell death (Figure 17 A and B). Our birthdating experiment also suggests that Atrx KO animals exhibit no defects in their neuroprogenitor pool as amacrine cells are born in appropriate numbers. Our data also contradicts a recent report which suggests that Atrx is required for cell cycle progression, more specifically for chromosome dynamics during mitosis (96). This suggests that Atrx may have cell type specific functions.

In support of the idea that chromatin remodeling associated with progenitor competence towards an amacrine and horizontal cell fate does not require Atrx, the expression of bHLH and HD transcription factors required for amacrine and horizontal specification such as, *Foxn 4, NeuroD, Math3, Pax6, Prox1, Ptf1a* were unaffected in our model as determined by qRT-PCR (Figure 16). Although there is some discrepancy between our *in situ* hybridization analysis and our qRT-PCR data, the increased sensitivity and the number of biological replicates used in our qRT-PCR analysis, makes a strong argument for the results obtained via this method. Thus, our data confirms that in the retina, in contrast to the forebrain and cortex, Atrx is not required for cell fate determination but may be required for differentiated cell function and plasticity.

4.4 Thinning of the INL and IPL in Atrx KO is due to the postnatal loss of amacrine cells

As amacrine and horizontal cell embryonic development appeared normal in Atrx KO mice we looked at the post-natal status of these cells. Consistent with normal amacrine cell genesis, the number of Pax6+ cells was similar at P7 and P10 in Atrx KO and wildtype littermates (Figure 18 C). However by P14, a small but non significant decrease in Pax6+ cells was observed in Atrx KO. By P17, a significant decrease in Pax6+ cells was evident in Atrx KO retinas. The decrease in Pax6+ cells was not accompanied by an increase in TUNEL positive nuclei in the INL (Figure 18 E). A possible explanation for such an observation is that amacrine loss occurs over several days and therefore the frequency of cell death may be too low to detect using this method as retinal sections only offer a snapshot of the whole retina.

Although our gene expression analysis suggests that horizontal cell development is normal in Atrx KO mice we were unable to confirm by immunohistochemistry if horizontal cells were properly generated in our model. As horizontal cells comprise less than 3% of the cells in the INL, we were unable to perform birthdating to conclusively determine if this cell type was generated in appropriate numbers (133). The mature horizontal cell marker calbindin was not distinguishable before P7, a timepoint where horizontal cells are already reduced by ~38% in Atrx KO mice (Figure 18 A). The LIM class homeodomain transcription factor *Lim1* is expressed in postmitotic, differentiating, and mature retinal horizontal cells (147). *Lim1* is thought to act cell autonomously to direct differentiating horizontal cells to the appropriate laminar position in the developing retina (147-149). Other groups have illustrated that Lim-1 expression can be detected by immunohistochemistry as early as E18.5 in the mouse retina (147, 149). However, in our hands numerous attempts with two different previously published and commercially available antibodies were unsuccessful.

Therefore we attributed the retinal dysplasia observed in Atrx KO animals to the gradual loss of amacrine cells in the postnatal period between P10 and P17. In addition, the *Lim1* expression profile at E17.5 as determined by qRT-PCR suggests that horizontal cell development is normal in Atrx KO retinas. However, we were unable to conclude when these cells were lost as they were already absent at P7, the earliest time point we were able to positively identify horizontal cells by immunohistochemistry. As cell death occurs much later in our model, in a post-mitotic cell population compared to the forebrain KO, this suggests that Atrx plays different roles within distinct cell types of the CNS.

Loss of horizontal and amacrine cells correlated with a change in Atrx subnuclear localization from pericentromeric heterochromatin to heterogeneous nuclear staining thus suggesting a shift in Atrx chromatin activity (Figure 18 B and D). Interestingly, the period of amacrine cell loss coincides with eye opening and retinal synaptic remodeling, which could be indicative that Atrx is important for chromatin reorganization in response to external stimuli as well as neurite extension and survival during synaptogenesis (131, 150).

Light stimulation has been shown to be required for the final maturation of ganglion and starburst of amacrine cells. While a strong link between activity-induced remodeling of ganglion cell dendrites and BDNF/TrkB receptors has been postulated, the underlying cause of the light-dependent changes on the spacing of the ChAT tracks in the IPL and the positioning of the cell bodies in the INL and GCL remains unknown (151-153). As loss of amacrine cells coincides with eye opening and a change in Atrx nuclear localization, it is possible that Atrx may be important for the epigenetic regulation of the genome during light induced synaptic remodeling.

Although the above mentioned mechanisms can explain the pan-amacrine cell death observed in Atrx KO mice, why the loss of amacrine cells is limited to 25% in regions of Atrx ablation is unknown. This phenotype is similar to the one observed when Atrx was deleted in the forebrain (100). Although there is a substantial increase in cell death, this only translates to a 20-30% reduction in cell number in the cortical plate. Previous unpublished work in our laboratory has shown that cell death in the absence of ATRX, occurs in a p53 dependent manner (DJP, unpublished). p53 is a tumor suppressor protein and an important transcriptional regulator of a number of signaling pathways

which play a role in cellular responses to various stress signals (154). Previous studies have shown that a certain threshold must be crossed in order to activate p53 dependent cellular apoptosis (155, 156). Thus, through epigenetic regulation of apoptotic pathways such as p53, Atrx may contribute to the balance between cellular apoptosis and survival.

4.5 Atrx ablation results in impaired visual function

Amacrine and horizontal cells are reduced by 25% and 37%, respectively in our Atrx KO model. This reduction, albeit restricted to the periphery, was sufficient to induce changes in ERG recording analyses on dark adapted animals. These results were somewhat surprising, as ERGs record the response from the whole retina (103). Our analysis revealed a significant decrease in INL function as measured by b-wave amplitude. Consistent with normal photoreceptor number and structure, the a-wave amplitude, was unaffected in our Atrx KO animals, as were the latency times.

While the a-wave is associated with photoreceptor response, the b-wave is associated with the combined activity of the depolarizing bipolar cells and bipolar dependent K+ currents affecting Müller cells (103). The reduction in b-wave amplitude thus suggests that the communication between photoreceptors and bipolar cells is defective although our immunohistochemical analysis did not provide any anatomical evidence to support this. The ERG component that is usually attributed to the interaction of amacrine cells with bipolar and ganglion cells is the oscillatory potentials (OP). Despite the reduction in amacrine cells in Atrx KO animals, OPs were clearly present in Atrx KO ERGs. Although the oscillatory potentials were not directly quantified, no gross delay or reduction was observed in Atrx KO animals although this may be due to the

subtlety of the phenotype which is confined to the peripheral retina in these animals. Attenuated ERG recordings in Atrx KO animals supports the notion that these animals exhibit altered retinal circuitry due in part to the loss of horizontal and amacrine cells.

Loss of amacrine interneurons is commonly observed in diabetic patients and diabetic animal models, such as the streptozotocin injected rat model and the $Ins2^{Akita}$ mouse (157, 158). Although a number of other retinal defects are present at various degrees, a reduction in b-wave amplitude and decreased OP amplitude has been reported in both animal models and diabetic patients suggesting that interneuron defects can indeed alter the b-wave response (159, 160).

Since Atrx is ubiquitously expressed in the INL it is possible that it impacts other cell types as well as amacrine and horizontal cells. Bipolar cells were expressed in normal numbers in Atrx KO mice as assayed by Chx10 staining. Furthermore, the rod bipolar marker PKC, and the Müller cell marker CRALBP also appeared normal in Atrx KO mice although absolute cell numbers were not quantified (132). However, normal number of Chx10 staining may not necessarily reflect normal bipolar function. For example, deletion of *VSX1* in mice results in normal Chx10 staining albeit a disruption in cone bipolar cell differentiation and a decrease in b-wave amplitude (161). In light of this, two other mechanisms may also contribute to the observed decrease in b-wave amplitude. Perhaps Atrx is required for the expression of proteins essential for synaptic transmission such as the inwardly rectifying K1 channel Kir4.1 on Müller glia cells or that synaptic dysfunction exists in Atrx KO animals beyond what has been observed (103, 162).

4.6 Visual system anomalies are present in ATR-X patients

Sensory organ phenotypes are often overlooked or mostly attributed to impaired cortex function in patients with severe mental retardation (163-168). The mosaic deletion of Atrx in our mouse model may therefore offer an interesting comparison to the retinal phenotype observed in ATR-X patients, as patient mutations have been shown to give rise to functional hypomorphs (89).

Here we present the first comprehensive report describing the prevalence of visual system anomalies in ATR-X patients. A review of the clinical information confirmed that 23% of ATR-X patients (N=202) presented with an ocular phenotype, although this number is probably still an underestimation due to the subtlety of such defects and the severity of their other clinical features. Under reporting of visual system anomaly has also been postulated in other rare mental retardation disorders such as Cri du Chat and Mowat-Wilson syndrome (163, 168).

Although the analysis of our animal model does not reveal a precise visual pathway phenotype, it does not recapitulate the phenotype observed in ATR-X patients. This may be partly due to the widespread loss of ATRX in all CNS tissues in patients, while in our mouse model; Atrx inactivation is restricted to the peripheral retina. Loss of interneurons is not a phenotype unique to our model. This phenotype is a common feature observed in animal models of diabetes and electrophysiologic studies in diabetic patients suggest alterations in the neural retina which result in a loss of contrast sensitivity (169). As ATR-X patients are unable to communicate, such a phenotype could only truly be assayed by electrical measurement of visual function. Overview of the clinical data

revealed that ERG analysis assessment had been performed on two patients although little could be concluded from these analyses.

4.7 Future directions

The present study brings into evidence the important biological role of Atrx as a key mediator of interneuron survival in the mammalian retina. In contrast to what has been previously published in other CNS tissues, Atrx was not required for early neuronal cell survival, but rather for interneuron survival in the postnatal period at a time in which the retina is prone to light induced synaptic remodeling. The molecular basis by which interneuron survival is compromised in Atrx KO retinas remains to be determined and therefore the first step in the understanding of this phenotype would be the identification of specific target genes which may be susceptible to the chromatin remodeling activity of Atrx. Microarray profiling experiments on retinal tissue derived from the peripheral retina may help refine the search for Atrx target genes. Candidate genes identified by this method would need to be prioritized on the basis of their pre-existing roles in synaptic remodeling or cellular survival as well as further validated by techniques such as qRT-PCR. Moreover, because amacrine cell loss coincides with eye opening, chromatin remodeling by Atrx at these target genes may be in part regulated by light activation. Dark rearing of animals may therefore provide valuable insight into the possible causes of the amacrine and horizontal cell loss in Atrx KO animals. Dark rearing of Atrx KO mice would enable us to determine whether Atrx ablation is associated with degenerative changes in interneurons induced by light-mediated visual activity.

ERG analysis revealed impaired visual transmission in Atrx KO mice. A closer look at synaptic connectivity in both the IPL and OPL may reveal valuable insight as to the nature of the visual pathway dysfunction in Atrx KO retinas. A number of synaptic markers can be visualized by IHC and may help us identify the underlying cause of the reduced b-wave amplitude in Atrx KO mice. In addition, abnormalities in synapse formation may also be examined at higher resolution by transmission electron microscopy.

An overview of the clinical data revealed a number of visual phenotype abnormalities in ATR-X patients. Additional consideration and reporting of ocular dysfunction in ATR-X patients is required in order to determine the frequency of this phenotype. If retinal dysfunction is found to be a hallmark of the ATR-X syndrome, ERG analysis, like in the case of diabetic retinopathy, may prove to be a useful non-invasive diagnostic tool for identifying ATR-X syndrome patients.

4.8 Conclusion

In conclusion, this is the first report which links with ATR-X syndrome with visual system anomalies. Our experiments enabled us to conclude that ATR-X is an important epigenetic regulator of amacrine and horizontal cell homeostasis in the mammalian retina. Perturbation of amacrine and horizontal cells may be partly responsible for the reduction in b-wave amplitude observed in Atrx KO mice and loss of these cell types likely contributes to the vision phenotype observed in ATR-X patients. In light of our findings, we speculate that investigation of an ocular phenotype by ERG

analysis may offer an interesting diagnostic tool for the ATR-X syndrome and other forms of severe mental retardation and thus warrants further investigation.

References

1. Chakravarthy, S., Y.J. Park, J. Chodaparambil, R.S. Edayathumangalam, and K. Luger. 2005. Structure and dynamic properties of nucleosome core particles. *FEBS Lett* 579:895-898.
2. Widom, J. 1998. Structure, dynamics, and function of chromatin in vitro. *Annu Rev Biophys Biomol Struct* 27:285-327.
3. Kornberg, R.D. 1974. Chromatin structure: a repeating unit of histones and DNA. *Science* 184:868-871.
4. De Koning, L., A. Corpet, J.E. Haber, and G. Almouzni. 2007. Histone chaperones: an escort network regulating histone traffic. *Nat Struct Mol Biol* 14:997-1007.
5. Shaw, B.R., T.M. Herman, R.T. Kovacic, G.S. Beaudreau, and K.E. Van Holde. 1976. Analysis of subunit organization in chicken erythrocyte chromatin. *Proc Natl Acad Sci U S A* 73:505-509.
6. Luger, K., A.W. Mader, R.K. Richmond, D.F. Sargent, and T.J. Richmond. 1997. Crystal structure of the nucleosome core particle at 2.8 A resolution. *Nature* 389:251-260.
7. Alberts, B.J., Alexander, Lewis, Julian; Raff, Martin; Roberts, Keith; Walter, Peter. 2002. Molecular Biology of the Cell. Garland Science, New York.
8. Grant, P.A. 2001. A tale of histone modifications. *Genome Biol* 2:REVIEWS0003.
9. Kouzarides, T. 2007. Chromatin modifications and their function. *Cell* 128:693-705.
10. Cosgrove, M.S., and C. Wolberger. 2005. How does the histone code work? *Biochem Cell Biol* 83:468-476.
11. Shogren-Knaak, M., H. Ishii, J.M. Sun, M.J. Pazin, J.R. Davie, and C.L. Peterson. 2006. Histone H4-K16 acetylation controls chromatin structure and protein interactions. *Science* 311:844-847.
12. Havas, K., I. Whitehouse, and T. Owen-Hughes. 2001. ATP-dependent chromatin remodeling activities. *Cell Mol Life Sci* 58:673-682.
13. Kagey, M.H., T.A. Melhuish, S.E. Powers, and D. Wotton. 2005. Multiple activities contribute to Pc2 E3 function. *Embo J* 24:108-119.
14. Wotton, D., and J.C. Merrill. 2007. Pc2 and SUMOylation. *Biochem Soc Trans* 35:1401-1404.
15. Wysocka, J., T. Swigut, H. Xiao, T.A. Milne, S.Y. Kwon, J. Landry, M. Kauer, A.J. Tackett, B.T. Chait, P. Badenhorst, C. Wu, and C.D. Allis. 2006. A PHD finger of NURF couples histone H3 lysine 4 trimethylation with chromatin remodelling. *Nature* 442:86-90.
16. Fazzio, T.G., and T. Tsukiyama. 2003. Chromatin remodeling in vivo: evidence for a nucleosome sliding mechanism. *Mol Cell* 12:1333-1340.
17. Wu, W.H., S. Alami, E. Luk, C.H. Wu, S. Sen, G. Mizuguchi, D. Wei, and C. Wu. 2005. Swc2 is a widely conserved H2AZ-binding module essential for ATP-dependent histone exchange. *Nat Struct Mol Biol* 12:1064-1071.

18. Mizuguchi, G., X. Shen, J. Landry, W.H. Wu, S. Sen, and C. Wu. 2004. ATP-driven exchange of histone H2AZ variant catalyzed by SWR1 chromatin remodeling complex. *Science* 303:343-348.
19. Flaus, A., and T. Owen-Hughes. 2004. Mechanisms for ATP-dependent chromatin remodelling: farewell to the tuna-can octamer? *Curr Opin Genet Dev* 14:165-173.
20. Whitehouse, I., A. Flaus, K. Havas, and T. Owen-Hughes. 2000. Mechanisms for ATP-dependent chromatin remodelling. *Biochem Soc Trans* 28:376-379.
21. Eberharter, A., and P.B. Becker. 2004. ATP-dependent nucleosome remodelling: factors and functions. *J Cell Sci* 117:3707-3711.
22. Wang, G.G., C.D. Allis, and P. Chi. 2007. Chromatin remodeling and cancer, Part II: ATP-dependent chromatin remodeling. *Trends Mol Med* 13:373-380.
23. Havas, K., A. Flaus, M. Phelan, R. Kingston, P.A. Wade, D.M. Lilley, and T. Owen-Hughes. 2000. Generation of superhelical torsion by ATP-dependent chromatin remodeling activities. *Cell* 103:1133-1142.
24. Saha, A., J. Wittmeyer, and B.R. Cairns. 2002. Chromatin remodeling by RSC involves ATP-dependent DNA translocation. *Genes Dev* 16:2120-2134.
25. Krebs, J.E., C.J. Fry, M.L. Samuels, and C.L. Peterson. 2000. Global role for chromatin remodeling enzymes in mitotic gene expression. *Cell* 102:587-598.
26. Armstrong, J.A., O. Papoulas, G. Daubresse, A.S. Sperling, J.T. Lis, M.P. Scott, and J.W. Tamkun. 2002. The Drosophila BRM complex facilitates global transcription by RNA polymerase II. *Embo J* 21:5245-5254.
27. Martens, J.A., and F. Winston. 2003. Recent advances in understanding chromatin remodeling by Swi/Snf complexes. *Curr Opin Genet Dev* 13:136-142.
28. Napolitano, M.A., M. Cipollaro, A. Cascino, M.A. Melone, A. Giordano, and U. Galderisi. 2007. Brg1 chromatin remodeling factor is involved in cell growth arrest, apoptosis and senescence of rat mesenchymal stem cells. *J Cell Sci* 120:2904-2911.
29. Reisman, D.N., M.W. Strobeck, B.L. Betz, J. Sciariotta, W. Funkhouser, Jr., C. Murchardt, M. Yaniv, L.S. Sherman, E.S. Knudsen, and B.E. Weissman. 2002. Concomitant down-regulation of BRM and BRG1 in human tumor cell lines: differential effects on RB-mediated growth arrest vs CD44 expression. *Oncogene* 21:1196-1207.
30. Xu, Y., J. Zhang, and X. Chen. 2007. The activity of p53 is differentially regulated by Brm- and Brg1-containing SWI/SNF chromatin remodeling complexes. *J Biol Chem* 282:37429-37435.
31. Kowenz-Leutz, E., and A. Leutz. 1999. A C/EBP beta isoform recruits the SWI/SNF complex to activate myeloid genes. *Mol Cell* 4:735-743.
32. Han, Q., J. Lu, J. Duan, D. Su, X. Hou, F. Li, X. Wang, and B. Huang. 2008. Gcn5- and Elp3-induced histone H3 acetylation regulates hsp70 gene transcription in yeast. *Biochem J* 409:779-788.
33. Inoue, H., T. Furukawa, S. Giannakopoulos, S. Zhou, D.S. King, and N. Tanese. 2002. Largest subunits of the human SWI/SNF chromatin-remodeling complex promote transcriptional activation by steroid hormone receptors. *J Biol Chem* 277:41674-41685.

34. Delmas, V., D.G. Stokes, and R.P. Perry. 1993. A mammalian DNA-binding protein that contains a chromodomain and an SNF2/SWI2-like helicase domain. *Proc Natl Acad Sci U S A* 90:2414-2418.
35. Hall, J.A., and P.T. Georgel. 2007. CHD proteins: a diverse family with strong ties. *Biochem Cell Biol* 85:463-476.
36. Simic, R., D.L. Lindstrom, H.G. Tran, K.L. Roinick, P.J. Costa, A.D. Johnson, G.A. Hartzog, and K.M. Arndt. 2003. Chromatin remodeling protein Chd1 interacts with transcription elongation factors and localizes to transcribed genes. *Embo J* 22:1846-1856.
37. Tai, H.H., M. Geisterfer, J.C. Bell, M. Moniwa, J.R. Davie, L. Boucher, and M.W. McBurney. 2003. CHD1 associates with NCoR and histone deacetylase as well as with RNA splicing proteins. *Biochem Biophys Res Commun* 308:170-176.
38. Kehle, J., D. Beuchle, S. Treuheit, B. Christen, J.A. Kennison, M. Bienz, and J. Muller. 1998. dMi-2, a hunchback-interacting protein that functions in polycomb repression. *Science* 282:1897-1900.
39. Schmidt, D.R., and S.L. Schreiber. 1999. Molecular association between ATR and two components of the nucleosome remodeling and deacetylating complex, HDAC2 and CHD4. *Biochemistry* 38:14711-14717.
40. de la Serna, I.L., Y. Ohkawa, and A.N. Imbalzano. 2006. Chromatin remodelling in mammalian differentiation: lessons from ATP-dependent remodellers. *Nat Rev Genet* 7:461-473.
41. Deuring, R., L. Fanti, J.A. Armstrong, M. Sarte, O. Papoulas, M. Prestel, G. Daubresse, M. Verardo, S.L. Moseley, M. Berloco, T. Tsukiyama, C. Wu, S. Pimpinelli, and J.W. Tamkun. 2000. The ISWI chromatin-remodeling protein is required for gene expression and the maintenance of higher order chromatin structure in vivo. *Mol Cell* 5:355-365.
42. Corona, D.F., G. Siriaco, J.A. Armstrong, N. Snarskaya, S.A. McClymont, M.P. Scott, and J.W. Tamkun. 2007. ISWI regulates higher-order chromatin structure and histone H1 assembly in vivo. *PLoS Biol* 5:e232.
43. Stopka, T., and A.I. Skoultchi. 2003. The ISWI ATPase Snf2h is required for early mouse development. *Proc Natl Acad Sci U S A* 100:14097-14102.
44. Barak, O., M.A. Lazzaro, W.S. Lane, D.W. Speicher, D.J. Picketts, and R. Shiekhattar. 2003. Isolation of human NURF: a regulator of Engrailed gene expression. *Embo J* 22:6089-6100.
45. Poot, R.A., L. Bozhenok, D.L. van den Berg, S. Steffensen, F. Ferreira, M. Grimaldi, N. Gilbert, J. Ferreira, and P.D. Varga-Weisz. 2004. The Williams syndrome transcription factor interacts with PCNA to target chromatin remodelling by ISWI to replication foci. *Nat Cell Biol* 6:1236-1244.
46. Poot, R.A., L. Bozhenok, D.L. van den Berg, N. Hawkes, and P.D. Varga-Weisz. 2005. Chromatin remodeling by WSTF-ISWI at the replication site: opening a window of opportunity for epigenetic inheritance? *Cell Cycle* 4:543-546.
47. Fraga, M.F., E. Ballestar, A. Villar-Garea, M. Boix-Chornet, J. Espada, G. Schotta, T. Bonaldi, C. Haydon, S. Ropero, K. Petrie, N.G. Iyer, A. Perez-Rosado, E. Calvo, J.A. Lopez, A. Cano, M.J. Calasanz, D. Colomer, M.A. Piris, N. Ahn, A. Imhof, C. Caldas, T. Jenuwein, and M. Esteller. 2005. Loss of acetylation at

Lys16 and trimethylation at Lys20 of histone H4 is a common hallmark of human cancer. *Nat Genet* 37:391-400.

48. Fraga, M.F., and M. Esteller. 2005. Towards the human cancer epigenome: a first draft of histone modifications. *Cell Cycle* 4:1377-1381.
49. Bhaumik, S.R., E. Smith, and A. Shilatifard. 2007. Covalent modifications of histones during development and disease pathogenesis. *Nat Struct Mol Biol* 14:1008-1016.
50. Yang, X.J., and M. Ullah. 2007. MOZ and MORF, two large MYSTic HATs in normal and cancer stem cells. *Oncogene* 26:5408-5419.
51. Peters, A.H., D. O'Carroll, H. Scherthan, K. Mechtler, S. Sauer, C. Schofer, K. Weipoltshammer, M. Pagani, M. Lachner, A. Kohlmaier, S. Opravil, M. Doyle, M. Sibilia, and T. Jenuwein. 2001. Loss of the Suv39h histone methyltransferases impairs mammalian heterochromatin and genome stability. *Cell* 107:323-337.
52. Huang, C., E.A. Sloan, and C.F. Boerkoel. 2003. Chromatin remodeling and human disease. *Curr Opin Genet Dev* 13:246-252.
53. Betz, B.L., M.W. Strobeck, D.N. Reisman, E.S. Knudsen, and B.E. Weissman. 2002. Re-expression of hSNF5/INI1/BAF47 in pediatric tumor cells leads to G1 arrest associated with induction of p16ink4a and activation of RB. *Oncogene* 21:5193-5203.
54. Versteege, I., N. Sevenet, J. Lange, M.F. Rousseau-Merck, P. Ambros, R. Handgretinger, A. Aurias, and O. Delattre. 1998. Truncating mutations of hSNF5/INI1 in aggressive paediatric cancer. *Nature* 394:203-206.
55. Biegel, J.A., L. Tan, F. Zhang, L. Wainwright, P. Russo, and L.B. Rorke. 2002. Alterations of the hSNF5/INI1 gene in central nervous system atypical teratoid/rhabdoid tumors and renal and extrarenal rhabdoid tumors. *Clin Cancer Res* 8:3461-3467.
56. Biegel, J.A., J.Y. Zhou, L.B. Rorke, C. Stenstrom, L.M. Wainwright, and B. Fogelgren. 1999. Germ-line and acquired mutations of INI1 in atypical teratoid and rhabdoid tumors. *Cancer Res* 59:74-79.
57. Sevenet, N., E. Sheridan, D. Amram, P. Schneider, R. Handgretinger, and O. Delattre. 1999. Constitutional mutations of the hSNF5/INI1 gene predispose to a variety of cancers. *Am J Hum Genet* 65:1342-1348.
58. Sansam, C.G., and C.W. Roberts. 2006. Epigenetics and cancer: altered chromatin remodeling via Snf5 loss leads to aberrant cell cycle regulation. *Cell Cycle* 5:621-624.
59. Roelfsema, J.H., and D.J. Peters. 2007. Rubinstein-Taybi syndrome: clinical and molecular overview. *Expert Rev Mol Med* 9:1-16.
60. Murata, T., R. Kurokawa, A. Krones, K. Tatsumi, M. Ishii, T. Taki, M. Masuno, H. Ohashi, M. Yanagisawa, M.G. Rosenfeld, C.K. Glass, and Y. Hayashi. 2001. Defect of histone acetyltransferase activity of the nuclear transcriptional coactivator CBP in Rubinstein-Taybi syndrome. *Hum Mol Genet* 10:1071-1076.
61. Nagarajan, R.P., A.R. Hogart, Y. Gwye, M.R. Martin, and J.M. LaSalle. 2006. Reduced MeCP2 expression is frequent in autism frontal cortex and correlates with aberrant MECP2 promoter methylation. *Epigenetics* 1:e1-11.
62. Nan, X., F.J. Campoy, and A. Bird. 1997. MeCP2 is a transcriptional repressor with abundant binding sites in genomic chromatin. *Cell* 88:471-481.

63. Wan, M., K. Zhao, S.S. Lee, and U. Francke. 2001. MECP2 truncating mutations cause histone H4 hyperacetylation in Rett syndrome. *Hum Mol Genet* 10:1085-1092.
64. Alarcon, J.M., G. Malleret, K. Touzani, S. Vronskaya, S. Ishii, E.R. Kandel, and A. Barco. 2004. Chromatin acetylation, memory, and LTP are impaired in CBP+/- mice: a model for the cognitive deficit in Rubinstein-Taybi syndrome and its amelioration. *Neuron* 42:947-959.
65. Hahnen, E., J. Hauke, C. Trankle, I.Y. Eyupoglu, B. Wirth, and I. Blumcke. 2008. Histone deacetylase inhibitors: possible implications for neurodegenerative disorders. *Expert Opin Investig Drugs* 17:169-184.
66. Osterod, M., E. Larsen, F. Le Page, J.G. Hengstler, G.T. Van Der Horst, S. Boiteux, A. Klungland, and B. Epe. 2002. A global DNA repair mechanism involving the Cockayne syndrome B (CSB) gene product can prevent the in vivo accumulation of endogenous oxidative DNA base damage. *Oncogene* 21:8232-8239.
67. Boerkoel, C.F., H. Takashima, J. John, J. Yan, P. Stankiewicz, L. Rosenbarker, J.L. Andre, R. Bogdanovic, A. Burguet, S. Cockfield, I. Cordeiro, S. Frund, F. Illies, M. Joseph, I. Kaitila, G. Lama, C. Loirat, D.R. McLeod, D.V. Milford, E.M. Petty, F. Rodrigo, J.M. Saraiva, B. Schmidt, G.C. Smith, J. Spranger, A. Stein, H. Thiele, J. Tizard, R. Weksberg, J.R. Lupski, and D.W. Stockton. 2002. Mutant chromatin remodeling protein SMARCAL1 causes Schimke immuno-osseous dysplasia. *Nat Genet* 30:215-220.
68. Kleefstra, T., and B.C. Hamel. 2005. X-linked mental retardation: further lumping, splitting and emerging phenotypes. *Clin Genet* 67:451-467.
69. Froyen, G., M. Bauters, T. Voet, and P. Marynen. 2006. X-linked mental retardation and epigenetics. *J Cell Mol Med* 10:808-825.
70. Ropers, H.H. 2006. X-linked mental retardation: many genes for a complex disorder. *Curr Opin Genet Dev* 16:260-269.
71. Lower, K.M., G. Turner, B.A. Kerr, K.D. Mathews, M.A. Shaw, A.K. Gedeon, S. Schelley, H.E. Hoyme, S.M. White, M.B. Delatycki, A.K. Lampe, J. Clayton-Smith, H. Stewart, C.M. van Ravenswaay, B.B. de Vries, B. Cox, M. Grompe, S. Ross, P. Thomas, J.C. Mulley, and J. Gecz. 2002. Mutations in PHF6 are associated with Borjeson-Forssman-Lehmann syndrome. *Nat Genet* 32:661-665.
72. Iwase, S., F. Lan, P. Bayliss, L. de la Torre-Ubieta, M. Huarte, H.H. Qi, J.R. Whetstine, A. Bonni, T.M. Roberts, and Y. Shi. 2007. The X-linked mental retardation gene SMCX/JARID1C defines a family of histone H3 lysine 4 demethylases. *Cell* 128:1077-1088.
73. Santos, C., L. Rodriguez-Revenga, I. Madrigal, C. Badenas, M. Pineda, and M. Mila. 2006. A novel mutation in JARID1C gene associated with mental retardation. *Eur J Hum Genet* 14:583-586.
74. Laumonnier, F., S. Holbert, N. Ronce, F. Faravelli, S. Lenzner, C.E. Schwartz, J. Lespinasse, H. Van Esch, D. Lacombe, C. Goizet, F. Phan-Dinh Tuy, H. van Bokhoven, J.P. Fryns, J. Chelly, H.H. Ropers, C. Moraine, B.C. Hamel, and S. Briault. 2005. Mutations in PHF8 are associated with X linked mental retardation and cleft lip/cleft palate. *J Med Genet* 42:780-786.

75. Picketts, D.J., D.R. Higgs, S. Bachoo, D.J. Blake, O.W. Quarrell, and R.J. Gibbons. 1996. ATRX encodes a novel member of the SNF2 family of proteins: mutations point to a common mechanism underlying the ATR-X syndrome. *Hum Mol Genet* 5:1899-1907.
76. Raymond, F.L. 2006. X linked mental retardation: a clinical guide. *J Med Genet* 43:193-200.
77. Gibbons, R. 2006. Alpha thalassaemia-mental retardation, X linked. *Orphanet J Rare Dis* 1:15.
78. Badens, C., N. Martini, S. Courrier, V. DesPortes, R. Touraine, N. Levy, and P. Edery. 2006. ATRX syndrome in a girl with a heterozygous mutation in the ATRX Zn finger domain and a totally skewed X-inactivation pattern. *Am J Med Genet A* 140:2212-2215.
79. Gibbons, R.J., and D.R. Higgs. 2000. Molecular-clinical spectrum of the ATR-X syndrome. *Am J Med Genet* 97:204-212.
80. Garrick, D., V. Samara, T.L. McDowell, A.J. Smith, L. Dobbie, D.R. Higgs, and R.J. Gibbons. 2004. A conserved truncated isoform of the ATR-X syndrome protein lacking the SWI/SNF-homology domain. *Gene* 326:23-34.
81. Stayton, C.L., B. Dabovic, M. Gulisano, J. Gecz, V. Broccoli, S. Giovanazzi, M. Bossolasco, L. Monaco, S. Rastan, E. Boncinelli, and et al. 1994. Cloning and characterization of a new human Xq13 gene, encoding a putative helicase. *Hum Mol Genet* 3:1957-1964.
82. Abidi, F.E., C. Cardoso, A.M. Lossi, R.B. Lowry, D. Depetris, M.G. Mattei, H.A. Lubs, R.E. Stevenson, M. Fontes, A.E. Chudley, and C.E. Schwartz. 2005. Mutation in the 5' alternatively spliced region of the XNP/ATR-X gene causes Chudley-Lowry syndrome. *Eur J Hum Genet* 13:176-183.
83. Howard, M.T., N. Malik, C.B. Anderson, J.L. Voskuil, J.F. Atkins, and R.J. Gibbons. 2004. Attenuation of an amino-terminal premature stop codon mutation in the ATRX gene by an alternative mode of translational initiation. *J Med Genet* 41:951-956.
84. Gibbons, R.J., A. Pellagatti, D. Garrick, W.G. Wood, N. Malik, H. Ayyub, C. Langford, J. Boultwood, J.S. Wainscoat, and D.R. Higgs. 2003. Identification of acquired somatic mutations in the gene encoding chromatin-remodeling factor ATRX in the alpha-thalassemia myelodysplasia syndrome (ATMDS). *Nat Genet* 34:446-449.
85. Xue, Y., R. Gibbons, Z. Yan, D. Yang, T.L. McDowell, S. Sechi, J. Qin, S. Zhou, D. Higgs, and W. Wang. 2003. The ATRX syndrome protein forms a chromatin-remodeling complex with Daxx and localizes in promyelocytic leukemia nuclear bodies. *Proc Natl Acad Sci U S A* 100:10635-10640.
86. Ishov, A.M., O.V. Vladimirova, and G.G. Maul. 2004. Heterochromatin and ND10 are cell-cycle regulated and phosphorylation-dependent alternate nuclear sites of the transcription repressor Daxx and SWI/SNF protein ATRX. *J Cell Sci* 117:3807-3820.
87. Gibbons, R.J., T. Wada, C.A. Fisher, N. Malik, M.J. Mitson, D.P. Steensma, A. Fryer, D.R. Goudie, I.D. Krantz, and J. Traeger-Synodinos. 2008. Mutations in the chromatin-associated protein ATRX. *Hum Mutat*

88. Tang, J., S. Wu, H. Liu, R. Stratt, O.G. Barak, R. Shiekhattar, D.J. Picketts, and X. Yang. 2004. A novel transcription regulatory complex containing death domain-associated protein and the ATR-X syndrome protein. *J Biol Chem* 279:20369-20377.
89. Berube, N.G., J. Healy, C.F. Medina, S. Wu, T. Hodgson, M. Jagla, and D.J. Picketts. 2008. Patient mutations alter ATRX targeting to PML nuclear bodies. *Eur J Hum Genet* 16:192-201.
90. Cardoso, C., Y. Lutz, C. Mignon, E. Compe, D. Depetris, M.G. Mattei, M. Fontes, and L. Colleaux. 2000. ATR-X mutations cause impaired nuclear location and altered DNA binding properties of the XNP/ATR-X protein. *J Med Genet* 37:746-751.
91. Le Douarin, B., A.L. Nielsen, J.M. Garnier, H. Ichinose, F. Jeanmougin, R. Losson, and P. Chambon. 1996. A possible involvement of TIF1 alpha and TIF1 beta in the epigenetic control of transcription by nuclear receptors. *Embo J* 15:6701-6715.
92. McDowell, T.L., R.J. Gibbons, H. Sutherland, D.M. O'Rourke, W.A. Bickmore, A. Pombo, H. Turley, K. Gatter, D.J. Picketts, V.J. Buckle, L. Chapman, D. Rhodes, and D.R. Higgs. 1999. Localization of a putative transcriptional regulator (ATRX) at pericentromeric heterochromatin and the short arms of acrocentric chromosomes. *Proc Natl Acad Sci U S A* 96:13983-13988.
93. Berube, N.G., C.A. Smeenk, and D.J. Picketts. 2000. Cell cycle-dependent phosphorylation of the ATRX protein correlates with changes in nuclear matrix and chromatin association. *Hum Mol Genet* 9:539-547.
94. Nan, X., J. Hou, A. Maclean, J. Nasir, M.J. Lafuente, X. Shu, S. Kriaucionis, and A. Bird. 2007. Interaction between chromatin proteins MECP2 and ATRX is disrupted by mutations that cause inherited mental retardation. *Proc Natl Acad Sci U S A* 104:2709-2714.
95. De La Fuente, R., M.M. Viveiros, K. Wigglesworth, and J.J. Eppig. 2004. ATRX, a member of the SNF2 family of helicase/ATPases, is required for chromosome alignment and meiotic spindle organization in metaphase II stage mouse oocytes. *Dev Biol* 272:1-14.
96. Ritchie, K., C. Seah, J. Moulin, C. Isaac, F. Dick, and N.G. Berube. 2008. Loss of ATRX leads to chromosome cohesion and congression defects. *J Cell Biol* 180:315-324.
97. Garrick, D., J.A. Sharpe, R. Arkell, L. Dobbie, A.J. Smith, W.G. Wood, D.R. Higgs, and R.J. Gibbons. 2006. Loss of Atrx affects trophoblast development and the pattern of X-inactivation in extraembryonic tissues. *PLoS Genet* 2:e58.
98. Berube, N.G., M. Jagla, C. Smeenk, Y. De Repentigny, R. Kothary, and D.J. Picketts. 2002. Neurodevelopmental defects resulting from ATRX overexpression in transgenic mice. *Hum Mol Genet* 11:253-261.
99. Betz, U.A., C.A. Vosshenrich, K. Rajewsky, and W. Muller. 1996. Bypass of lethality with mosaic mice generated by Cre-loxP-mediated recombination. *Curr Biol* 6:1307-1316.
100. Berube, N.G., M. Mangelsdorf, M. Jagla, J. Vanderluit, D. Garrick, R.J. Gibbons, D.R. Higgs, R.S. Slack, and D.J. Picketts. 2005. The chromatin-remodeling

protein ATRX is critical for neuronal survival during corticogenesis. *J Clin Invest* 115:258-267.
101. Young, R.W. 1985. Cell proliferation during postnatal development of the retina in the mouse. *Brain Res* 353:229-239.
102. Chow, R.L., and R.A. Lang. 2001. Early eye development in vertebrates. *Annu Rev Cell Dev Biol* 17:255-296.
103. Smith, R., S; Simon W.M John; Patsy M. Nishina; John P. Sundberg. 2002. Systemic Evaluation of the Mouse Eye Anatomy, Pathology and Biomethods. CRC Press,
New York.
104. Prada, C., J. Puga, L. Perez-Mendez, R. Lopez And, and G. Ramirez. 1991. Spatial and Temporal Patterns of Neurogenesis in the Chick Retina. *Eur J Neurosci* 3:1187.
105. Cepko, C.L., C.P. Austin, X. Yang, M. Alexiades, and D. Ezzeddine. 1996. Cell fate determination in the vertebrate retina. *Proc Natl Acad Sci U S A* 93:589-595.
106. Wang, J.C., and W.A. Harris. 2005. The role of combinational coding by homeodomain and bHLH transcription factors in retinal cell fate specification. *Dev Biol* 285:101-115.
107. Marquardt, T., and P. Gruss. 2002. Generating neuronal diversity in the retina: one for nearly all. *Trends Neurosci* 25:32-38.
108. Harris, W.A. 1997. Pax-6: where to be conserved is not conservative. *Proc Natl Acad Sci U S A* 94:2098-2100.
109. Chalupa, L.M., and E. Gunhan. 2004. Development of On and Off retinal pathways and retinogeniculate projections. *Prog Retin Eye Res* 23:31-51.
110. Xu, H., and N. Tian. 2004. Pathway-specific maturation, visual deprivation, and development of retinal pathway. *Neuroscientist* 10:337-346.
111. Tian, N. 2004. Visual experience and maturation of retinal synaptic pathways. *Vision Res* 44:3307-3316.
112. Famiglietti, E.V., Jr., and H. Kolb. 1976. Structural basis for ON-and OFF-center responses in retinal ganglion cells. *Science* 194:193-195.
113. Marquardt, T., R. Ashery-Padan, N. Andrejewski, R. Scardigli, F. Guillemot, and P. Gruss. 2001. Pax6 is required for the multipotent state of retinal progenitor cells. *Cell* 105:43-55.
114. Truett, G.E., P. Heeger, R.L. Mynatt, A.A. Truett, J.A. Walker, and M.L. Warman. 2000. Preparation of PCR-quality mouse genomic DNA with hot sodium hydroxide and tris (HotSHOT). *Biotechniques* 29:52, 54.
115. Dakubo, G.D., Y.P. Wang, C. Mazerolle, K. Campsall, A.P. McMahon, and V.A. Wallace. 2003. Retinal ganglion cell-derived sonic hedgehog signaling is required for optic disc and stalk neuroepithelial cell development. *Development* 130:2967-2980.
116. Jensen, A.M., and V.A. Wallace. 1997. Expression of Sonic hedgehog and its putative role as a precursor cell mitogen in the developing mouse retina. *Development* 124:363-371.
117. Leonard, K.C., D. Petrin, S.G. Coupland, A.N. Baker, B.C. Leonard, E.C. LaCasse, W.W. Hauswirth, R.G. Korneluk, and C. Tsilfidis. 2007. XIAP

protection of photoreceptors in animal models of retinitis pigmentosa. *PLoS ONE* 2:e314.

118. Mears, A.J., M. Kondo, P.K. Swain, Y. Takada, R.A. Bush, T.L. Saunders, P.A. Sieving, and A. Swaroop. 2001. Nrl is required for rod photoreceptor development. *Nat Genet* 29:447-452.
119. Ozawa, Y., K. Nakao, T. Shimazaki, S. Shimmura, T. Kurihara, S. Ishida, A. Yoshimura, K. Tsubota, and H. Okano. 2007. SOCS3 is required to temporally fine-tune photoreceptor cell differentiation. *Dev Biol* 303:591-600.
120. Wang, Y., G.D. Dakubo, S. Thurig, C.J. Mazerolle, and V.A. Wallace. 2005. Retinal ganglion cell-derived sonic hedgehog locally controls proliferation and the timing of RGC development in the embryonic mouse retina. *Development* 132:5103-5113.
121. Yaron, O., C. Farhy, T. Marquardt, M. Applebury, and R. Ashery-Padan. 2006. Notch1 functions to suppress cone-photoreceptor fate specification in the developing mouse retina. *Development* 133:1367-1378.
122. Stacy, R.C., J. Demas, R.W. Burgess, J.R. Sanes, and R.O. Wong. 2005. Disruption and recovery of patterned retinal activity in the absence of acetylcholine. *J Neurosci* 25:9347-9357.
123. Chen, D., R. Opavsky, M. Pacal, N. Tanimoto, P. Wenzel, M.W. Seeliger, G. Leone, and R. Bremner. 2007. Rb-Mediated Neuronal Differentiation through Cell-Cycle-Independent Regulation of E2f3a. *PLoS Biol* 5:e179.
124. MacNeil, M.A., and R.H. Masland. 1998. Extreme diversity among amacrine cells: implications for function. *Neuron* 20:971-982.
125. Voigt, T., and H. Wassle. 1987. Dopaminergic innervation of A II amacrine cells in mammalian retina. *J Neurosci* 7:4115-4128.
126. Li, S., Z. Mo, X. Yang, S.M. Price, M.M. Shen, and M. Xiang. 2004. Foxn4 controls the genesis of amacrine and horizontal cells by retinal progenitors. *Neuron* 43:795-807.
127. Inoue, T., M. Hojo, Y. Bessho, Y. Tano, J.E. Lee, and R. Kageyama. 2002. Math3 and NeuroD regulate amacrine cell fate specification in the retina. *Development* 129:831-842.
128. Dyer, M.A., F.J. Livesey, C.L. Cepko, and G. Oliver. 2003. Prox1 function controls progenitor cell proliferation and horizontal cell genesis in the mammalian retina. *Nat Genet* 34:53-58.
129. Nakhai, H., S. Sel, J. Favor, L. Mendoza-Torres, F. Paulsen, G.I. Duncker, and R.M. Schmid. 2007. Ptf1a is essential for the differentiation of GABAergic and glycinergic amacrine cells and horizontal cells in the mouse retina. *Development* 134:1151-1160.
130. Fujitani, Y., S. Fujitani, H. Luo, F. Qiu, J. Burlison, Q. Long, Y. Kawaguchi, H. Edlund, R.J. MacDonald, T. Furukawa, T. Fujikado, M.A. Magnuson, M. Xiang, and C.V. Wright. 2006. Ptf1a determines horizontal and amacrine cell fates during mouse retinal development. *Development* 133:4439-4450.
131. Young, R.W. 1985. Cell differentiation in the retina of the mouse. *Anat Rec* 212:199-205.
132. Haverkamp, S., and H. Wassle. 2000. Immunocytochemical analysis of the mouse retina. *J Comp Neurol* 424:1-23.

133. Jeon, C.J., E. Strettoi, and R.H. Masland. 1998. The major cell populations of the mouse retina. *J Neurosci* 18:8936-8946.
134. Wulle, I., and J. Schnitzer. 1989. Distribution and morphology of tyrosine hydroxylase-immunoreactive neurons in the developing mouse retina. *Brain Res Dev Brain Res* 48:59-72.
135. Cellerino, A., G. Pinzon-Duarte, P. Carroll, and K. Kohler. 1998. Brain-derived neurotrophic factor modulates the development of the dopaminergic network in the rodent retina. *J Neurosci* 18:3351-3362.
136. Calamusa, M., P.P. Pattabiraman, N. Pozdeyev, P.M. Iuvone, A. Cellerino, and L. Domenici. 2007. Specific alterations of tyrosine hydroxylase immunopositive cells in the retina of NT-4 knock out mice. *Vision Res* 47:1523-1536.
137. Chen, W.G., Q. Chang, Y. Lin, A. Meissner, A.E. West, E.C. Griffith, R. Jaenisch, and M.E. Greenberg. 2003. Derepression of BDNF transcription involves calcium-dependent phosphorylation of MeCP2. *Science* 302:885-889.
138. Martinowich, K., D. Hattori, H. Wu, S. Fouse, F. He, Y. Hu, G. Fan, and Y.E. Sun. 2003. DNA methylation-related chromatin remodeling in activity-dependent BDNF gene regulation. *Science* 302:890-893.
139. Wang, H., S.A. Chan, M. Ogier, D. Hellard, Q. Wang, C. Smith, and D.M. Katz. 2006. Dysregulation of brain-derived neurotrophic factor expression and neurosecretory function in Mecp2 null mice. *J Neurosci* 26:10911-10915.
140. Chang, Q., G. Khare, V. Dani, S. Nelson, and R. Jaenisch. 2006. The disease progression of Mecp2 mutant mice is affected by the level of BDNF expression. *Neuron* 49:341-348.
141. Kljavin, I.J., C. Lagenaur, J.L. Bixby, and T.A. Reh. 1994. Cell adhesion molecules regulating neurite growth from amacrine and rod photoreceptor cells. *J Neurosci* 14:5035-5049.
142. Tanabe, K., Y. Takahashi, Y. Sato, K. Kawakami, M. Takeichi, and S. Nakagawa. 2006. Cadherin is required for dendritic morphogenesis and synaptic terminal organization of retinal horizontal cells. *Development* 133:4085-4096.
143. Masai, I., Z. Lele, M. Yamaguchi, A. Komori, A. Nakata, Y. Nishiwaki, H. Wada, H. Tanaka, Y. Nojima, M. Hammerschmidt, S.W. Wilson, and H. Okamoto. 2003. N-cadherin mediates retinal lamination, maintenance of forebrain compartments and patterning of retinal neurites. *Development* 130:2479-2494.
144. Bai, S., K. Ghoshal, and S.T. Jacob. 2006. Identification of T-cadherin as a novel target of DNA methyltransferase 3B and its role in the suppression of nerve growth factor-mediated neurite outgrowth in PC12 cells. *J Biol Chem* 281:13604-13611.
145. Fuerst, P.G., A. Koizumi, R.H. Masland, and R.W. Burgess. 2008. Neurite arborization and mosaic spacing in the mouse retina require DSCAM. *Nature* 451:470-474.
146. Yamagata, M., and J.R. Sanes. 2008. Dscam and Sidekick proteins direct lamina-specific synaptic connections in vertebrate retina. *Nature* 451:465-469.
147. Liu, W., J.H. Wang, and M. Xiang. 2000. Specific expression of the LIM/homeodomain protein Lim-1 in horizontal cells during retinogenesis. *Dev Dyn* 217:320-325.

148. Margeta, M.A. 2008. Transcription factor Lim1 specifies horizontal cell laminar position in the retina. *J Neurosci* 28:3835-3836.
149. Poche, R.A., K.M. Kwan, M.A. Raven, Y. Furuta, B.E. Reese, and R.R. Behringer. 2007. Lim1 is essential for the correct laminar positioning of retinal horizontal cells. *J Neurosci* 27:14099-14107.
150. Horsburgh, G.M., and A.J. Sefton. 1987. Cellular degeneration and synaptogenesis in the developing retina of the rat. *J Comp Neurol* 263:553-566.
151. Zhang, J., Z. Yang, and S.M. Wu. 2005. Development of cholinergic amacrine cells is visual activity-dependent in the postnatal mouse retina. *J Comp Neurol* 484:331-343.
152. Tian, N., and D.R. Copenhagen. 2001. Visual deprivation alters development of synaptic function in inner retina after eye opening. *Neuron* 32:439-449.
153. Liu, X., R.N. Grishanin, R.J. Tolwani, R.C. Renteria, B. Xu, L.F. Reichardt, and D.R. Copenhagen. 2007. Brain-derived neurotrophic factor and TrkB modulate visual experience-dependent refinement of neuronal pathways in retina. *J Neurosci* 27:7256-7267.
154. Levine, A.J., W. Hu, and Z. Feng. 2006. The P53 pathway: what questions remain to be explored? *Cell Death Differ* 13:1027-1036.
155. Chen, X., L.J. Ko, L. Jayaraman, and C. Prives. 1996. p53 levels, functional domains, and DNA damage determine the extent of the apoptotic response of tumor cells. *Genes Dev* 10:2438-2451.
156. Nakano, H., H. Yonekawa, and K. Shinohara. 2007. Threshold level of p53 required for the induction of apoptosis in X-irradiated MOLT-4 cells. *Int J Radiat Oncol Biol Phys* 68:883-891.
157. Barber, A.J., D.A. Antonetti, T.S. Kern, C.E. Reiter, R.S. Soans, J.K. Krady, S.W. Levison, T.W. Gardner, and S.K. Bronson. 2005. The Ins2Akita mouse as a model of early retinal complications in diabetes. *Invest Ophthalmol Vis Sci* 46:2210-2218.
158. Park, S.H., J.W. Park, S.J. Park, K.Y. Kim, J.W. Chung, M.H. Chun, and S.J. Oh. 2003. Apoptotic death of photoreceptors in the streptozotocin-induced diabetic rat retina. *Diabetologia* 46:1260-1268.
159. Hancock, H.A., and T.W. Kraft. 2004. Oscillatory potential analysis and ERGs of normal and diabetic rats. *Invest Ophthalmol Vis Sci* 45:1002-1008.
160. Bresnick, G.H., and M. Palta. 1987. Temporal aspects of the electroretinogram in diabetic retinopathy. *Arch Ophthalmol* 105:660-664.
161. Chow, R.L., B. Volgyi, R.K. Szilard, D. Ng, C. McKerlie, S.A. Bloomfield, D.G. Birch, and R.R. McInnes. 2004. Control of late off-center cone bipolar cell differentiation and visual signaling by the homeobox gene Vsx1. *Proc Natl Acad Sci U S A* 101:1754-1759.
162. Maxeiner, S., K. Dedek, U. Janssen-Bienhold, J. Ammermuller, H. Brune, T. Kirsch, M. Pieper, J. Degen, O. Kruger, K. Willecke, and R. Weiler. 2005. Deletion of connexin45 in mouse retinal neurons disrupts the rod/cone signaling pathway between AII amacrine and ON cone bipolar cells and leads to impaired visual transmission. *J Neurosci* 25:566-576.
163. Garavelli, L., and P.C. Mainardi. 2007. Mowat-Wilson syndrome. *Orphanet J Rare Dis* 2:42.

164. Van der Geest, J.N., G.C. Lagers-van Haselen, J.M. van Hagen, E. Brenner, L.C. Govaerts, I.F. de Coo, and M.A. Frens. 2005. Visual depth processing in Williams-Beuren syndrome. *Exp Brain Res* 166:200-209.
165. Castelo-Branco, M., M. Mendes, A.R. Sebastiao, A. Reis, M. Soares, J. Saraiva, R. Bernardes, R. Flores, L. Perez-Jurado, and E. Silva. 2007. Visual phenotype in Williams-Beuren syndrome challenges magnocellular theories explaining human neurodevelopmental visual cortical disorders. *J Clin Invest* 117:3720-3729.
166. Kogan, C.S., I. Boutet, K. Cornish, S. Zangenehpour, K.T. Mullen, J.J. Holden, V.M. Der Kaloustian, E. Andermann, and A. Chaudhuri. 2004. Differential impact of the FMR1 gene on visual processing in fragile X syndrome. *Brain* 127:591-601.
167. Binder, J., S. Hofmann, S. Kreisel, J.C. Wohrle, H. Bazner, J.K. Krauss, M.G. Hennerici, and M.F. Bauer. 2003. Clinical and molecular findings in a patient with a novel mutation in the deafness-dystonia peptide (DDP1) gene. *Brain* 126:1814-1820.
168. Cerruti Mainardi, P. 2006. Cri du Chat syndrome. *Orphanet J Rare Dis* 1:33.
169. Gastinger, M.J., R.S. Singh, and A.J. Barber. 2006. Loss of cholinergic and dopaminergic amacrine cells in streptozotocin-diabetic rat and Ins2Akita-diabetic mouse retinas. *Invest Ophthalmol Vis Sci* 47:3143-3150.

Appendix 1: Sequence of primers used for qRT-PCR

Gene	Primer sequence
18 S	5'- CGG CTA CCA CAT CCA AGG -3' 5'-CTG GAA TTA CCG CGG CT -3'
GAPDH	5'-TGA AGG GGT CGT TGA TGG -3' 5'-AAA ATG GTG AAG GTC GGT GT -3'
ATRX	5'-TGC ATT CTT GCC CAC TGT ATGG -3' 5'-CGT GCT GAA ATC CAG TTT GTC ACAC -3'
CHX 10	5'-CGG CTT TAA ACC AGA CCA AG -3' 5'-GGG CGT AGA CAT CTG GGT AG -3'
FOXN 4	5'- GCA CAA GTG GAA ACG AAA GGA -3' 5'-CGG GCG GTC TGA GAT GAG -3'
Lim1	5'-TTA TCT CCG GAT TCC CAA GATC -3' 5'-CTG AGA CGT TGG CA CTT TCA GA -3'
Neuro D1	5'-GAA CAC GAG GCA GAC AAG AAA GA -3' 5'-CTC CCC CGT TTC TCA GAG AGT -3'
Neuro D4	5'-GAG TCA AGG CCA ATG CTA GAG AA -3' 5'-CCT AAG ATT ATC CAA GGC ATC ATT C -3'
Pax6	5'-GGC TAT TTT GCT TAC AAC TTC TGG -3' 5'-GTG CTG GAC AAT GAA AAC GTA T -3';
Ptf1 a	5'-GCA CTC TCT TTC CTG GAC TGA -3' 5'-TCC ACA CTT TAGC TGT ACG GA -3'

Appendix 2: Markers of Amacrine cell subtypes

Marker	Amacrine cell subtype
Calbindin	AII some overlap with calretinin
Calretinin	AII small to medium-field diffuse amacrine and large-field stratified A19; Starburst
ChAT	Starburst
Syntaxin	Pan-amacrine
Pax6	Pan-amacrine (also stains horizontal and ganglion cells)
Prox1	AII (also stains horizontal and bipolar cells)
TH	Dopaminergic

Appendix 3: Contribution from Collaborators

Collaborators are listed in alphabetical order of their surname

Stuart G. Coupland: Associate Professor of Ophthalmology, University of Ottawa Eye Institute. Dr. Coupland was instrumental in setting up the ERG protocol in order to examine the oscillatory potential in ATRX KO mice. He also analyzed and interpreted the patient ERG data as described in section 3.5.2.

Richard J. Gibbons: Scientist, Medical Research Council Molecular Haematology Unit, Weatherall Institute of Molecular Medicine, John Radcliffe Hospital, Oxford, United Kingdom. Dr. Gibbons provided the clinical data described in 3.5.2. More specifically, he provided us with a list of ATR-X patients who had visual problems previously annotated by a physician in their files. He also provided access to clinical notes and ERG results for interpretation.

Chantal Mazerolle: Research Technician, Dr. Valerie Wallace's lab, Vision Program, Ottawa Health Research Institute. Ms. Mazerolle performed the initial characterization of ATRX KO animals (Figure 9 panels D, H, I, J, K and O) and performed some of the *in situ* hybridization experiments on P0 animals as described in section 3.3.1.

YaPing Wang: Research Associate, Valerie Wallace's lab, Regenerative Medicine Program, Ottawa Health Research Institute. Dr. Wang assisted with the execution of the ERG analysis on adult wildtype and ATRX KO mice as described in section 3.5.1.